UNIVERSITY OF BIRMINGHAM

Investigation of the validity of using 3D printed teeth to replace human teeth for *in-vitro* endodontic research

by

Chuta Kooanantkul

A thesis submitted to the University of Birmingham for the degree of Master of Science

School of Dentistry

College of Medical and Dental Sciences

The University of Birmingham

August 2020

ACKNOWLEDGEMENTS

I would like to express my deepest sense of gratitude to all of my supervisors, Dr. Josette Camilleri, Dr. Phillip Tomson and Dr. Richard Shelton, for their thoughtful guidance and their critical comments and correction of the thesis. I extend my gratitude to Dr. Parastoo Jamshidi for her valuable guidance and instruction provided in the additive manufacturing experiment. Thank you for all laboratory technicians, especially, Gay Smith and Jianguo Liu, for their technical guidance and endless cooperation. Thank you for post-graduate students, whom I met during my study, for sharing their research experiences and their friendly companionship. I extend thanks to Dr. Robert Harper and Rafaela Fernandes Zancan for the time and help provided in the microCT experimentation.

Thank you XDC badminton club, Birmingham IVC badminton club, Aston hawk badminton club and Thai student in Birmingham society for providing invaluable experience and make Birmingham as my second home. Finally, I must thank my parents for their support inspired me the strength to continue my study.

Table of Contents

List of illustrations

List of tables

List of abbreviations

Abbreviation	Meaning
2D	Two-dimension
3D	Three-dimension
3DP	Three-dimensional printing
3DPT	Three-dimensional printed teeth
µCT	Micro-computed tomography
ANOVA	Analysis of variance
BC cone	Bioceramic coated gutta-percha cone
CAD	Computer-aided design
CBCT	Cone-beam computed tomography
CEJ	Cemento−enamel junction
CT	Computed tomography
DLP	digital light processing
EDS	Energy dispersive X-ray spectroscopy
EDTA	Ethylenediaminetetraacetic acid
FDM	Fused deposition modelling
GP	Gutta-percha
HA	Hydroxyapatite
HBSS	Hanks balanced salt solution
HCSC	Hydraulic calcium silicate cement
HeCd	Helium-Cadmium
ICC	Intraclass correlation coefficient
kV	Kilovoltage
LED	Light emitting diode
LOM	Laminated object manufacturing
mA	Milliampere

Abbreviation	Meaning
mbar	Millibar
MI	Mechanical instrument
MTA	Mineral trioxide aggregate
NaOCl	Sodium hypochlorite
Nd:Yag	neodymium-doped yttrium aluminium garnet
NiTi	Nickel-titanium
Pa	Pascal
pA	Picoampare
PDL	Periodontal ligament
ppm	Parts per million
ROI	Region of interest
SEM	Scanning electron microscopy
SD	Standard Variation
SLA	Stereolithography
SLS	Selective laser sintering technique
UV	Ultraviolet
w/v	Weight per volume
WL	Working length
WVC	Warm vertical compaction

ABSTRACT

Introduction: Root canal obturation aims at eliminating the communication between the root canal and the peri-radicular tissues. Obturating materials fill the root canal space and the adequacy of obturation is usually assessed as a marker of sealer performance. One of the methods used to measure quality of obturation is the calculation of obturated volume of the root canal by microcomputed tomography (µCT). Human teeth are usually used for such analysis but the diversity in anatomy and the need of ethical approval limits their use. Human teeth with a particular anatomy can be 3-D printed with a polymer model being very popular for teaching and in vitro research. The polymer model is not suitable to test hydraulic calcium silicate (HCSC)-based sealers as it does not interact with the sealers and it also prevents surrounding moisture from reaching them. Thus, this research aimed to manufacture a root model composed of hydroxyapatite (HA), to assess the obturation efficacy of sealers and comparing this to that in contact with natural teeth and 3-D printed polymer teeth using µCT.

Methods: Sealers and GP were characterised by the scanning electron microscopy (SEM) and energy dispersive spectroscopy (EDX). Forty-seven incisors and mesial roots of lower molars were sectioned at the cement-enamel junction, prepared with the Protaper Gold and scanned with µCT. One incisor and molar 3D data were selected as digital model for 3DPT. 40% and 45% of HA slurry were prepared and characterised by SEM, EDX and rheometer. HA-3DPT was printed with Admaflex-130 and characterised with SEM and EDX. Five lower premolars and five polymer incisors were used to test the effect of the moisture, position and temperature on µCT accuracy. Forty-five of each polymer and natural incisors and molars were divided into 9 groups

equally and were obturated with either AH Plus (Dentsply Maillefer, Tulsa, OK, USA), Totalfill BC (FKG Dentaire SA, La Chaux-de-Fonds, Switzerland), BioRoot RCS (Septodont, Saint-Maur-des, Fossés, France) or Bio-C sealer (Angelus, Londrina, PR, Brazil) with either warm vertical compaction (WVC) or single-cone technique. Teeth were scanned immediately after obturation, at 3-month and 6-month interval. Obturated roots were kept in Hank's balanced salt solution (HBSS). HBSS was collected at 3 and 6 months to measure the calcium ion leaching with inductively coupled plasma mass spectroscopy (ICP-MS).

Results: The moisture content, positioning and temperature fluctuations inside the μCT chamber did not affect the mean root canal volume. 40% and 45% HA slurry had the same characteristics as the Admatec alumina slurry (control for printable slurry specific to the machine used). 45% HA slurry could be used to print the HA tooth model. The HA tooth model's appearances including size and shape were similar to the digital model except it had no root canal. When comparing the same sealer obturated with different obturation technique, the polymer molar obturated with Totalfill BC WVC had significantly less gap and void volume percentages than the Totalfill BC with BC cone ($p \leq 0.05$), the Bio-C WVC had significantly less gap and void volume percentages than the Bio-C single-cone ($p \leq 0.05$). When comparing the same obturation technique with different sealer, there was no significantly different between each group ($p > 0.05$). When comparing different sealer with different obturation technique, Both AH Plus WVC and Totalfill BC WVC had significantly less gap and void volume percentages than the BioRoot RCS single-cone in natural tooth ($p \leq 0.05$). For the polymer molar, the Totalfill WVC had significantly less gap and void volume percentages than the Bio-C single-cone and the Bio-C WVC had significantly less gap and void volume percentages than the Totalfill BC cone ($p \leq 0.05$). Gaps and voids volume percentages decreased in the AH

Plus single-cone in natural teeth and increased in the BioRoot single-cone of natural incisors and Bio-C WVC of polymer incisors. The highest calcium ions released at 3 months was found in the Totalfill BC cone in every tooth type. At 6 months, the highest calcium ion release was found in the BioRoot RCS single-cone for both natural tooth types, Total fill BC cone for polymer incisors and Bio-C WVC for polymer molars.

Conclusion: Variations in pre-testing parameters had no effect on the μCT measurement. 40% and 45% HA slurry had potential to be 3D printed. Polymer teeth could be used in endodontic research instead of the natural teeth to assess the filling quality and amount of calcium ion leaching. Increasing the polymer teeth's radiopacity could improve the reliability of the result. All HCSC-based sealers could be used to obturate the root canal with either single cone technique or WVC technique. Gutta-percha mass was still needed to adapt the sealers into the root canal wall and irregularity. The Totalfill BC and the BioRoot RCS obturated with single cone technique should be used whenever the clinician needs the effects of calcium ion released from the sealer.

CHAPTER I

INTRODUCTION

The primary goal of endodontic treatment is to prevent and treat apical periodontitis, which is usually bacterial in origin (1). To achieve this, the root canal system needs to be cleared of microorganisms and their by-products as well as remnants of necrotic tissue (which provide a nutrient source). The disinfection protocols in endodontic treatments include mechanical instrumentation, irrigation with antimicrobial agents and intra-canal medication.

Despite the best of efforts to clean root canals, bacteria cannot always be completely eradicated (2, 3) due to the complexity of the root canal space. It is generally accepted that some debris and unprepared surfaces (4) are always left inside the root canal system. Although the host defence mechanism can heal tissues in the body if the microbial load is reduced, remnant bacteria inside the root canal can recolonize and lead to treatment failure (5). Thus, using obturation techniques that provide a hermetic seal of the root canal are necessary to prevent communication between the root canals and surrounding tissues. To achieve this, obturation materials are used to entomb microorganisms together with their by-products and seal the root canal (6). Root canal filling materials are generally considered in two categories: core materials and root canal sealers.

1.1 Root canal core filling materials

Grossmann (7) described the ideal characteristics of a root canal core filling material as needing to:

- be easily introduced into the root canal system;
- seal the canal laterally as well as apically;
- not shrink after insertion;
- be impervious to moisture;
- be bacteriostatic or at least not encourage bacterial growth;
- be sterile or easily and quickly sterilized immediately before insertion;
- not stain the tooth structure;
- not irritate periapical tissue;
- be radiopaque;
- be easily removed from the root canal if necessary.

Many core materials have been used to fill the root canal, however the most commonly used is gutta-percha (GP). GP has been used as a root canal filling material to obturate root canals since 1847 (8). Its properties are close to the ideal characteristics of the filling material as suggested by Grossman above (7). It is composed of 70% zinc oxide, 20% natural rubber, which is a polymer of polyisoprene in the form of trans-1,4-polyisoprene and other substances such as a radiopacifier (9).

The polyisoprene of the naturally occurring GP has two crystalline forms an α-phase and a β-phase. GP is thermoplastic and occurs in the β-phase at room temperature. This phase is dimensionally stable and relatively inert. However, it cannot flow and take the shape of the irregularities of the root canal system. When heated above 42 °C, the β-phase is converted into the plastic α-phase. On cooling it is reconverted to the β-phase with a resultant shrinkage from 0.96% to 6.5% caused by the phase change (10-12).

1.2 Root canal sealers

As previously described, GP alone cannot completely fulfil the objectives of a root canal obturating material; therefore, a sealer is used as an adjuvant to the GP to fill the space between GP cones and the walls of the root canal system. Grossman (7) suggested the ideal properties of root canal sealer needed to:

- exhibit tackiness when mixed to provide excellent adhesion between it and the canal wall when set;
- establish a hermetic seal;
- be bacteriostatic or at least not encourage bacterial growth;
- exhibit a slow set;
- be tissue tolerant; that is, non-irritating to peri-radicular tissue;
- be radiopaque so that it can be seen on a radiograph;
- be of a very fine powder so that it can mix easily with liquid;
- not shrink on setting;
- not stain the tooth structure;
- be soluble in common solvents should it become necessary to remove the root canal filling;
- be insoluble in tissue fluids.

Nowadays, there are many types of sealers that are used in endodontic treatment that can be categorized according to composition including: zinc oxide eugenol, calcium hydroxide, epoxy resin and hydraulic calcium silicate -based sealers.

1.2.1 Zinc oxide eugenol-based sealers

Zinc oxide eugenol-based sealers set via a chelation reaction between zinc oxide powder and eugenol (4-alkyl-2-methoxy phenol). The use of this sealer has demonstrated long-lasting antimicrobial activity

(13, 14), ease of handling and has enough radiopacity (equivalent to approximately 3-4 mm of aluminium) (15) to fulfil the requirement of ANSI/ADA 57/2000 and ISO 6878/2001 (each root canal filling should have radiopacity at least equivalent to 3 mm of aluminium) (16). Moreover, some studies have shown that this sealer expands slightly when the ratio of eugenol is increased (17, 18); and consequently generates a good sealing of a root canal (17, 18).

Although a commonly used sealer, it has several disadvantages which include its inability to bond with GP or root dentine and high solubility (19). It dissolves when in contact with tissue fluid which will compromise seal. In addition, some zinc oxide eugenol-based sealers also release formaldehyde which can be cytotoxic (20).

1.2.2 Calcium hydroxide-based sealers

Calcium hydroxide has been used since 1838 in endodontics for various clinical applications including the disinfection of the root canal system, inhibition of a root resorption and pulp capping promoting apexification arising from the formation of a hard tissue barrier (21). The mechanisms involved in this activity include a prolonged high pH (12.5 when mixed and above 10 after 28 days of placing inside the root canal) (22) and calcium ion release. The high pH alters the catalytic activity of bacterial enzymatic systems and denatures the proteins on bacterial cell membrane; thus, calcium hydroxide acts as an antibacterial agent (23). When in contact with hard dental tissues, the calcium ions together with a high pH act in synergistic way to promote mineralisation of the dentine. The elevated pH activates the alkaline phosphatase enzyme, whereas the calcium ions accelerate the pyrophosphatase enzyme (24). Both enzymes are important factors during the mineralisation process of the dentine (23).

Nonetheless, research using calcium hydroxide as a sealer indicated a lower pH was generated when compared with the calcium hydroxide paste (not exceeding 9.57 in the first hour) (25, 26) alongside an inability to eradicate some microorganisms, including *Candida albicans* and *Staphylococcus aureus* (25-27). Secondly, this sealer has not been associated with a rapid healing of periapical lesions (28). However, the advantage of this sealer is that its cytotoxicity has been shown to be lower than that of most sealers in clinical use (29, 30).

1.2.3 Epoxy resin-based sealers

There are a large number of epoxy resin-based sealers on the market, the most commonly used is AH Plus (Dentsply Maillefer, Tulsa, OK, USA). This sealer is presented as a 2-paste system and is composed of bisphenol-A epoxy resin, bisphenol-F epoxy resin, calcium tungsten, zirconium oxide, silica, iron oxide and silicone oil (31). AH Plus has lower polymerisation shrinkage and lower solubility compared with other resin-based sealers (31). The shrinkage rate of AH Plus is 1.76% whereas the others are around 2.31% to 9.33% (31, 32).

AH Plus has many advantages. When compared with conventional zinc oxide eugenol sealers, AH Plus demonstrated the lowest solubility in distilled water (33). It also demonstrated a thinner film thickness than the ISO requirement for root canal sealing materials (31). When used after ethylenediaminetetraacetic acid (EDTA) irrigation, it penetrated into open dentinal tubules and this resulted in good adhesion of the sealer to the root canal wall (34). It also physically bonded the GP together, so it is the recommended sealer for use with the lateral condensation technique.

When compared with the previous formulation (AH 26), AH Plus exhibited better adhesion to the root canal wall and lower release of formaldehyde (35). AH 26 contains bismuth oxide as a radiopacifier which causes potential tooth discolouration and it was therefore removed in AH Plus; the latter contains zirconium oxide and calcium tungsten instead (36). AH Plus is generally considered as the gold standard for comparisons with other sealers (37).

1.2.4 Hydraulic calcium silicate-based sealers

Bioceramic materials have been widely used in medicine especially in orthopaedics including: being used as a prosthetic joint and scaffold for tissue regeneration (38) as they demonstrate biocompatibility and interact with surrounding tissues. In dentistry, the hydraulic calcium silicate cement (HCSC)-based materials such as mineral trioxide aggregate (MTA) have been used primarily for root-end fillings or root perforation repairs. These materials are hydrophilic and their hydration reaction results in the release of calcium ions (39-41), thus promoting cell attachment, proliferation, migration and differentiation (31). Calcium hydroxide is released from the hydration reaction which raises the pH to above 12 during the setting process; this alkaline pH is high enough to eradicate most bacteria (42).

These benefits resulted in the use of HCSC as a sealer with GP to obturate the root canal system. The first commercially available sealer incorporating MTA was MTA Fillapex (Angelus, Londrina, Brazil). It is composed of the salicylate resin matrix, silica and a small amount of MTA. Unlike the other sealer types, the MTA Fillapex does not shrink. Instead, it expands slightly when set (43, 44). However, MTA Fillapex is inert and the amount of calcium hydroxide released when setting is negligible (45).

A disadvantage of the MTA-based sealer is tooth discolouration caused by bismuth oxide used as a radiopacifier (46). Moreover, bismuth oxide may interfere with the hydration process of tricalcium silicate particles (41). The disadvantages of MTA Fillapex, meant other HCSC-based sealers were developed which were composed of synthetic calcium silicate and used alternative radiopacifiers to bismuth oxide.

BioRoot RCS (Septodont, Saint-Maur-des, Fossés, France) is composed of synthetic tricalcium silicate and includes zirconium oxide as a radiopacifier instead of bismuth oxide to reduce the tooth discolouration reported for sealers including MTA. It induced the angiogenic and osteogenic growth factors produced from periodontal ligament cells (47). It also had antimicrobial activity and low cytotoxicity (48).

BioRoot RCS is mixed with water and this evaporates when the sealer is used with warm vertical compaction obturation techniques leading to changes in sealer properties such as flow, film thickness and setting time (49). Moreover, when compared with AH Plus, BioRoot RCS exhibited a significantly higher amount of voids (50). It also requires manual mixing of powder and liquid, and some clinicians may find this inconvenient. The sealer may also dry out if a tooth with multiple canals is being obturated.

Other types of HCSC-based sealers are the premixed ones such as EndoSequence Bioceramic Sealer (Brasseler, Savannah, GA, USA), which is also marketed as Totalfill BC (FKG Dentaire SA, La Chaux-de-Fonds, Switzerland) and iRoot SP (Innovative BioCeramix, Inc., Vancouver, Canada). They have the same chemical compositions, namely zirconium oxide, calcium silicates, calcium phosphate monobasic, calcium hydroxide, fillers and thickening agents.

When compared with AH Plus, the premixed HCSC-based sealers release higher amounts of calcium ions, demonstrate higher flow rates, higher pH and lower cytotoxicity (51-53). These sealers also exhibit chemical and micromechanical bonds with the dentine (31). The iRoot SP has the highest bond strength to dentine compared with AH Plus and MTA Fillapex (54, 55). Furthermore, the iRoot SP exhibited a similar sealing ability to resin-based sealers (56, 57) and an antimicrobial effect due its high pH. However, this sealer does not bind to GP (58) and its alkalinity may weaken the tooth structure (31).

Bio-C (Angelus, Londrina, PR, Brazil) is a new premixed HCSC-based sealer. It is composed of tricalcium silicate, calcium aluminate, calcium oxide, zirconium oxide, iron oxide, silicon dioxide and dispersing agent. It also has a small particle size (<2 μm) (59), which improves the rheological properties and rate of calcium and hydroxyl ion release (60). Bio-C has a similar radiopacity, volumetric change and pH to Totalfill BC sealer (59). Bio-C also has the highest flow and shortest setting time compared with Totalfill BC and AH Plus (59). To date, there is no research regarding the gaps and voids analysis of the Bio-C sealer.

Due to the development of HCSC-based materials, the bioceramic coated GP cone (BC cone) was introduced (Brassler, Georgia, USA). This type of GP is coated and impregnated with calcium silicate nanoparticles. This cone aims to create an interaction with a hydraulic calcium silicate sealer to form an actual gap-free seal (monoblock system). To date, there are relatively few studies that have evaluated this type of GP in terms of filling quality and ion leaching.

1.3 Root canal filling techniques

The root canal filling technique is also one of the factors affecting the quality of root canal obturation. The objective of each technique is to fill all space inside the root canal with GP or sealer and spreading both materials into the root canal irregularities. Several techniques are used for the obturation of the root canal with GP and sealers.

1.3.1 Lateral condensation technique

This is an established technique that has been used since 1914 (61) because of its simplicity. Before obturation, a master GP cone is inserted to the working length (WL) which generates some resistance when pulled out of the root canal (tug back). While the GP is in the root canal, the spreader size is selected to find the proper size which can be inserted to 1-2 mm from the WL. After the fit of the master cone and checking of the spreader size, the root canal is obturated using the master GP cone coated with sealer. The GP cone is inserted to the WL and pressed laterally against the root canal wall using a selected spreader to create a room for an accessory GP cone. A spreader matched-size accessory GP cone is coated with sealer and inserted into the space created by the spreader. The spreader is inserted into the root canal alongside the GP cones. Apical pressure is applied to push the spreader in as deep as possible and then the GP cones are pressed laterally with the spreader again to create room for another accessory GP cone. This method is repeated until a dense filling is achieved (Figure 1A-1F).

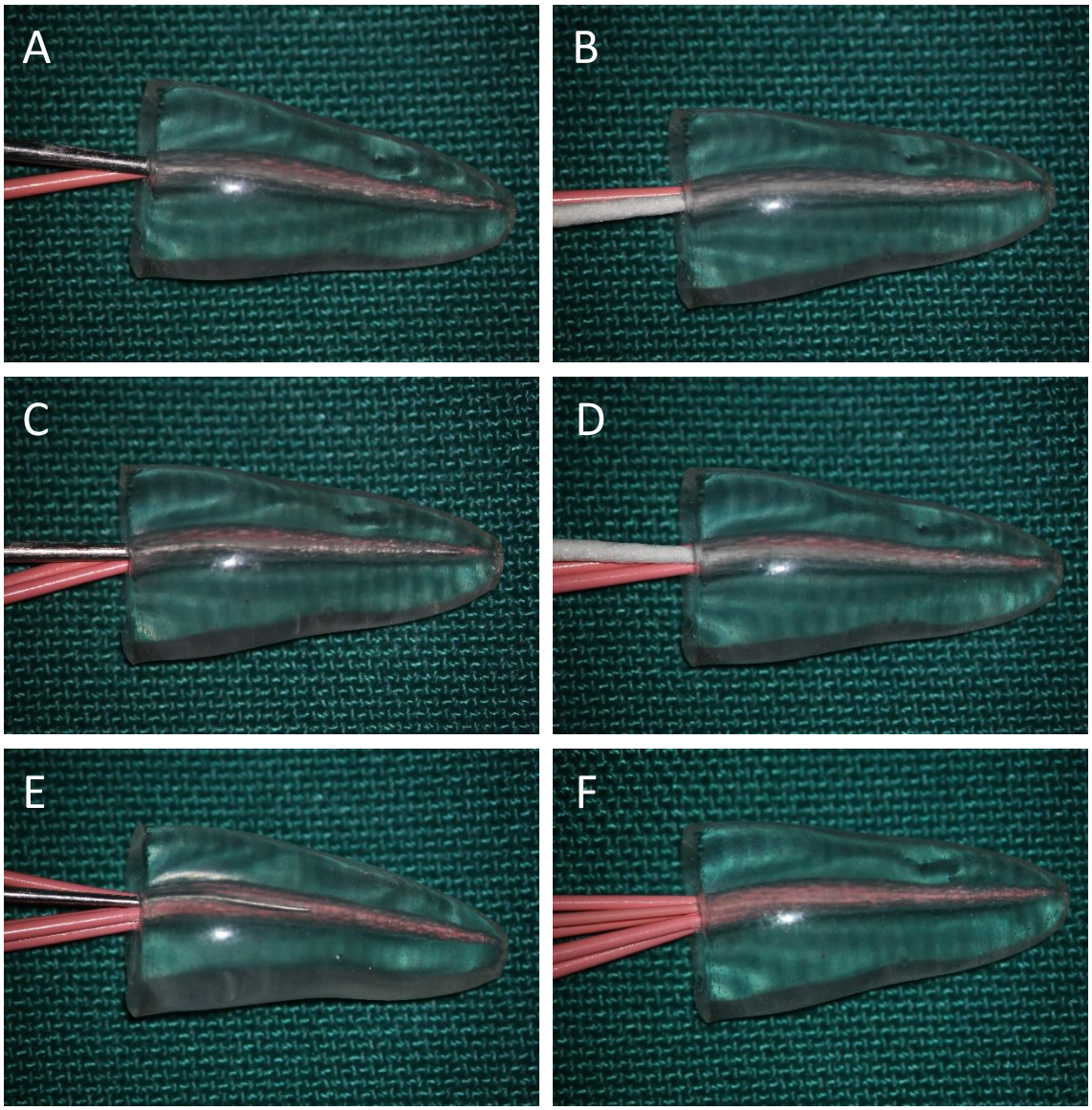

Figure 1: Lateral condensation technique*. Note that for clarity, a paper point is used to represent a new accessory cone and the sealer is not used. A: master GP cone is inserted to the WL and a selected spreader is inserted 1-2 mm from WL to create a space, B: an accessory cone is inserted into the space created by the spreader, C: the spreader is inserted as deep as possible into the root canal, D: another accessory cone is inserted to the space, E: the spreader is inserted into the root canal again. Note the decreased depth the spreader can penetrate into the canal and F: the filled root canal*

This technique is often used as a standard for comparison with new obturation techniques. The advantages of this technique are that it does not require special instruments, it generates dimensionally stable root fillings as there are no phase changes between the α- and β-phase of the GP and the working length is easily controlled (62).

The major drawbacks of this technique are that the GP does not adapt to the irregularities of the root canal (Figure 2A) and the mass generated is not homogeneous (Figure 2B) (63, 64). Also, this technique may cause vertical root fractures arising presumably from the force applied by the spreader (65, 66).

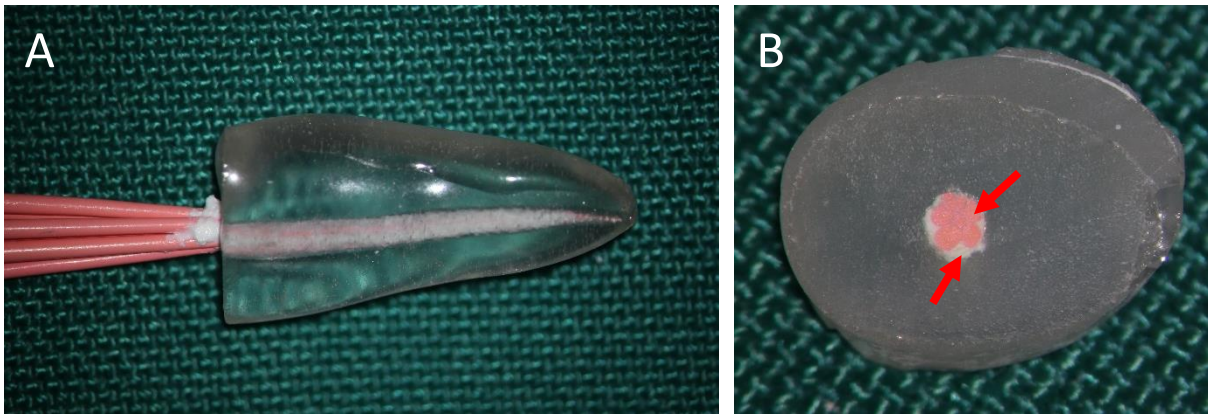

Figure 2: Root canal filled using the lateral condensation technique; *A: lateral view of a root canal filled with GP cones (pink material) and sealer (white material) and B: cross-section of the root canal filled using the lateral condensation technique. Note that GP alone cannot completely fill the root canal; therefore, the remaining space is filled with a sealer*

1.3.2 Warm vertical compaction technique (WVC)

This method was introduced by Schilder in an attempt to find an obturation method that filled all the root canal irregularities (63). The master cone is inserted to the working distance, then it is cut at 3–4 mm from the WL and is compacted vertically with heat. After that, small pieces of GP are softened with heat, inserted into the canal above the master cone and compacted vertically. This procedure is repeated until

the root canal is filled completely. This process aims to overcome the disadvantages of the lateral condensation technique. The GP cones used in the lateral condensation technique are rigid; they cannot completely fill the root canal system. Several studies have shown that warm vertically compacted GP can fill canal irregularities, such as lateral canals, better than the lateral condensation technique (67-69). The disadvantage of the WVC technique is that the incidence of GP and sealer extrusion beyond the apex of the root canal is higher than with the lateral condensation technique (62).

To date, there are several modifications and developments to the WVC technique. These include injecting a small amount of GP with a heated device into the root canal instead of using small pieces of GP when filling the coronal two thirds of the canal. Another variation is the continuous wave WVC technique developed by Buchanan (70) (Figure 3). The master cone is inserted and cut using the same approach as the conventional WVC, following by continuously injecting the GP in one movement until it fills the rest of the root canal. Whilst heated, the coronal GP is packed vertically with a matched-size cold plugger. The continuous wave WVC takes advantage of the master cone fitting to reduce apical extrusion and advantage of WVC to fill the irregularities of the canal (71).

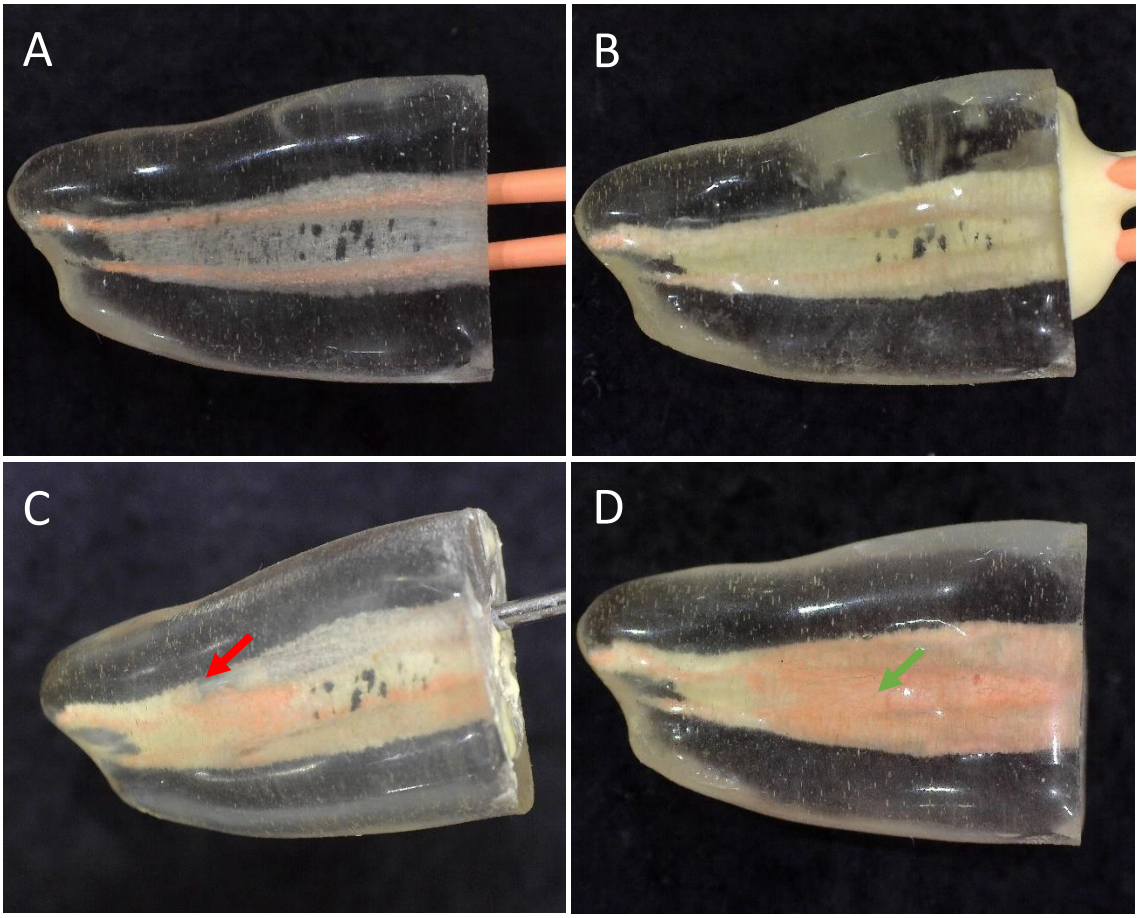

Figure 3: continuous wave warm vertical compaction technique*; A: master cones are inserted to the working length (trial main cone), B: sealer is injected directly or delivered into the root canal and master cones are inserted back to the working length, C: master cones are cut 3-4 mm above the working length and compacted vertically with a heat carrier (red arrow shows the tip of the plugger) and D: warm GP is injected into the root canal in one movement until it fills the root canal. Note the pink colour of GP at the isthmus area (green arrow)*

1.3.3 Single-cone obturation technique

This technique was originally used to obturate the root canal using a silver cone. However, when the lateral condensation technique was developed, this technique became unpopular. It made a return with the development of nickel-titanium (NiTi) rotary files, greater taper GP cones, matched size GP cones and HCSC sealers. NiTi rotary files can predictably shape the canal, while the HCSC sealers possess many of the benefits described in Section 1.2.5. The properties of HCSC sealers

depend on the environment they are placed in. Thus, when placed in a root canal, the moisture imbibed from the surrounding periodontium will result in sealer expansion and more importantly, the antimicrobial activity from the hydration reaction. As a consequence, the root canal can be obturated with a substantial amount of sealer and a matched size of GP cone (72) (Figure 4 and 5B). Other reasons that have popularised this technique are the perceived homogeneity of the GP mass formed and it is less time-consuming when compared with other techniques (73, 74).

***Figure 4: Single-cone technique**; after try main cone and deliver sealer into the root canal as the WVC technique, master cones are cut at the 2 mm below the access instead of the 3-4 mm from the working length as the WVC technique. Note the white colour of the sealer at the isthmus area (red arrow)*

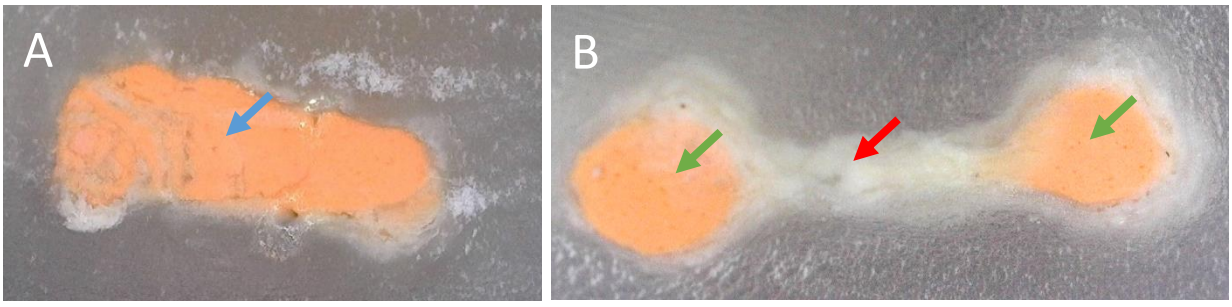

***Figure 5: cross-sectional images of filled root canal**; A: with WVC technique. Root canals and isthmus (blue arrow) are mainly filled with GP and B: with single-cone technique. Root canals are filled with master cones (green arrows), whereas the isthmus area (red arrow) is filled with sealer (sealer-based)*

To date, there is no consensus on the quality of this technique. Some literature that used radiograph and bacterial leakage test to evaluate the filling quality (describe later in 1.4) stated that the quality of the filling using this technique is similar to or better than others (75, 76). Other research that used bacterial leakage test showed worse outcomes for the single-cone technique compared with other techniques (77, 78). The main shortcoming of this technique is that it is sealer-dependent. Since most of the conventional sealers exhibit shrinkage when set, leakage is likely to occur more frequently in the single-cone technique, which requires a large amount of sealer (sealer-based technique). The adaptability of this technique is also questionable when being used with an irregular root such as an oval shape or C-shaped root canal (79, 80). As a consequence, the obturation quality of the single-cone technique should be investigated further with this type of sealer.

1.4 Root canal filling quality test

Root canal obturation quality can be measured as a sealing ability as the well-obturated root canal means the root canal is sealed well and contains no spaces. Hence, microorganisms from the oral cavity or remaining microorganisms inside the root canal are unlikely to leak to the periradicular area through the root canal (good sealing). The general concept of the sealing ability test is to pass dyes, bacteria or glucose from coronal to apical through the filled root canal. The results are usually reported as time it takes for the tracer to penetrate or pass through the root canal or the quantity of tracer present in the root canal system at defined time points. The amount of tracers are then assessed by photography or microscopy. Radiography and computed tomography for qualitative assessment of the voids in root canals has also been used.

There are many testing materials and techniques to evaluate the sealing ability *in vitro*.

1.4.1 Dye leakage test

This method involves the immersion of a tooth post-obturation into various dyes such as 0.5−2% methylene blue, 0.5% Rhodamine B, or 0.5−1% India ink. After that, the tooth is sectioned transversely or longitudinally and dye penetration recorded.

Methylene blue is the most frequently used dye because of its high degree of staining, it is inexpensive and has a low molecular weight, which facilitates dye penetration along the root canal (81). Nevertheless, this dye has some limitations as it dissolves during the demineralization and clearing process. Unfortunately, the small probability of obtaining a longitudinal section which demonstrates the deepest dye penetration point tends to generate unreliable data (82). Moreover, the dye is acidic, which may demineralize the root dentine, thus leading to increased leakage values (83). Some authors recommend using Rhodamine B instead of methylene blue (84) as Rhodamine B has a particle size of 0.1−2 μm, which is similar to many endodontic pathogens (85). As a result, it seems suitable to use this dye to measure obturation quality.

A disadvantage of the dye leakage test is the variation in the results due to many variable factors, including the dye immersion time, immersion periods, tracers used and the thermal cycling (83). Therefore, it is difficult to compare the results of each study when using this method. Another limitation is the vapour-lock effect caused by air trapping, which prevents dye penetration (83, 86).

1.4.2 Fluid filtration method

This method uses an air bubble to measure the sealing ability of a root canal obturation material. The coronal portion of the sample is connected to a tube filled with water, while the apical portion of the sample is connected to a liquid-filled capillary tube with an air bubble inside. Then constant pressure is applied to the coronal portion in order to force the water into the apical portion through the obturated root canal. The length of air bubble displacement is measured and used as a sign of leakage.

The significant advantages of this technique are the ability to measure the filling quality without damaging the specimen (87, 88) and the sensitivity of this method is dependent on the passage of the water, which can be adjusted by altering the diameter of the tube and the pressure (89).

1.4.3 Bacteria and toxin infiltration method

This technique uses bacteria or their by-products to evaluate leakage. It is believed to be more clinically relevant compared with other methods. The system comprises a dual-chamber apparatus. A bacterial-infected upper chamber is connected to the coronal part of the filled root. Many species of bacteria are used, such as *Staphylococcus epidermidis*, *Streptococcus salivarius* and *Streptococcus mutans*. However, the most frequently used species is *Enterococcus faecalis*, since it is a fast-growing bacterium. Another chamber, which contains a broth, is connected to the apical portion of the filled root. The whole system is kept in the incubator and observed until there is a sign of turbidity of the lower portion, which means there is a bacterial contamination.

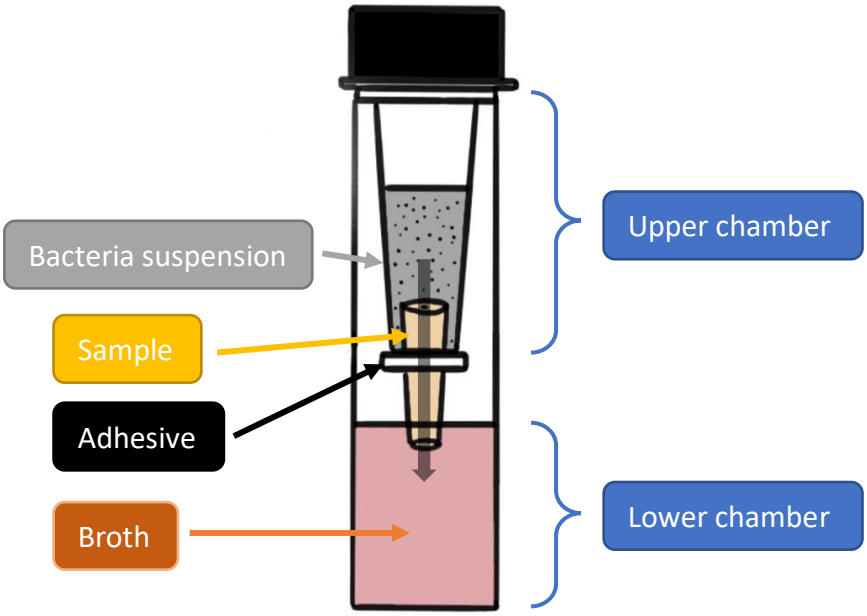

Figure 6: Bacteria infiltration method model. *Adhesive is used to attach a sample to the upper chamber contained bacteria suspension and separate the upper chamber from the lower chamber contained broth. With this setting, bacteria from the upper chamber can infiltrate into the lower chamber throught a sample only.*

The result of this method depends on the species of bacteria used (81) as the different growth rate of various bacterial species. The fast-growing bacteria generate turbidity more rapidly than the slow-growing bacteria. Notwithstanding its clinical relevance, it may not be suitable for measuring the quality of a root canal filled using a hydraulic calcium silicate-based sealer, which exhibits antimicrobial activity preventing the bacteria from leaking into the root canal. In other words, any antibacterial property of the hydraulic calcium silicate-based sealer may influence the test result. As a result, the bacterial infiltration method should be used in conjunction with other methods, including histological sections and micro-computed tomography to confirm the route of contamination (90). Another limitation of this method is that it does not completely relate to the clinical periradicular inflammation as the leaked bacteria does not always cause a periapical lesion (91). It is dependent on the species, virulence factors and amount of the bacteria as well as

the patient's immune status. This test also need histological investigation to prove the pathway of the leakage (92).

1.4.4 Glucose penetration method

Glucose is used to test sealing ability because its molecular weight is low and it is a nutrient for microorganisms in the root canal (93). In this technique, the upper chamber described in 1.4.3 is filled with glucose instead of the bacteria used in a bacteria infiltration method. The pressure is applied to the upper chamber forcing the glucose to penetrate through the obturated root canal to the lower chamber. The quantity of glucose in the lower chamber can be quantified by spectrophotometry or the concentration of leaked glucose; therefore, it is considered a sensitive and clinically relevant test. However, its drawbacks include requiring a long experimental period resulting in the difficulty of maintaining a sterile system and the risk of water evaporation affecting the glucose concentration (81).

1.4.5 Protein microleakage test

This technique uses similar methodology as that used in the glucose penetration method but bovine serum albumin is used instead of the glucose. The Bradford indicator filling the lower chamber is used to determine the concentration of albumin that leaks from the upper chamber by the formation between the indicator and serum albumin. The dye-protein complex shifts the maximum absorption wavelength of the Brilliant Blue G, which can be detected by spectrophotometer (81).

1.4.6 Cone-beam computed tomography technique (CBCT)

Another way to measure the quality of a root canal obturation is to measure the voids in the root canal by using cone-beam computed tomography (CBCT). This technique was developed by Arai (94). CBCT generates a higher resolution image whilst using a lower radiation dose when compared with traditional computed tomography (CT). Owing to the isotropic voxels of CBCT, an accurate three dimensional (3D)-image can be made without damaging the specimen.

Nowadays, CBCT plays an essential role in clinical studies because it provides information about root canal morphology in three planes (coronal, sagittal and axial) without damaging specimens (95-97). When compared with conventional two-dimension radiography, CBCT does not have a problem with superimposition. However, the limitations of CBCT are metal scattering (96) and the CBCT's volumetric pixel (voxels) size (0.4−0.125 mm) is not small enough to measure the root canal filling quality (98).

1.4.7 Micro-computed tomography technique

Micro-computed tomography (µCT) is another 3D technique being used for both qualitative and quantitative analysis in many fields include: material sciences, additive manufacturing (3D printing) and biological sciences as it can generate voxels in the size range from 5-50 µm (99). In other words, µCT provides much greater detail and resolution than CBCT. In the general scanning process, a sample is fixed onto a rotating base. The X-rays are focussed onto the sample while the base is slowly rotated projecting images on a planar detector (Figure 7). Projecting images are reconstructed and segmented into several sliced images, and subsequently, the sliced images are merged into a 3D image.

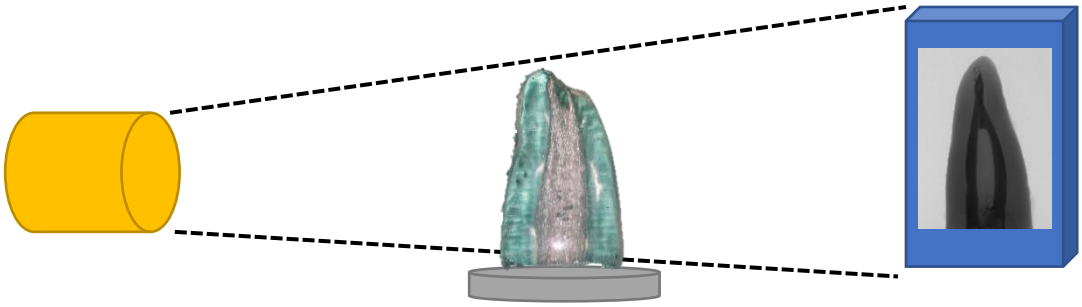

Figure 7: Schematic µCT process. *A sample - in this case, a tooth - is fixed to the rotating base. The base slowly rotates receiving X-ray beam and projecting images on the planar detector*

Three scanning parameters involve in this process which need optimization for each type of sample:

1. Voltage: The voltage required depends on the sample density. A denser object requires a higher voltage for better penetration. However, using a high voltage results in a reduction in contrast between materials with the same density (100).
2. X-ray current: This parameter determines the signal to noise ratio. The higher X-ray current gives a better signal to noise ratio.
3. Voxels size: This parameter determines the images' resolution. The smaller voxels size, a higher resolution is generated but the scanning time is also increased.

In endodontics, µCT is widely used for both qualitative and quantitative studies of root canal cleaning and obturation quality as it has many benefits described above. The tooth is scanned and reconstructed in µm resolution then superimposed to create 3D images. The structure of the root filling materials, dentine and enamel are colour-coded by the software. Based on this procedure, the structure of the root canal can be seen in three dimensions related to the external tooth surface (101-103). For root canal obturation quality assessment, µCT has

been used to show the amount, size and location of gaps (space between the material and dentine) and voids (space inside the material).

However, µCT has some limitations, including not being suitable for clinical use (102) as it requires long term exposure to X-rays (usually several hours for a high-quality scan) and the size of the sample must be smaller than the size of a µCT machine. To date, no study has reported the precision and accuracy of µCT used for a quantitative study in endodontics.

1.5 Three-dimensional printing techniques for development of 3D models for in-vitro endodontic research

A 3D printer generates an object from a digital model created using software (computer-aided design; CAD), CT scan, or µCT (104, 105). The 3D image can be converted to a .stl file, which changes the image's surface into the mesh of triangular sections. The .stl file is imported into the printing software for a 3D printing.

In dental research that uses human teeth, the physiological standardization of the natural teeth is impossible. In some countries, there are also limitations in using human teeth due to ethical issues. Some specific diseases and complex anatomies, such as C-shaped root canal, *dens invaginatus*, or root resorption, are rare. Thus, research on those teeth is limited because of the scarcity of the samples. In conclusion, there are many limitations to conducting research on human teeth. When considering the dental education field, endodontic procedures require an in-depth knowledge of root canal anatomy, which is generally taught by the preparation of extracted natural human teeth in dental school. Unfortunately, the anatomy of natural teeth can only be observed by the two-dimensional (2D) radiograph. Moreover, 2D or

3D visualizations on a computer screen can be inadequate for obtaining a thorough understanding of the complex root canal anatomy.

Currently, rapid prototyping or 3D printing (3DP) has been introduced in the dental and medical fields. It has been used in many applications, including as a research and training tool, as it can overcome those limitations described above. In education, students can observe tooth anatomy using translucent 3D models. Furthermore, training dental procedures in rare diseases and anatomy are becoming possible. In the research field, 3DP can reproduce exact the physiological anatomy of the tooth. Hence, bias from the sample standardization is eradicated.

1.5.1 Stereolithography technique (SLA)

SLA is the first commercialized 3DP method (106) that uses an ultraviolet (UV) beam to polymerize a light-cured resin liquid that fills a bath (107), described as the 'bath configuration'. The type of UV light source varies depending on the type of resin. The most common sources are helium-cadmium (HeCd) laser and the xenon lamp (104). After completing the first 2D cross-section, the base lowers further into the resin pool and the UV beam begins to polymerize the next layer on top of the previous one. This process repeats until the 3D object is completed. The vertical resolution of this technique can be determined by the thickness of the cured layer, which is dependent on the intensity of the light source, the critical energy of the resin and the depth of light penetration. The horizontal resolution of this technique depends on the diameter of the UV beam.

The bath configuration has some drawbacks. First of all, the size of the object is restricted by the height of the bath. Secondly, this configuration wastes significant amounts of resin. As a consequence,

another configuration of the SLA technique called 'layer configuration' has been invented. This configuration uses the same process as the bath configuration, but the movable part is placed above the resin reservoir and the light source is placed beneath it. This set-up results in less resin waste and no height limitation.

The other improvement of the SLA technique is a masked lamp technique. Unlike the conventional method that cures the resin line by line, the masked lamp technique cures an entire layer at a time. Thereby, the time used to print the 3D object is reduced (104).

Another variation of SLA is digital light processing (DLP). Instead of using a laser beam to cure the resin in a series of points, DLP uses a projector to flash an image throughout the platform at once. An example of this technique is Admaflex 130 (Admatec Europe B.V., Alkmaar, Netherland) (Figure 8). It is an industrial 3D printing machine used SLA technique to print both ceramic and metal materials. Material powders are mixed with light-cured resin. The powder-resin solution known as a slurry is delivered into the machine, which it is solidified layer after layer by a light projector.

The advantages of the SLA technique are its capability to make high-resolution and complex shapes with internal structure and the ease of removal of the residual resin. The challenges of this technique are the entrapment of crosslinked monomers and the inability to process different types of resin at the same time. Furthermore, resins that are used in this technique are epoxy or acrylic resins, which shrink and become brittle when polymerized (104). Moreover, this technique needs temporary support structures to fabricate unsupported parts. Complete removal of the supporting structure can be difficult.

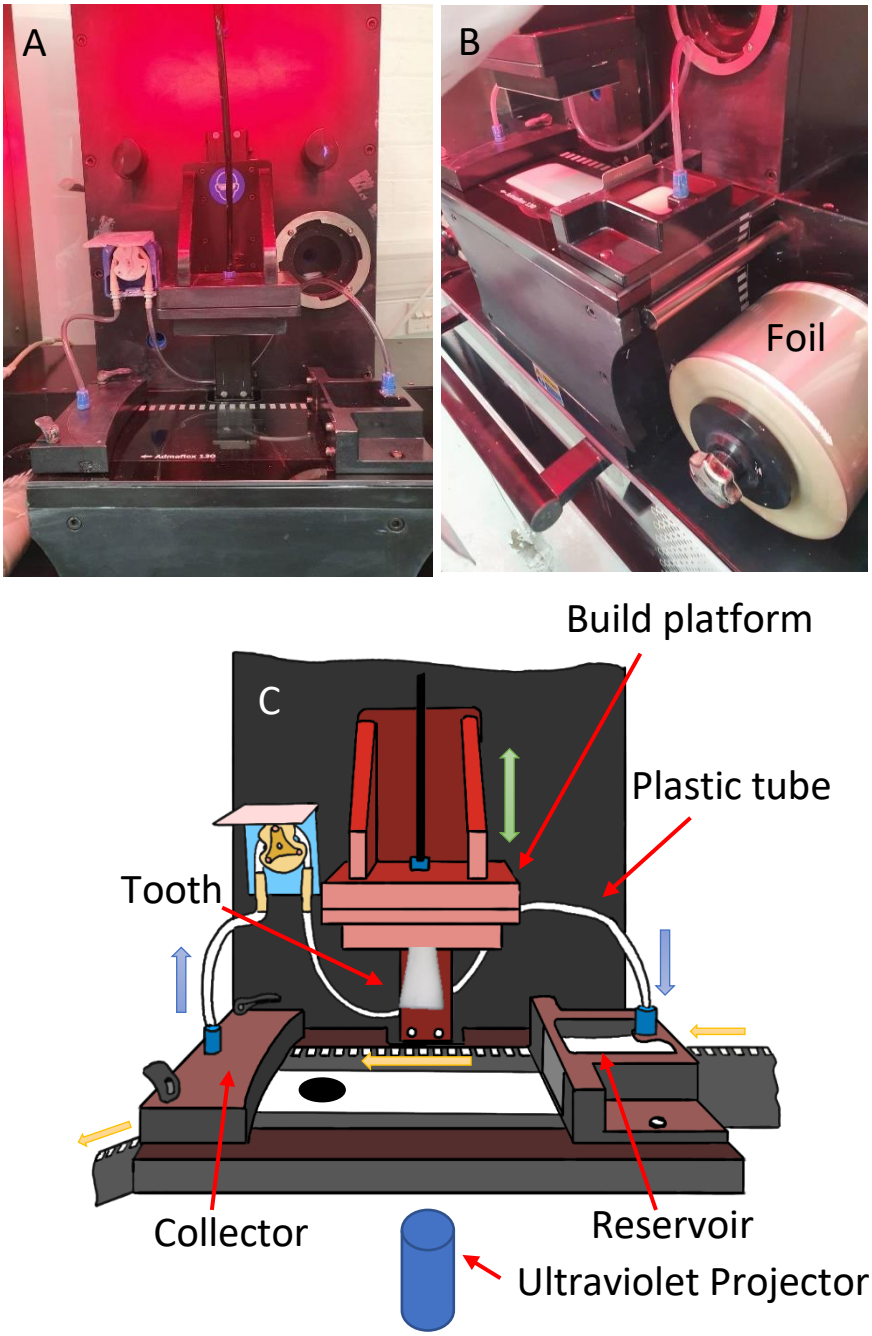

Figure 8: Admaflex 130 machine*; A: Admaflex 130 machine, B: Admaflex 130 during printing process and C: Schematic of the Admaflex 130 machine during printing and B: the printing process. The slurry was poured into the reservoir then it was carried with plastic foil to the collector (yellow arrows show the flow direction). Meanwhile, the build platform moved down toward the slurry. When the platform touched the slurry, the foil stopped moving and the light was emitted from the projector to cure the slurry. After curing, the platform moved back to its initial position and the foil together with the remaining slurry continued moving toward the collector where the remaining resin was circulated back to the reservoir through plastic tubes. This process was repeated until the printing was finished.*

1.5.2 Inkjet printing technique

The inkjet printing technique is usually a powder-based method. The layer of solid particles is bound together by printed liquid material. The first layer of the solid particle is spread on a support stage by a roller. The print head then prints droplets of liquid onto the solid particle. After completing the first layer, the stage is lowered and the next layer of the solid particles is deposited again. These steps are repeated until the object is created. Finally, a complete model is generally heat-treated to improve the fusion of the powders.

Inkjet 3D printing is commonly considered as a hybrid of two different types of technique. The continuous type requires electrostatic plates to guide ink droplets onto the paper. The size and the spacing of droplets are controlled by a pressure wave pattern. Another type of an inkjet technique is the drop-on-demand type. Unlike the former type, this type uses voltage and a pressure pulse to direct the ink droplets.

The advantages of this technique over SLA is the variety of materials that can be used. As it is a powder-based technique, powder from glass, ceramic or monomers can be used. Still, this technique has some drawbacks as it cannot be used for tissue scaffold fabrication due to the cytotoxicity of the ink droplets (108). In addition, incomplete interaction between solid particles and liquid can affect the transparency, surface roughness and porosity.

1.5.3 Selective laser sintering technique (SLS)

Although SLS is a powder-based system like the inkjet printing technique, this technique uses a high-power laser such as the neodymium-doped yttrium aluminium garnet (Nd: Yag) laser to sinter polymer powders (84). The first solid powder is distributed as with the

inkjet technique, but it is heated to a temperature below melting point. A laser beam is then directed at the powder to raise the temperature above the glass transition temperature which fuses the powder together. Then the next layer of solid powder is distributed. These steps are repeated until the object is fabricated.

The advantage of this technique is that many materials can be used. Unlike SLA, SLS does not require temporary support since unbound particles can support any cantilever part. Moreover, this technique can be used to fabricate models that have internal porosity because the sintering method does not cause complete melting of the particles. Nonetheless, the pore sizes are limited by the powder size used, as previously mentioned. On the other hand, models printed from this technique suffer deformation from the change of heat. In addition, the conduction and diffusion of heat from the laser beam can fuse unwanted neighbouring powders. The limit of the particle size used in this technique is 10 µm since poor spreading and sintering too quickly cause inaccuracies at margins.

1.5.4 Fused deposition modelling (FDM)

This technique is one of the most widely used. It works by moving the thermoplastic filament by rollers to the print tip. Then, the filament is heated to a semi-molten stage and injected onto the platform. The platform is lowered down and another layer is deposited in the same way. The controllable parameters are raster thickness, raster gaps width, raster angle and layer thickness.

Advantages of this technique are that it can create models with multiple material types by subsequently changing the filament and it can fabricate high-porosity models with excellent mechanical strength.

However, this technique results in a staircase effect. Moreover, internal defects can result from heterogeneities of the filament diameter and density (104). Apart from that, the complexity of the shape of models is limited due to the properties of the materials, which have to have high enough viscosity to solidify but low enough viscosity to be ejected.

1.5.5 Laminated object manufacturing (LOM)

This technique generates 3D models by stacking layers of sheet materials. After loading the material onto the stage, the laser beam traces the outline of the pattern and the excess sheet is removed. After that, a second sheet covers the previous one and a laser beam is used to retrace the outline. Adjacent sheets are fused with adhesive or welding (104).

The advantage of this technique is the deformation from the thermal process of this technique is minimal when compared with other techniques. Nevertheless, if a local temperature of the sheet is not well controlled, the sheets could be delaminated due to adhesive failure.

1.6 3D-printing materials used in dentistry

1.6.1 Acrylic resin

In endodontics, acrylic resin has been used to make tooth models for several years because it is inexpensive and it can be 3D-printed by many techniques. The acrylic model also precisely replicates the tooth anatomy. Moreover, its translucence also makes the root canal visible; therefore, it helps in teaching and training. Nevertheless, acrylic models have some limitations which are the low melting point (160 ^{o}C) and its properties that differ from the natural tooth. Although the actual

working temperature of the warm vertical compactor is lower than displayed (200 ^{o}C) (109), it still may have some effect on the acrylic resin. Also, the feeling provided by the acrylic during instrumentation is not the same as the feeling of a natural tooth. There have also been some problems, such as canal blockage by acrylic debris. Finally, a hydraulic calcium silicate-based sealer does not react with the acrylic resin and it may not set because of the lack of moisture.

1.6.2 Hydroxyapatite (HA)

Most human teeth and bone structures are mainly composed of HA (110), HA models were made to mimic the natural hard tissue. There have been many articles regarding HA models in terms of bone grafting materials which showed promising outcomes (111-113). HA demonstrates excellent biocompatibility and fulfils all standard requirements of bone tissue engineering scaffolds (111). However, to date no study has been conducted regarding tooth models made from HA.

1.7 Aims of this study

To achieve the highest success rate of the root canal treatment, one of the most important factors is to find the optimal root canal obturation technique and material. To date, many HCSC-based sealers have been introduced to the market. As mentioned before, some sealers such as BioRoot RCS change properties when heated during WVC. Thus, research about the obturation quality of root canal filled with these sealers using different techniques is necessary to create an in-depth understanding of the sealers' properties and to identify the best technique to be used with these sealers.

In-vitro endodontics research and studies are usually carried out on extracted natural teeth because natural teeth can easily be related to the clinical situation. However, natural teeth also have disadvantages which include the anatomical variation and scarcity of samples. As a result, polymer 3DPT teeth can be used to overcome these limitations. However, a limitation of polymer teeth is a lack of interaction with calcium silicate-based sealers. To overcome this problem, HA, the major component found in natural teeth could be used instead of the polymer. To the best of the authors' knowledge, no 3DPT teeth made of HA have been fabricated.

Other disadvantages of polymer teeth are its porosity and hardness also differ from natural teeth; therefore, data obtained from polymer teeth may differ from that obtained in natural teeth. To date, no study has ever compared data from research using polymer and natural teeth. Due to the gaps in knowledge and the limitations of the materials mentioned above, the aims of this study were:

1. to manufacture a root model made of HA;
2. to assess the obturation efficacy of a number of sealers using natural teeth and polymer teeth models using µCT;
3. to assess the hydration of hydraulic calcium silicate sealers in contact with the different tooth models and natural teeth;
4. to measure calcium ion leaching from a number of sealers at specific time points.

1.8 Hypothesis

From the assessment of the obturation efficacy of a number of sealers using natural teeth and polymer teeth models using µCT, the null (H_0) and alternative hypotheses (H_1) were tested as follows:

Hypothesis 1: Root canal filling technique H_0: There is no significant difference in the quality of the root canal filling obturated with the single cone technique and the WVC technique.

H_1: There is a significant difference in the quality of the root canal filling obturated with the single cone technique and the WVC technique.

Hypothesis 2: Root canal sealerH_0: There is no significant difference in the quality of the root canal filling among sealers.

H_1: There is a significant difference in the quality of the root canal filling among sealers.

Hypothesis 3: Tooth type

H_0: There is no significant difference in the results performed in the natural and polymer teeth.

H_1: There is a significant difference in the results performed in the natural and polymer teeth.

Hypothesis 4: Effect of sample's temperature, moisture and position on the accuracy of µCT measurement

H_0: There is no significant difference in the accuracy of µCT measurement among sample's status.

H_1: There is a significant difference in the accuracy of µCT measurement among sample's status.

CHAPTER II

MATERIALS AND METHODS

To assess the validity of using 3DPT to replace human teeth for assessment of the quality of endodontic obturation a study was designed where two obturation techniques were compared, namely, warm vertical compaction and single-cone obturation using different types of GP and sealer. GP and BC cones (only for the Totalfill BC; FKG Dentaire SA, La Chaux-de-Fonds, Switzerland) were matched to the final size of root canal preparation and used with the following sealers:

1. AH Plus (Dentsply Maillefer, Tulsa, OK, USA)
2. BioRoot RCS (Septodont, Saint-Maur-des Fossés, France)
3. Totalfill BC (FKG Dentaire SA, La Chaux-de-Fonds, Switzerland)
4. Bio-C (Angelus, Londrina, PR, Brazil)

Obturation was carried out in human teeth or 3DPT made of either resin or HA. Two different anatomical variations of 3DPT were used: either single-rooted teeth for simple root canal anatomy or mesiobuccal roots of lower molars with two canals joined by an anastomosis to represent complex root canal anatomy. One 3DPT of each anatomy was made from both resin and HA.

2.1 Material characterisation

The four sealers and the two types of GP were characterised using scanning electron microscopy (SEM; EVO MA10, Carl Zeiss, Cambridge, UK) and energy dispersive X-ray spectroscopy (EDS; EVO MA10, Carl Zeiss, Cambridge, UK). The sealers were injected into circular rubber moulds 10 mm internal diameter and 2 mm high placed on mixing glass slab and kept at 37 ^{o}C and 100% humidity until the surface was resistant to indentation. Sealers were considered as set entirely when no physical mark was made on the sealer surface visually.

After setting, each sealer was removed from the rubber mould and embedded in epoxy resin (EpoFix, Struers, Ballerup, Denmark). Resin blocks were put in a fume hood at room temperature for one day for polymerisation. After setting, the resin blocks were polished using 220, 500 and 1,200 grit diamond discs (MD-Piano, Struers ApS, Denmark) with water coolant for 1 min each, using an automatic grinding and polishing machine (Phoenix Beta, Buehler, Lake Bluff, IL, USA) followed by polishing with cloth discs (MD Largo, Dac, Nap, Struers Aps, Ballerup, Denmark) using 9, 3 and 1 µm diamond impregnated polishing liquids (DiaPro, Struers ApS, Ballerup, Denmark) for 3 mins, respectively.

Samples including the Protaper GP cones, GP pellets used in WVC and BC cone were dried in a desiccator containing silica gel at room temperature for one day. All the specimens were mounted on aluminium stubs with double-sided carbon tape. Each sample was sputter-coated with gold (EMITECH K550X; Carl Zeiss, UK, needle value adjustment was set to give 0.1 mbar of Argon gas at a nominal 0.3 bar, a deposition current of 25 mA and deposition time 2 mins) before examination using SEM and EDS for elemental analysis (working distance 8.5 mm, I Probe 1,000 pA and accelerating voltage 20 kV). Images in backscatter mode

were captured at 1 K and 2 K X magnification. The type and weight fraction of the elements were recorded from EDS.

2.2 Tooth selection and preparation

To assess the quality of obturation, two types of root canals were selected. These included upper central incisors as these have round canals and are considered as uncomplicated to manage. The mesiobuccal root of lower molars were also selected as complicated root canals. For each tooth type, a resin and a hydroxyapatite replica were made of the prepared canal.

2.2.1 Selection and preparation of natural teeth

The use of human teeth for research was approved by the Research and Innovation Department, Birmingham Community Healthcare Trust (14/EM/1128). A total of 47 upper incisors, 47 lower molars and five lower premolars were obtained from the tooth bank at Birmingham Dental Hospital, Birmingham, UK. The apices were checked to ensure they were fully formed. Teeth with caries or restorations on the root, or fractures of the root were excluded. Remnants of periodontal ligament (PDL) and bone were gently removed using a Gracey curette (SG11/12, Hu-Friedy, Chicago, IL, USA). The crowns were sectioned off with a diamond disk and the roots of the incisors and lower premolars were standardized to 16 mm while the mesio-buccal roots were sectioned off and standardized to 12 mm in length.

For the single-root group, teeth were decoronated perpendicular to the long axis of the tooth 16 mm above the root apex with a low-speed rotary diamond saw (ISOMET®, Buehler, Lake Bluff, IL, USA) with water coolant at maximum speed. When the coronal root canal orifice was not found, a high-speed tapered diamond bur with water coolant was used

to open the access before insertion of a K-file No.10 (Dentsply Maillefer, Ballaigues, Switzerland) into the canal with a watch-winding motion. The files were advanced within the canal until the tip of the file was observed flush with the apical foramen using loupe magnification (x4) (EyeMag® Pro, Carl Zeiss, Bangkok, Thailand) with maximum brightness from a dental light-emitting diode (LED) headlight (Lumadent, Reno, NV, USA). The rubber stop was moved until in contact with the top of the access (coronal reference point) and the canal length was measured using a ruler from the rubber stop to the tip of the file to determine thelength of the canal. WL was calculated by subtracting 0.5 mm from the canal length. If the canal could not be fully negotiated to achieve patency, the tooth was excluded from the study.

For the molar group, teeth were decoronated perpendicular to the long axis of the tooth, 12 mm from the tip of the root using the low-speed rotary saw. These teeth were sectioned into two through the furcation to isolate the mesial root. The WLs of the two canals in the mesial root were then calculated as described for the incisor group.

A total of 47 upper incisors, 47 mesial roots of lower molars and five lower premolars were collected. All teeth were kept hydrated at 37 °C in an incubator by immersion in Hanks balanced salt solution (HBSS H6648; Sigma Aldrich, Dorset, UK) throughout the experiment.

The root canals were prepared using ProTaper Gold Sx (Dentsply Maillefer, Ballaigues, Switzerland) files used for coronal flaring to 12 mm depth in the incisor group and 8 mm in the molar group. Initial foramen size was evaluated with the largest K-file that could be inserted to the WL using a watch-winding motion pressureless technique. Root canals were enlarged at the working length sequentially from ProTaper Gold S1 to ProTaper Gold F3 (Dentsply Maillefer, Ballaigues, Switzerland) for the incisor group. The molar group was enlarged with ProTaper Gold S1 to

ProTaper Gold F2 with a brushing motion against the outer part of the curvature of the canal (if it existed) on the outstroke. Each ProTaper Gold instrument was used to prepare five incisors and five mesial roots before discarding.

Throughout the preparation, canals were irrigated using a 27-gauge side-vent needle which was inserted to a maximum of 2 mm short of the apical foramen between each mechanical instrumentation (MI) step to deliver a total of 6 mL 2% sodium hypochlorite (NaOCl; Cerkamed, Stalowa Wola, Poland) per root. After completing MI, 3 mL 17% EDTA (Cerkamed, Stalowa, Wola, Poland) was used to rinse the canal for 1 min, followed by 3 mL 2% NaOCl for 1 min.

A matched GP cone for ProTaper Gold system (Dentsply Maillefer, Ballaigues, Switzerland) was inserted into each root canal to the WL and tug back was checked to verify cone fitting. If the main cone did not reach the WL, the largest rotary file size used in each tooth type was used to enlarge the canal again. If the main cone went beyond the apical foramen, the length from the tip of the main cone to the apical foramen was measured using a ruler. The GP was then cut at that length plus 0.5 mm from the tip end. Then, all teeth were kept in a moist condition by using a tissue napkin soaked with HBSS and put in the 37 $^{\circ}$C incubator.

2.2.2 Selection and preparation of model 3DPT

To select natural teeth for creating the digital template of 3DPT, upper central incisors and lower molar teeth were selected from the tooth bank with the same criteria as the natural tooth outlined above. The upper central incisor group was used to represent round simple root canal anatomy whereas the lower molar was used to represent a root canal containing isthmus and thus a more complex anatomy. Teeth were

scanned with µCT (Bruker Skyscan MicroCT model 1172, Billerica, MA, USA) from apex to crown at 11 µm intervals, using an accelerating voltage of 70 kV at 140 mA and medium camera pixels (2K x 1K). These conditions were used for all scans unless indicated otherwise. Scanned images were reconstructed using NRecon software (Bruker, Billerica, MA, USA) and saved in .tiff file format.

These procedures were repeated until the following criteria were met:

For the incisor group (Figure 9A)

1. The model should have a circular continuously tapered canal from the coronal to the apical part of the root.
2. The model must have an apical stop.

For the molar group (Figure 9B)

1. The model should have two continuously tapered canals from the coronal to the apical part of the root.
2. The model should have two apical foramina, each with an apical stop.
3. The model must have a continuous isthmus along the root length.

One selected tooth from each group was prepared with the same procedures as the natural tooth. 3D root canals and dentine images of these teeth were created using CTAn software (Bruker, Billerica, Massachusetts, United States) and were saved in the .stl file format. The selected digital files were sent for 3D-polymer printing (RepliDens®, Smartodont, Zurich, Switzerland) (Figure 9C and 9D).

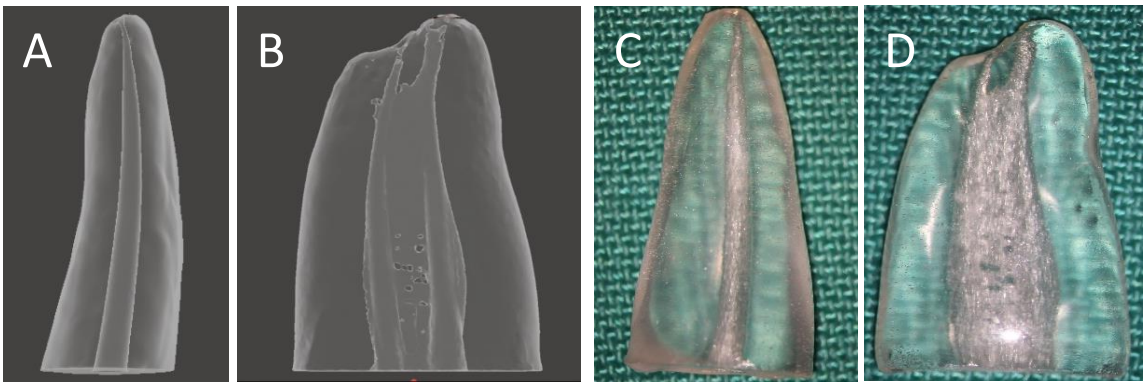

Figure 9: Digital and polymer printed tooth model*; A: digital model of the incisor, B: digital model of the molar, C: polymer printed incisor, and D: polymer printed molar. Note the similarity of the root canal morphology of polymer teeth compared with digital models*

2.2.3 Preparation and testing of HA-3DPT

A 3D printer (Admaflex 130, Admatec Europe, Alkmaar, Netherlands) was used to print the photocurable HA root replica. Following Admatec's recommendations (114), the following materials were used to 3DPT:

1. The HA powder was high-purity (99.9% purity or higher) with uniform particle size. The mean particle size was less than 0.5 µm and a specific surface area in the vicinity of 7 m^2/g;

2. The polymeric resin was made of a monofunctional binder together with a di- and a tetra-functional crosslinker. The photo-initiator was activated by the 3DPT device's light engine wavelength (405 mm).

Materials used for slurry preparation included:

1. HA powder (CAPTAL® R, Plasma Biotal, Buxton, UK)
2. Light-curable resin (Admatec Europe B.V., Alkmaar, Netherlands)
3. Dispersant (Disperplast 1142, BYK-CHEMIE GMBH, Wesel, Germany)

4. Photo-initiator (2,2-dimethoxy-2-phenylacetophenone, DMPA; Sigma-Aldrich, Dorset, UK)

The HA powder was characterised using SEM with the same parameters as described in 2.1. A pilot study was carried out to investigate the highest solid loading composition to use for the printing. The HA slurry used for pilot study was prepared by mixing HA with the light-cured resin. The dispersant was added into the suspension to adjust the viscosity. Finally, the photo-initiator was included into the slurry suspension. The pilot studies aimed to optimise the slurry by:

1. Altering the light-cured resin to dispersant ratio;
2. Trying different mixing processes: manual mixed with spatula or mechanical mixing (Cap-Vibrator, Ivoclar Vivadent, Schaan, Liechtenstein).
3. Increasing the mixing time when using the mechanical mixer (30 s, 5 min and 10 min).

These pilot studies aimed to create an HA slurry which had the same viscosity as the Admatec's alumina slurry which was the control and printable. The printing time was around 4 hours thus a slurry that maintained the same viscosity as the control for that period of time was required.

Two prototype slurries were selected and rheology testing was performed. This was done by preparing 1 mL of each slurry type with a mechanical mixer which was then placed into the rheometer at 20 $^{\circ}$C. The dynamic viscosity was analysed by increasing the shear rate from 0.01 to 1,000 s^{-1} while measuring the torque. The test was performed an hour after preparation to imitate the actual printing procedure.

The printing procedure is shown in Figure 6. A prototype model and circular discs 10 mm in diameter and 1 mm thickness needed for

measuring the radiopacity (115) were printed and compared with the radiopacity of the filling materials. A preliminary test was performed to find the optimum parameters for the printing. The machine parameters at each slice are shown in Table 1.

***Table 1: Parameters for HA 3D printing**; * means data came from the preliminary study*

Parameters \ Slice	0 (base)	1−20	21−524
Thickness (μm)*	30	50	30
Repeat	2	1	1
LED power*	500	800	800
Pixel value	1,000	1,000	1,000
Exposure time (ms)*	1,000	5,000	5,000
Delay before exposure (ms)	35,000	8,000	4,000
Delay after exposure (ms)	500	50	500
Transport speed (μm/s)	25,000	25,000	25,000
Transport acceleration (μm/s^2)	25,000	25,000	25,000
Transport distance margin (μm)	35,000	50,000	5,000
Up/down distance (μm)	6,000	8,000	4,000
Up/down speed (μm/s)	1,500	1,500	1,500
Up/down acceleration (μm/s^2)	1,000	1,000	1,000
Slow up distance (μm)	1,000	1,00	1,000
Slow up speed (μm/s)	200	200	200
Slow down distance (μm)	300	200	200
Slow down speed (μm/s)	200	200	200

The evaluation of the radiopacity of the HA-printed root and HA disc was assessed using radiographs both on the same X-ray film as an aluminium step-wedge (Gammex model 117, 11 steps with 3.2 mm increments, Gammex rmi, Middleton, WI, USA) on a phosphor plate (DÜrr Dental, Bietigheim-Bissingen, Germany). The X-ray beam was

directed perpendicular to a phosphor plate using an intraoral X-ray machine (Progeny Preva DC, Midmark, Dayton, Ohio, USA) at 60 kV, 7mA and exposure time of 0.050 s. A digital greyscale image was saved as .jpeg and imported into ImageJ software version 1.52a (National Institute of Health, Bethesda, MD, USA). To calculate the radiopacity (116), the grey pixel value of the HA-printed root, HA disc and each step of an aluminium step-wedge images were measured. A spreadsheet program (Microsoft Office Excels 2020; Microsoft Corp., Redmond, WA, USA) was used to plot a graph between grey pixel of aluminium step-wedge versus the thickness of aluminium and the best-fit logarithmic trendline was drawn through the points. The equation of the trend line gave the grey pixel value of an object on the image as a function of the object's thickness in mm of aluminium (Figure 10). The mean grey pixel values of the HA printed root and HA disc were calculated with this equation and expressed in mm of aluminium. The 3D printed root was characterised by SEM.

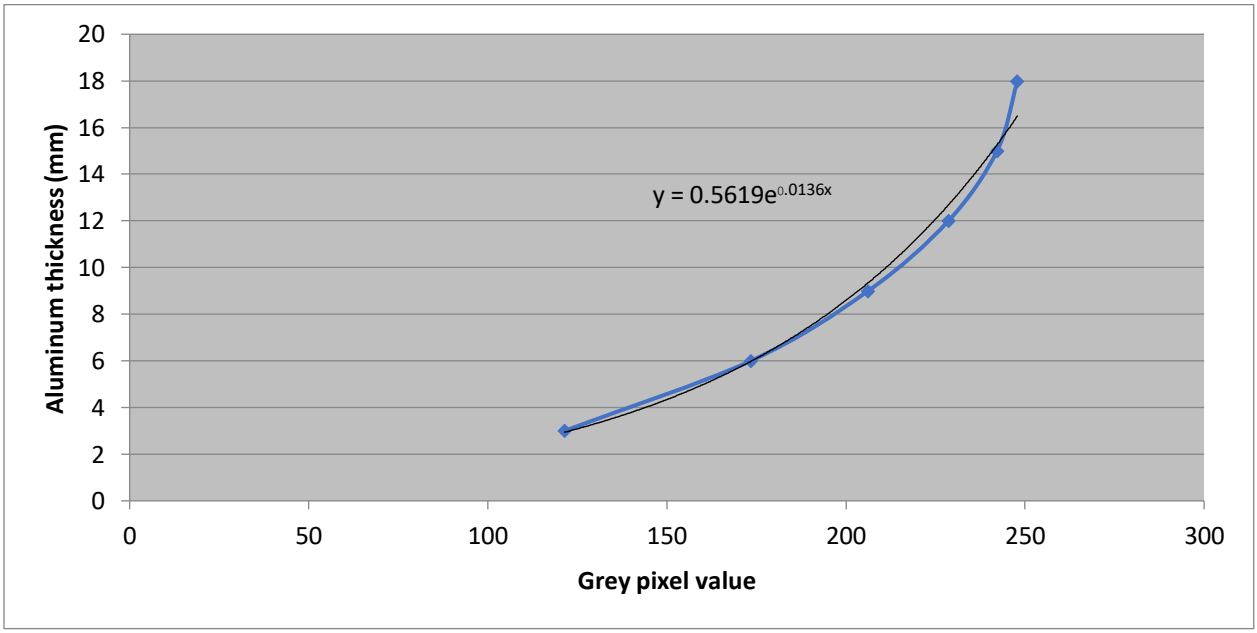

Figure 10: Graph between Aluminium thickness and grey pixel value. *A grey pixel value of Aluminium step-wedges is plotted in a blue graph, whereas the trendline is plotted in a black graph*

2.3 Root canal obturation of natural teeth and root replicas

The 45 incisor and molar of both root replicas and natural teeth were randomly divided into nine groups depending on the sealer/cone used and obturation method (n = 5 per group) and were obturated as follows:

1. AH Plus
    1. Single-cone obturation
    2. Warm vertical compaction
2. BioRoot RCS
    1. Single-cone obturation
    2. Warm vertical compaction
3. Totalfill BC
    1. Single-cone obturation
    2. Single-cone obturation with bioceramic coated cone
    3. Warm vertical compaction
4. Bio-C
    1. Single-cone obturation
    2. Warm vertical compaction

For single-cone obturation groups, root canals were filled using the following protocol:

1. In the BioRoot RCS group and AH Plus group, the sealer was prepared according to the manufacturer's instructions. Then, the sealer was delivered into the canal using the master cone and distributed within the canal using a back and forth motion. This step was repeated until the sealer was inundate out of the orifice.
2. For sealers that were presented in a proprietary syringe (Totalfill BC and Bio-C), the tip of the syringe was inserted to 2 mm short of the WL and the sealer was expelled whilst the syringe was withdrawn with a slow backward movement until the canal was filled.

3. A matched ProTaper GP cone was coated with sealer and slowly inserted in one movement until it reached the WL.
4. To establish the coronal seal, excess GP was cut to 4 mm below the orifice with a heating device (EQ-V, Meta Biomed, Chungcheongbuk-do, Republic of Korea) to create a space for glass ionomer cement (ChemFil® Superior, Dentsply DeTrey, Konstanz, Germany). While still warm, the coronal GP was compacted vertically using a No. 4 hand plugger (Dentsply Maillefer, Surrey, UK).

For warm vertical compaction groups, root canals were obturated using the following protocol:

1. Heat carriers and pluggers were inserted into the canal at 4 mm above the WL prior to obturation to check the best fitting size.
2. Sealers were inserted into the canal and the master cone seated as previously described. The heat was applied to a heat carrier that fitted tightly into the empty canal 4 mm from the WL.
3. When the heat carrier indicated 200 °C, it was driven into the GP with apical pressure.
4. When 2 mm above the binding point of the selected heat carrier was reached, the heat was removed, but apical pressure maintained until the carrier reached the binding position. The heat was reapplied and the heat carrier was then rotated around its axis and immediately removed from the canal, removing coronal GP.
5. While still warm, the GP was compacted vertically with the selected hand plugger.
6. The remainder of the canal was filled with GP using a backfill device (EQ-V, Meta Biomed, Chungcheongbuk-do, Republic of Korea) at 200 °C in one continuous movement for the back-packing stage until the GP reached the orifice. While still warm, the GP was

compacted vertically with a No. 4 hand plugger until the coronal level of the GP was at 4 mm below the orifice.

All procedures were carried out with magnification (x4) with maximum brightness from a dental LED headlight.

After completion of the root canal obturation, the coronal seal was established by filling the orifice with 4 mm of glass ionomer cement. The external root surface was cleaned with a gauze soaked with distilled water. For the control group, two teeth from each tooth type were used. Their orifices were filled with 4 mm of glass ionomer cement without root canal obturation. All teeth were stored in 1.5 mL HBSS at 37 $^{\circ}$C incubator. The gaps and voids volume percentages calculations were performed immediately after obturation and after 3 and 6 months after storage in HBSS.

2.4 Effect of temperature, object position and moisture levels on accuracy of µCT analysis of natural and polymer teeth.

Testing parameters, such as fluctuations in machine temperature, tooth positioning and the moisture conditions of the specimens, could affect the µCT measurements. In order to assess this a pilot study was designed to determine how these parameters affected the readings of the µCT. Five human lower premolars extracted for orthodontic and periodontal reasons were selected and prepared using the same protocol for the incisors described previously (2.2.1). These teeth and five polymer incisors were used to determine the effect of the moisture on the µCT calculation. Ten polymer incisors were used to determine the effect of the temperature and tooth position on the µCT calculation because they were insensitive to moisture.

2.4.1 Testing the effect of temperature on the precision of µCT

The µCT machine was warmed up for 3 hours at 11 µm intervals, using an accelerating voltage of 70 kV at 140 mA and medium camera pixels (2K x 1K). After that, a thermocouple device (data logger model TC-08, Pico® technology, Saint Neots, UK) was used to measure the temperature inside the µCT machine by continuously recording every second for five hours. The µCT machine was operated in two different ways:

1. Interrupted scan: the X-ray beam was stopped every 53 mins, the µCT chamber was opened for 1 min, then closed and the X-ray beam was started again. This method was repeated five times.
2. Continuous scan: the X-ray beam was used continuously without opening the µCT chamber. µCT parameters were the same as the interrupted scan except the software was set to continuous scan for 5 cycles.

The interrupted scan temperature was used to represent the temperature during measuring the gaps and voids volume percentage in this study. 53 mins was the scanning time for one cycle when using the parameters described above. The µCT chamber was opened for 1 min to represent the time used for changing the sample during each scan. The continuous scan temperature was used to compare the fluctuation rate of the temperature with the interrupted scan to test the hypothesis that the temperature measuring during the continuous scan was stable. This mode was used for testing the position effect described in 2.4.2 to eliminate the temperature that could affect the measurement.

The initial, maximum and average working temperatures were recorded by Picolog version 6.1.14 software (Pico® technology, Saint Neots, UK). 3DPT polymer teeth acclimatized at the temperature

measured inside the machine were tested. Furthermore, teeth kept at room temperature were scanned, were placed in incubator at 37 °C and rescanned were also tested. The temperature of the teeth was measured with the same thermocouple. Silicone putty was used as a mould to stabilise and fix each tooth's position on the µCT base before scanning. Five teeth were used for each temperature tested and the scanning was repeated five times.

All scanned images were reconstructed using NRecon software (ring artefact reduction = 13, beam-hardening correction = 20% and dynamic image range from 0.001 to 0.05) and saved in a .tiff file format. All reconstructed images were imported into Dataviewer software (Bruker, Billerica, MA, USA). The 3D-registration method was used to overlap two images from different scans together. The same tooth position between each scan was confirmed by completely overlapping between each image. After that, only apical to middle-third reconstructed images were imported into ImageJ.

In order to calculate root canal volume, the scale was calibrated according to the µCT setting (one pixel = 0.011 mm). Then, the wand tracing tool was used together with the 3D measure stack plugin to locate the outline of the root canal. The threshold of the tool was set to 22 and the slice spacing was set to 0.011. These procedures were used to calculate the root canal volume of all the teeth used in the preliminary study.

2.4.2 Testing the effect of tooth position on the precision of µCT

Five 3DPT polymer teeth were stored in an incubator at an average working temperature within the µCT measured previously and confirmed using the thermocouple device. Silicone putty was used as a

mould to fix the tooth's position and stabilise it to the µCT base. A tooth was continuously scanned at 11 µm intervals, using the same parameters as previously described (2.4.1) for 5 cycles. After scanning was complete, the tooth was kept in an incubator again until its temperature was equal to the average working temperature of the µCT. This method was repeated five times to generate an identical tooth position using the same silicone putty mould.

Then, both tooth position and angulation were altered by purposefully placing the tooth in a completely different orientation on the µCT platform each time. The tooth was fixed with silicone putty in the new position and scanned again with the same parameters as before. After scanning was complete, the tooth was stored in an incubator again until its temperature was equal to the average µCT working temperature. This method was repeated five times with different tooth positions and angles between each scan.

All scanned images were reconstructed using NRecon software (ring artefact reduction = 13, beam-hardening correction = 20% and dynamic image range from 0.001 to 0.05), saved to .tiff file format and imported into Dataviewer software. Tooth position was adjusted with a 3D-segmentation method, where the first scanned tooth image was imported as a reference, whilst another tooth image was imported as the target image. The target image was adjusted until it completely overlapped the reference image before exporting the adjusted image in a .tiff file format. The root canal volume of the initial position, altered position and software-adjusted position were calculated with ImageJ, as described previously (2.4.1).

2.4.3 Testing the effect of moisture on the qualitative analysis of µCT

Five 3DP polymer incisors and five natural human lower premolar teeth were immersed in tap water at room temperature. The weight of teeth was used as an indicator for the moisture change. Teeth were immersed in the water and their weight was measured every day until it was stable to at least two decimal places (fully hydrated). Then, silicone putty was used as a mould to fix the tooth's position and stabilise it to the µCT base. Teeth were scanned five times at 11 µm intervals using the same conditions as described previously (2.4.1) and stored at room temperature for seven days. Teeth were weighed again before fixing individual teeth back onto the silicone mould and scanning again using the same parameters. Finally, teeth and silica gel were stored in a desiccator and teeth were weighed each day until their weight was stable (complete dryness). Each tooth was fixed back onto the silicone mould and scanned again using the same parameters.

All scanned images were reconstructed using NRecon software (ring artefact reduction = 13, beam-hardening correction = 20% and dynamic image range from 0.001 to 0.05) and saved to a .tiff file format. Dataviewer software was used to confirm a similar tooth position between each scan. The root canal volume of the fully hydrated, room-conditioned and thoroughly dried roots were calculated with ImageJ as described previously (2.4.1).

2.5 Gaps and voids volume percentage calculation of obturated roots

Obturated roots were scanned with µCT using the same parameters as described for pre-obturation immediately after

obturation. All post-obturation scanned images were reconstructed using NRecon software with the same parameters described in 2.4.1 and saved as .tiff file format.

All images were loaded into Dataviewer software and 3D-image registration of post-obturation images was carried out using pre-obturation images as references. The post-obturation image was adjusted until it completely overlapped the reference image, before exporting the adjusted image as a .tiff file format.

Images within 16 mm from the WL were used to calculate the total gaps and voids volume percentage in the incisor group, while images within 12 mm from the WL were used to calculate the molar group. Total gaps and voids volume percentages were assessed with CTAn software using the following method:

To determine thresholding range for type of sample, a cross-sectional image was randomly picked and was zoomed to the highest magnification allowed by the software. The thresholding range was selected by slowly adjusting the value until it gave a black and white image, which visually had an identical outline to the original image. A threshold value was tested again with different cross-sections and different teeth in the same group to confirm the correct value.

Thresholding ranges from 150−255 were used to calculate the filling volume for the single-cone group and single-cone part of the warm vertical compaction group. In contrast, thresholding from 130−255 was used to calculate the volume of warm GP in the warm GP group.

Thresholding from 0−150 was used to calculate the gaps and voids volume percentages in the single-cone group and single-cone part of the warm vertical compaction group. In contrast, thresholding from 0−130 was used to calculate the gaps and voids volume percentages in the

warm GP area of the warm GP group. Finally, the region of interest (ROI) was identified, following the outline of the gaps and voids area.

The total percentage of gaps and voids volumes was calculated and compared between each group by these equations:

$$\%Gap\ volume = \frac{gap\ volume}{canal\ volume} \times 100$$

$$\%Void\ volume = \frac{void\ volume}{canal\ volume} \times 100$$

$$Canal\ volume = gap\ volume + void\ volume + filling\ volume$$

To imitate the periodontal ligament, collagen-agarose gels containing 1 mg/mL of collagen and 1% w/v agarose were prepared by adding 3 g of agarose (Bioline, London, UK) into 2.6 mL of HBSS and microwaving for 30 s. If the gel did not dissolve completely, it was reheated in a microwave oven again for another 30 s. Then, 0.3 mL of 10% collagen (FibriCol®, Advanced BioMatrix, San Diego, CA, USA) was added to the agarose gel. Finally, 0.03 mL of 0.1N NaOH was used to adjust the pH of the gel to 7.4.

After a 3D-scan was completed, the external root surfaces of natural teeth were coated by dipping the teeth into the gel until a total thickness range between 0.1 and 0.4 mm of the gel was achieved to mimic the PDL. Gel thickness was confirmed using a stereomicroscope (Dino-Lite Edge AM4115ZT, Chosen Technology, Bangkok, Thailand). After the gel had polymerised, the teeth were immersed in HBSS and were stored in an incubator at 37 ^{o}C.

After 3 and 6 months, the collagen-agarose gel was removed from the tooth surface. Then, teeth were scanned, reconstructed and 3D-segmented using the same methods as before to enable calculation of gaps and voids volume percentages, as described previously. Finally, the

tooth was coated with gel and immersed in HBSS in an incubator at 37 ^{o}C. The percentage of gaps and voids data obtained immediately after obturation was compared with 3 months and 6 months data.

2.6 Leachate analysis

Two teeth from each tooth type (natural incisor, natural molar, polymer incisor and polymer molar) were used as the control group. The orifices of these teeth were filled with 4 mm of glass ionomer cement and the roots were coated with collagen-agarose gel as described in 2.5. The control group was immersed in HBSS in an incubator at 37 ^{o}C at the same time as the experimental groups.

After 3 months' immersion of teeth in HBSS, 1 mL HBSS from two samples from each group were collected and diluted 10-fold. Leachate analysis was performed using inductively coupled plasma mass spectroscopy (Optima 8000; Perkin Elmer, Waltham, MA, USA). Argon was used as the plasma gas with a flow rate of 8 mL/ min and 1,300 wattage. The samples' flow rates were 1.0 mL/ min. The amount of calcium ion from each group was calculated using the following equation:

$$Net\ calcium\ ion\ (ppm) = 10 \times (Calcium\ ion_t - Calcium\ ion_c)$$

Where: $Calcium\ ion_t$ represents the amount of calcium ion from each group;

$Calcium\ ion_c$ represents the amount of calcium ion from the control group.

Another 1 mL of HBSS was added back to the tooth containers to immerse the tooth. All sample was kept in an incubator at 37 ^{o}C. These

methods were repeated with the other three samples from each group at six monthly periods.

2.7 Statistical analysis

All statistics were performed using SPSS software version 23 (IBM, North Castle, NY, USA). Material characterisation, HA 3DPT characterisation and leachate analysis were analysed using descriptive statistics. A Kolmogorov−Smirnov test was used to test the normality of the data. A confidence interval for intraclass correlation for kappa measurement was used to calculate the amount of sample used for intraclass correlation coefficient (ICC) calculation (confidence level; $1-\alpha = 0.95$, 2-sided, number of raters; $k = 2$, expected interclass correlation; $\rho = 0.8$ and distance from correlation to limit; $\omega = 0.2$). Intrarater reliability was calculated by using ICC with 14 samples at a 2 weeks' interval.

The Wilcoxon signed-rank test was used to test the effect of the temperature of the tooth on the precision of µCT. The Friedman test was used to test the effect of the moisture and the position of the tooth on the precision of µCT. The mean of the canal volume between each group in the same tooth type was compared using one-way analysis of variance (ANOVA) test and post hoc Tukey analysis.

The percentage of gaps, voids and gaps and voids volumes at each period (immediately after obturation, 3 months and 6 months) were compared between different sealers using Kruskal−Wallis test and Dunn−Bonferroni analysis. The percentage of gaps, voids and gaps and voids volumes from the same sealer group at the different periods were compared between each sealer using the Friedman test and Dunn-Bonferroni analysis.

CHAPTER III

RESULTS

3.1 Material characterisation

The 2,000x backscattered images of each sealer are shown in Figure 11. AH Plus was composed of discrete particles of different opacities made up of zirconium and tungsten embedded in a carbon-rich matrix. BioRoot RCS, Totalfill BC and the Bio-C were composed of numerous calcium-rich particles with zirconium particles scattered within the cement matrix. The particle size found in AH Plus and BioRoot RCS was approximately 2-10 µm, whilst in Totalfill BC was approximately 4-15 µm. The smallest particle size among all of the sealers was found in Bio-C (approximately 1 µm).

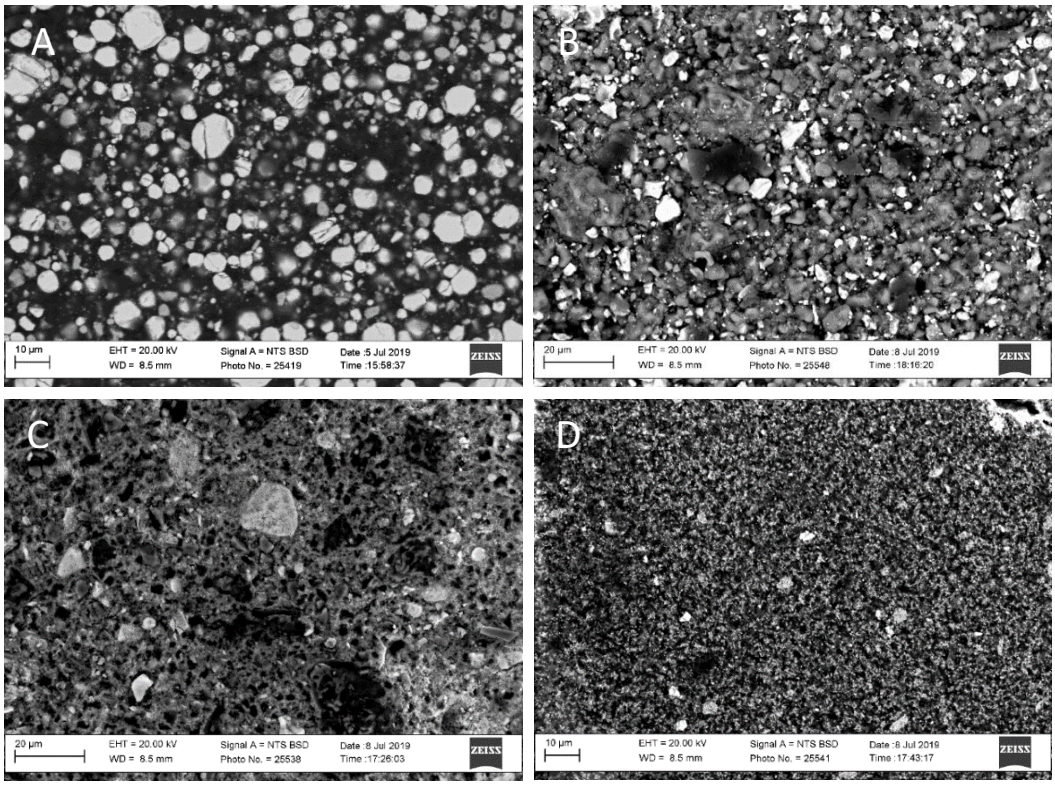

Figure 11: Backscatter images at 2,000x; *A: AH plus, B: BioRoot RCS, C: Totalfill BC and D: Bio-C sealer*

The elements found in all the sealers included calcium and zirconium. The type and mean weight fraction of the ion in each sealer are shown in Table 2 and Figure 12. The highest mean percent weight fraction of calcium was found in the BioRoot RCS group (23.78%) followed by Totalfill BC (9.74%), Bio-C (4.32%) and the AH Plus group (2.53%), respectively. Tungsten was found only in the AH Plus group, whereas silicon was found only in the HCSC-based sealer group. The highest mean percent weight fraction of silicon was also found in the BioRoot RCS group (6.48%) followed by Totalfill BC (2.93%) and Bio-C (1.18%).

Table 2: Mean percentage of weight fraction of element found in the sealers (%±SD) (n=3). *Calcium, oxygen and zirconium are the common elements found in all sealers*

	AH Plus	BioRoot RCS	Totalfill BC	Bio-C
Calcium	2.52±0.47	23.78±2.94	9.47±0.81	4.34±2.67
Zirconium	10.85±0.49	16.97±1.50	24.3±1.98	17.25±5.68
Tungsten	12.68±2.42	0	0	0
Silicon	0	6.48±0.71	2.93±0.20	1.18±0.57

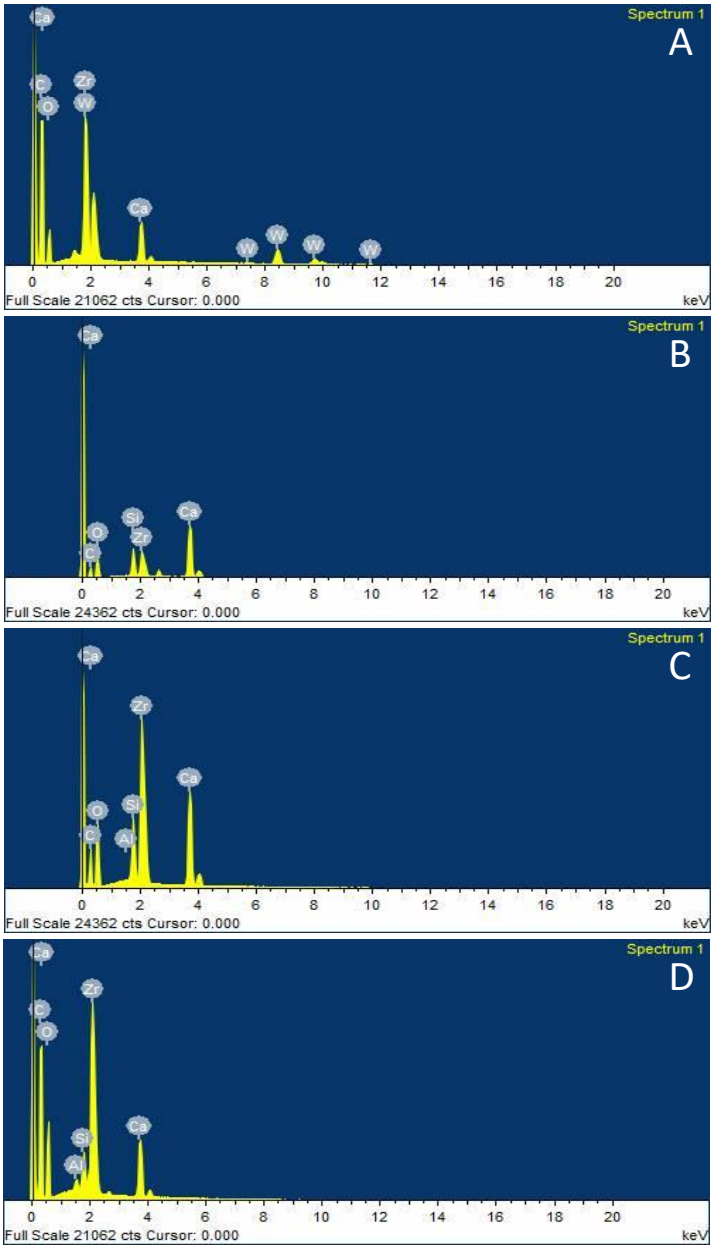

Figure 12: EDS analysis of the sealers; *A: AH Plus, B: EDS analysis of BioRoot RCS, C: EDS analysis of Totalfill BC and D: EDS analysis of Bio-C. Calcium and Zirconium were the common element found in all sealers. Silicon was found in all BioRoot RCS, Totalfill BC and Bio-C. Tungsten was found only in the AH Plus*

The 2,000x backscattered images of GP cones, GP pellets and BC cones are shown in Figure 13. At room temperature, warm pellet GP injected from heated device had a smooth external surface, whereas the

matched ProTaper Gold GP cones and BC cones showed numerous crystals deposited on the surface.

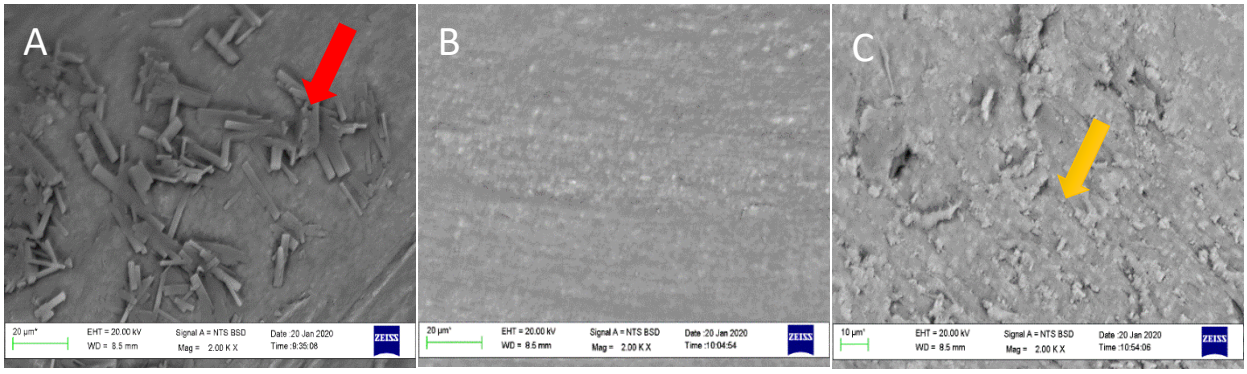

Figure 13: Backscatter images at 2,000x; *A: matched GP cone. The surface composed of rod shape of zinc oxide crystal size ≈ 20x0.3 µm (red arrow), B: Warm GP. The surface was smooth and C: BC cone. The surface composed of submicron size calcium crystal (yellow arrow)*

The type and mean weight fraction of the elements for the GP are shown in Table 3 and Figure 14. Zinc was the most frequently identified element in each type of GP. Barium was found in the matched ProTaper Gold GP cones and warm GP. Silicon and zirconium were found only in the BC cones. Calcium was found in the warm GP and BC cones.

Table 3: Mean percentage of weight fraction of element found in GPs (%±SD) (n=3). *Zinc was the most abundant element found in all GP.*

	Match GP cone	GP pellet (warm GP)	BC cone
Zinc	35.57±11.62	61.21±22.73	38.24±8.65
Calcium	0	0.37±0.64	0.74±0.77
Silicon	0	0	0.32±0.28
Barium	9.57±2.85	9.58±1.17	0
Zirconium	0	0	11.00±9.93

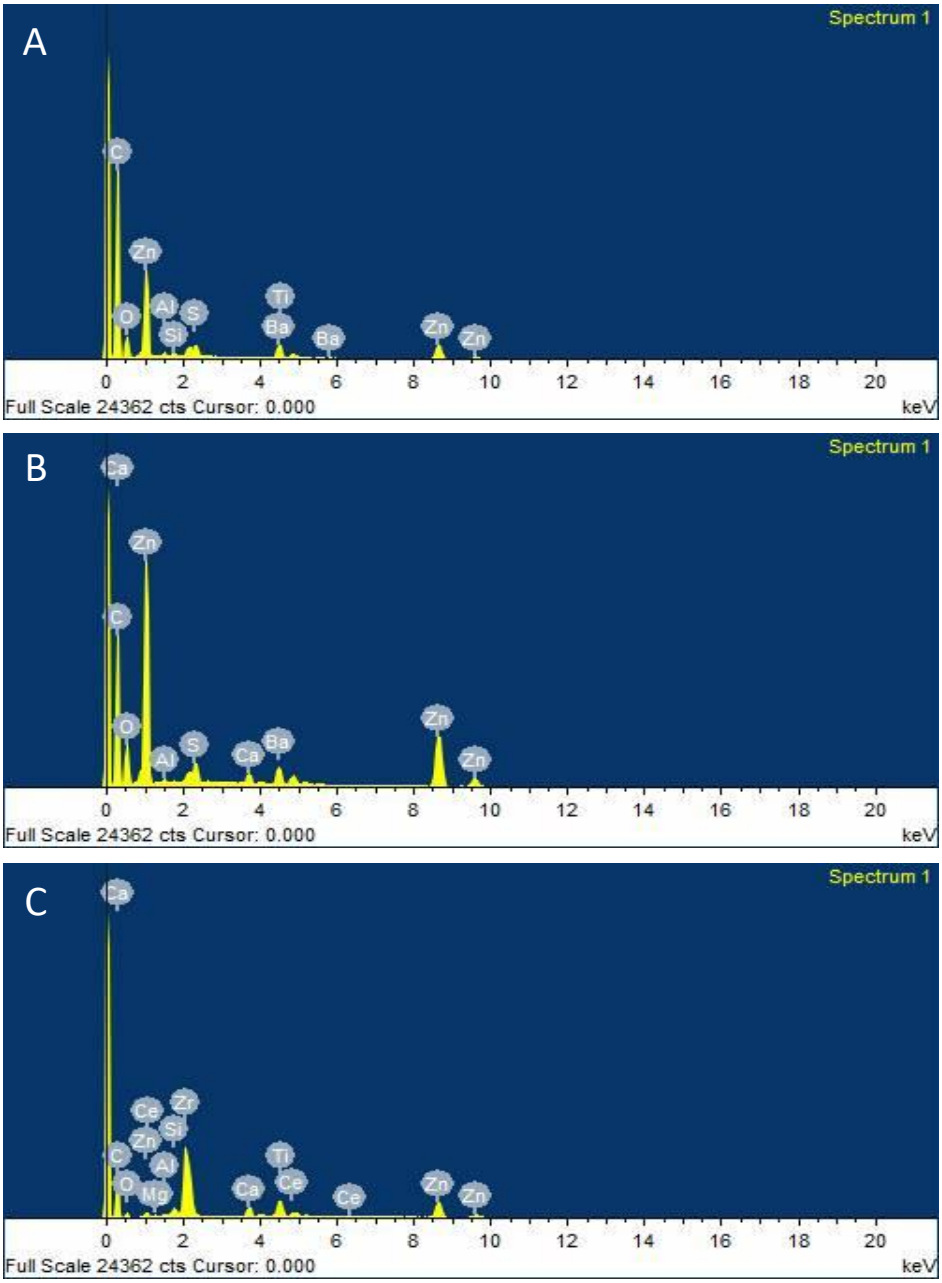

Figure 14: EDS analysis of the GP; *A: matched GP cone, B: Warm GP and C: BC cone. All sealer composed of zinc which is the main composition of the GP. Barium was found in the matched GP cone and warm GP whereas zirconium was found in BC cone. Calcium was found in warm GP and BC cone. Silicon was found only in the BC cone*

3.2 HA-3DPT characterisation

A SEM micrograph (8,000x) of the HA powder used in printing is shown in Figure 15. The HA powder was in a cluster of needle-like crystals with a homogeneous crystal size range from 0.2-0.5 µm, approximately.

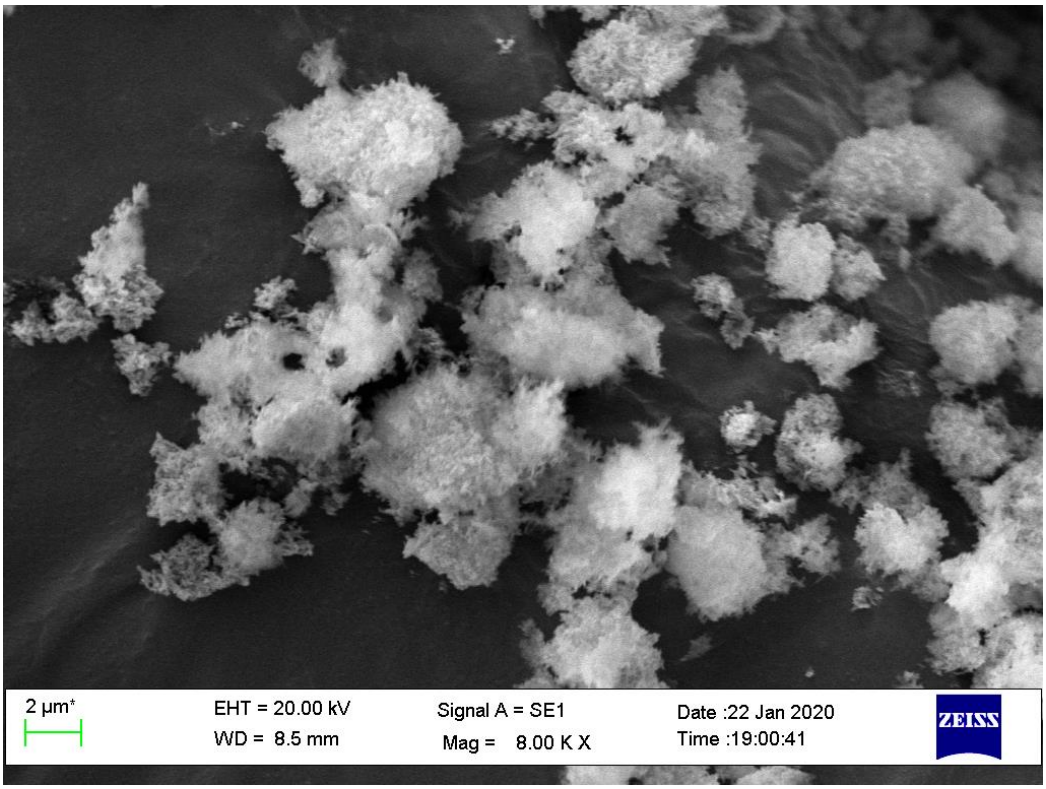

Figure 15: SEM image of the HA powder at 8,000X. *HA powder is in a cluster of needle-like crystal form size range from 0.2-0.5 µm*

3.3 Testing of HA slurry

The final composition of 40% solid loading of HA slurry was HA; resin; dispersant; photo-initiator equal to 4: 2: 3.95: 0.05, whereas 45% solid loading of HA slurry was HA; resin; dispersant; photo-initiator equal to 4.5: 2: 3.45: 0.05. The slurry was mixed with a mechanical mixer for 5 mins. After mixing, it was kept in a light-tight container and was used within an hour after mixing.

The rheology tests of 40% and 45% HA slurry are shown in Figure 17. The viscosity of both slurries was reduced when the shear stress was increased (shear-thinning characteristic). This was similar to the reference Admatec alumina slurry. (Figure 16).

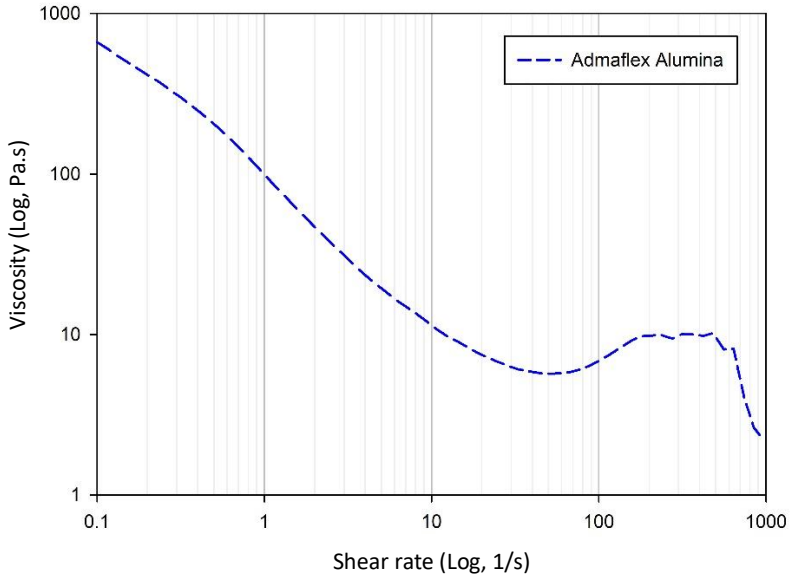

Figure 16: The rheology test of the Admatec alumina slurry (Log)*. A viscosity of the Admatec alumina lower when shear rate is increased (shear-thinning)*

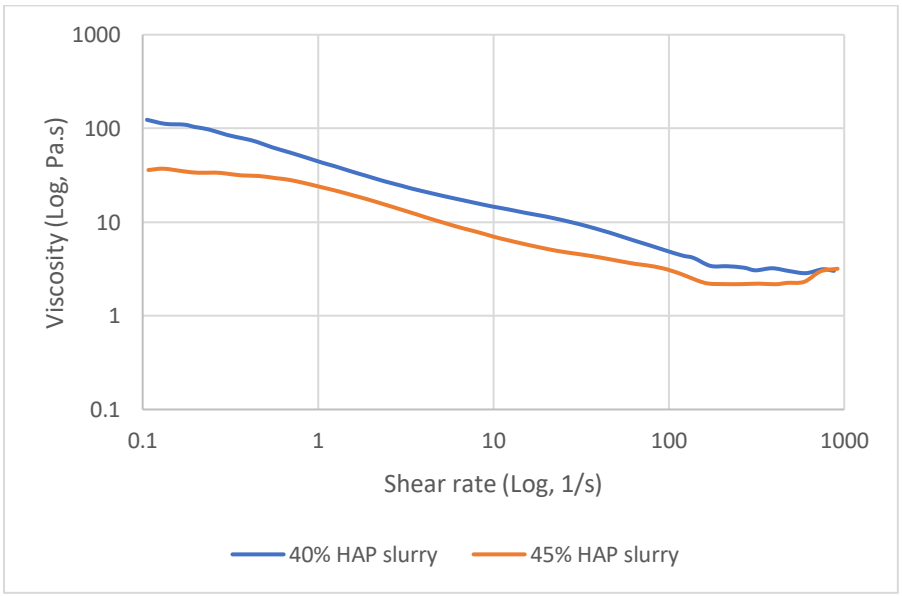

Figure 17: The rheology test of 40% and 45% HA slurry (Log). *A viscosity of both composition is lower when shear rate is increased (shear-thinning)*

The HA printed is shown in Figure 18 and 19A. The root surface was smooth and a base layer of the HA printed tooth comprised three different areas with a different microstructure (Figure 19B) The SEM images of the base layer of the printed root are shown in Figures 19B and 20. The outer area had a smooth surface whereas the inner area had a rough surface (Figure 20A and 20B). The canal-like area was agglomerated with fused HA crystals (Figure 20C and 20D).

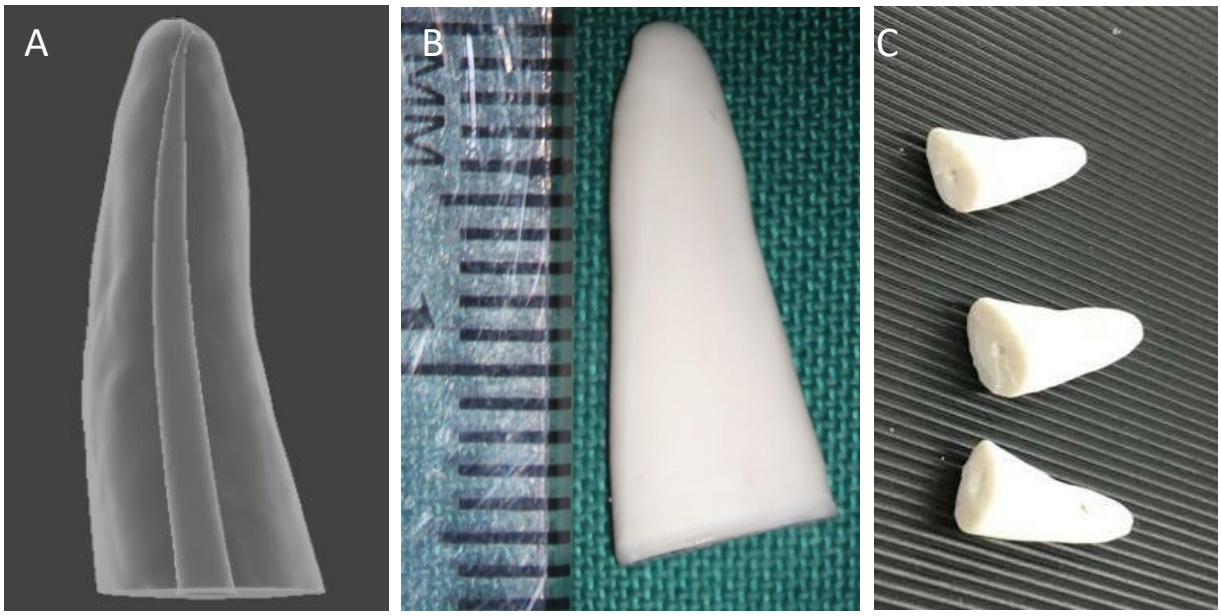

Figure 18: HA printed root. *Note the resemble of the external shape between the HA-3DPT and the digital model*

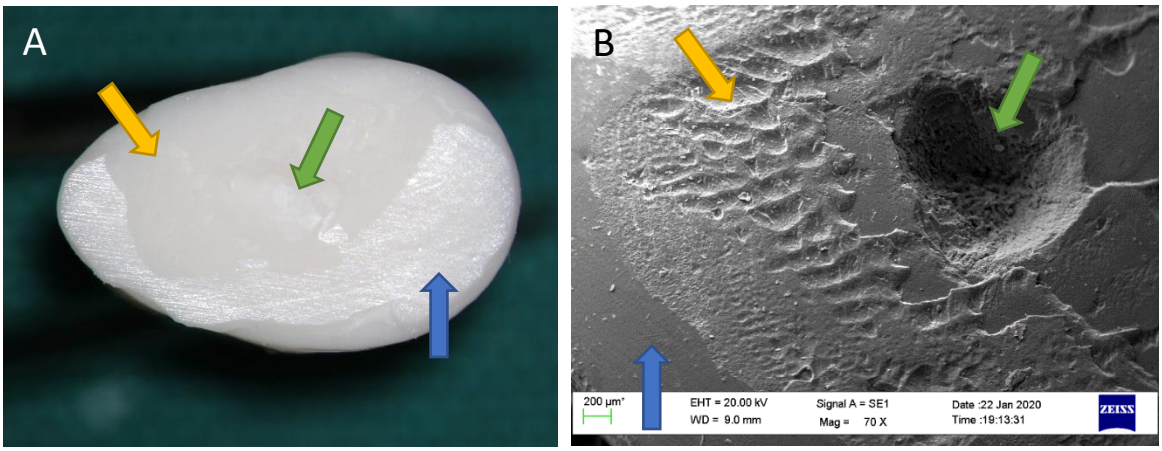

Figure 19: Macroscopic and microscopic appearance of HA printed tooth; *A: a base layer of HA printed tooth made up of a glossy area (blue arrow), matte area (yellow arrow) and root canal-like area (green arrow) and B: SEM image of the base layer of HA printed tooth at 70x*

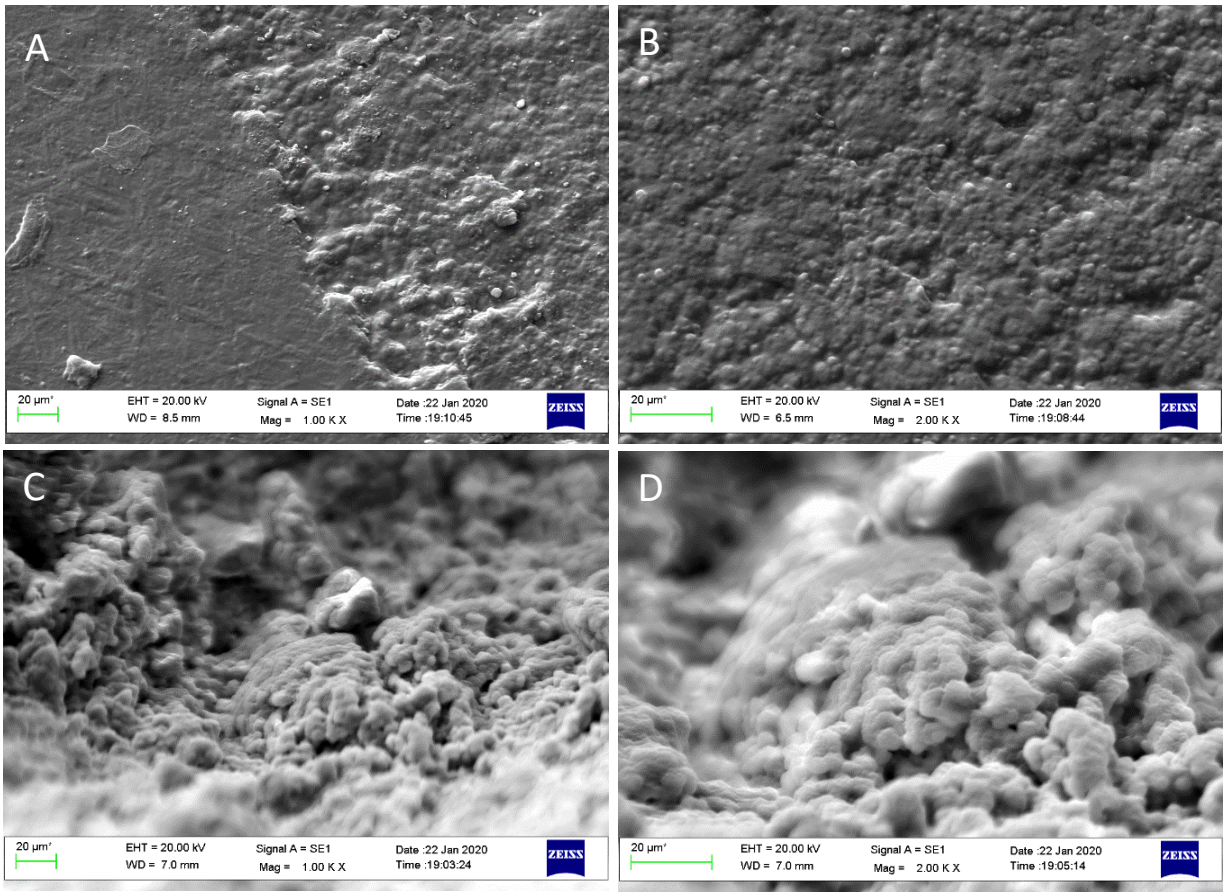

Figure 20: The SEM images of the HA printed tooth*; A: at the junction between the outer smooth area and the middle rough area (1,000x), B: at middle area at 2,000x, C: at innermost area at 1,000x, and D : at the innermost area at 2,000x. The middle and innermost area were composed of fused-globular HA crystral.*

The radiopacity of the HA printed root is 2.30 mm of aluminium, whereas the radiopacity of the HA disc is 1.25 mm of aluminium (Figure 21).

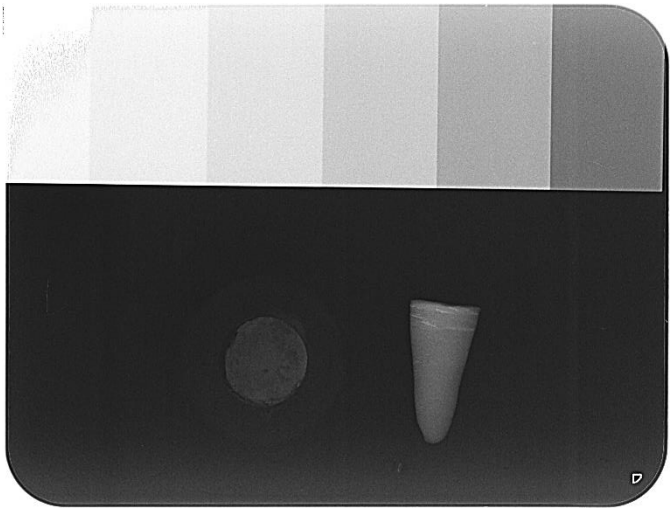

Figure 21: Radiopacity of HA printed root and HA disc compared with the aluminium step wedge. *The radiopacity of HA printed root and the HA disc was approximately equivalent to 2 and 1 mm of aluminium thickness, respectively*

3.4 Effect of temperature, object position and moisture levels on accuracy of µCT analysis of natural and polymer teeth.

The intraclass correlation coefficient for measuring the root canal volume twice at 2 weeks' interval was 0.95, which indicated very close agreement between both measurements.

3.4.1 The effect of temperature on the precision of µCT

The working temperature from a non-continuous scan is shown in Figure 22. The average temperature during scanning was 23.84±0.67°C. The temperature tended to increase between each scan with an abrupt change in the temperature when a scan ended and the sample was changed to carry out another scan.

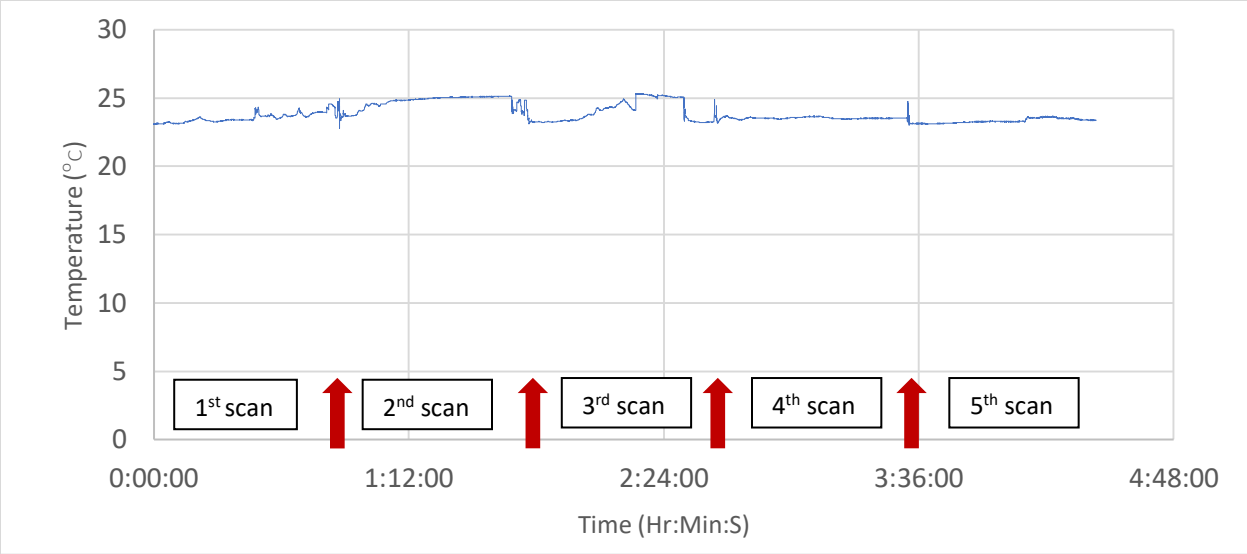

Figure 22: The µCT working temperature from a non-continuous scan. *Red arrows show the temperature when the µCT chamber was opened. Some temperature fluctuation is occurred during each scan with abrupt temperature change when the µCT chamber is opened*

The working temperature from a continuous measurement is shown in Figure 23. The maximum, minimum and average working temperature are 24.79, 23.29 and 24.46±0.21°C, respectively.

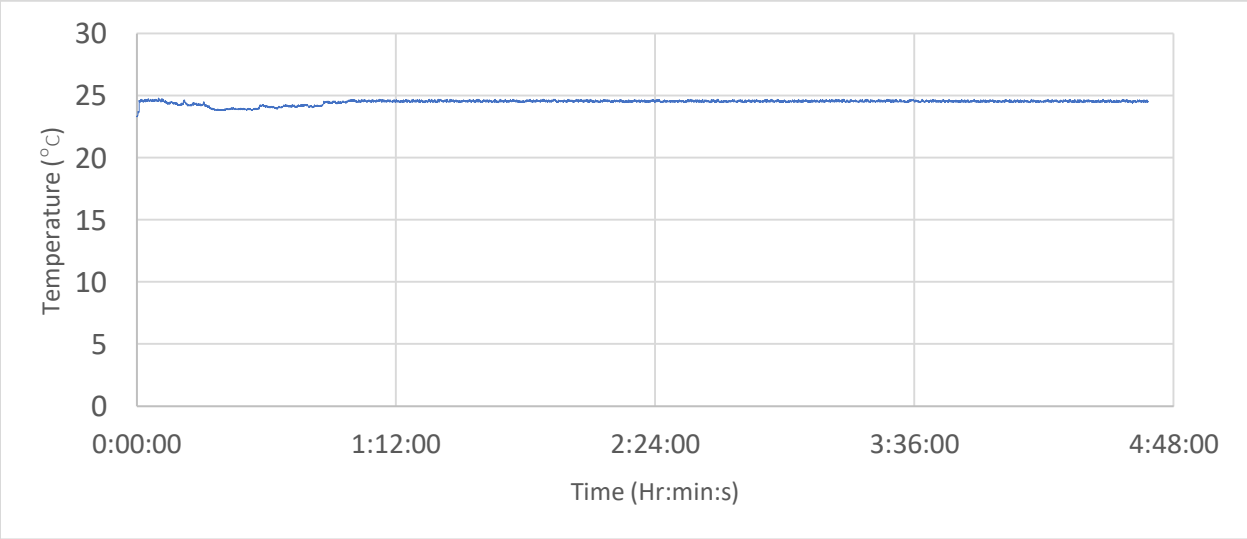

Figure 23: The µCT working temperature temperature from a continuous scan*. The temperature was stable approximately 50 min after initiating the µCT scan*

The mean root canal volume measured at 24 °C and 37 °C is shown in Figure 24. There was no significant difference ($p > 0.05$) in root canal volume measured at the two different temperatures.

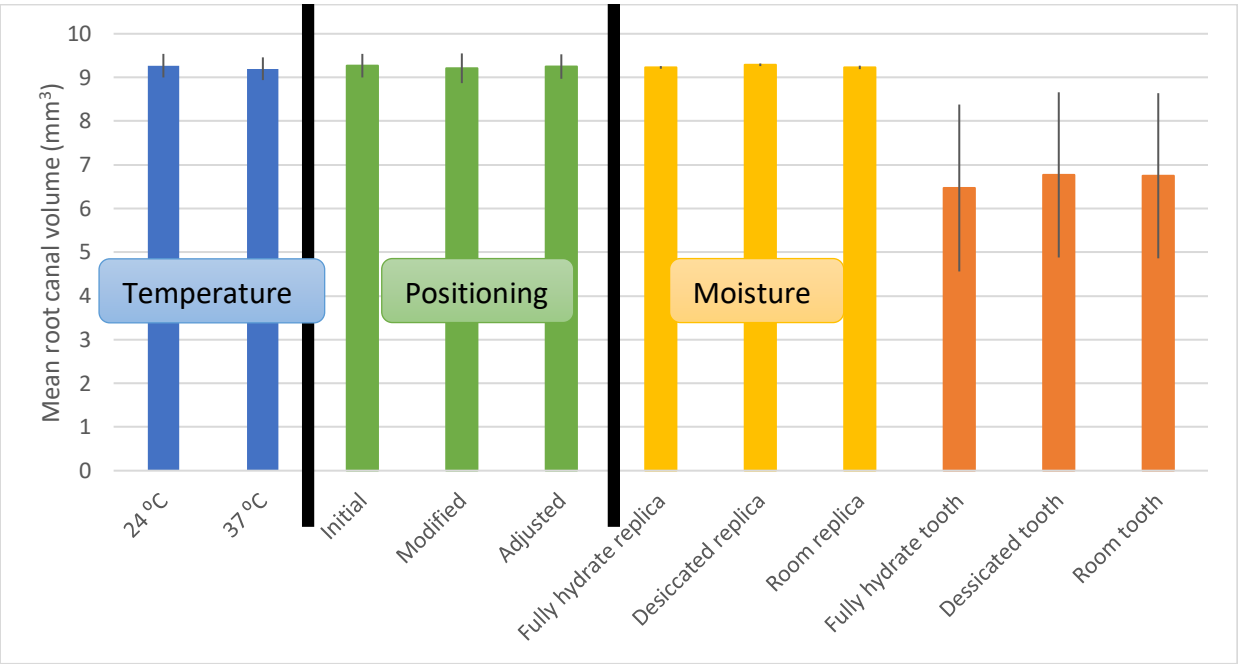

Figure 24: Mean root canal volume of natural teeth (mm³) (n=5). *There was no significant difference between the mean root canal volume at 24 °C and 37 °C (blue columns), between each position (green columns) and each moisture condition (yellow and orange columns).*

3.4.2 The effect of tooth position on the precision of µCT

The mean root canal volume at the initial, changed and software-adjusted position are shown in Figure 24. There was no significant difference ($p > 0.05$) in root canal volume between each position.

3.4.3 The effect of moisture on the precision of µCT

The mean root canal volumes of the room-conditioned, fully hydrated natural and polymer teeth and their complete dryness are shown in Figures 24. There was no significant difference ($p > 0.05$) in root canal volume among each moisture condition.

3.5 Gaps and voids volume percentages calculation

3.5.1 Natural incisor group

The mean empty root canal volume in the incisor group was 7.58 ± 1.41 mm^3. There was no significant difference ($p > 0.05$) among each group in the same tooth type.

Typical obturated roots are shown in Figure 25 and 27. The common gaps and voids areas were found at the lateral canals (Figure 26A and 28A), the junction between warm GP and matched GP cones (Figure 26B and 28B), inside the warm GP (Figure 28C) and within canal irregularities (Figure 26C and 28D). The mean gaps and voids volume percentages of each group are shown in Figure 33 and 35. The highest amount of the mean gaps and voids volume percentage was found in the Totalfill BC single-cone group immediately after obturation and the BioRoot RCS single-cone at three and six months, whereas the lowest amount of the mean gaps and voids volume percentage was found in the AH Plus WVC group at all times.

When comparing between each sealer from the same period, there were significant difference at three months between the AH Plus warm vertical compaction and the BioRoot RCS single-cone group ($p \leq 0.05$) and between the Totalfill BC cone and the BioRoot RCS single-cone group ($p \leq 0.05$) (Figure 33).

When comparing the same sealer at different time periods, there were significant differences between the AH Plus single-cone immediately after obturation and at 6 months ($p \leq 0.05$). Another significant difference was found in the BioRoot single-cone immediately after obturation and at 6 months ($p \leq 0.05$; Figure 33).

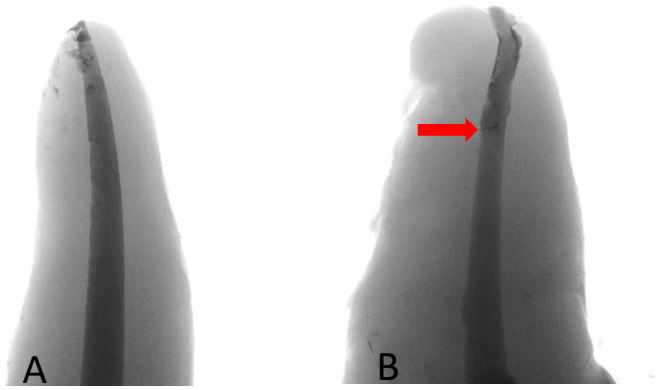

Figure 25: Inverted colour of the reconstructed images showing the typical µCT appearance of obturated natural incisors. *A: single-cone technique and B: WVC technique. Root canals are filled with root canal filling. Note the difference in radiopacity between the matched GP cone (darker) and warm GP (brighter) at the junction between warm GP and the matched single-cone (red arrow)*

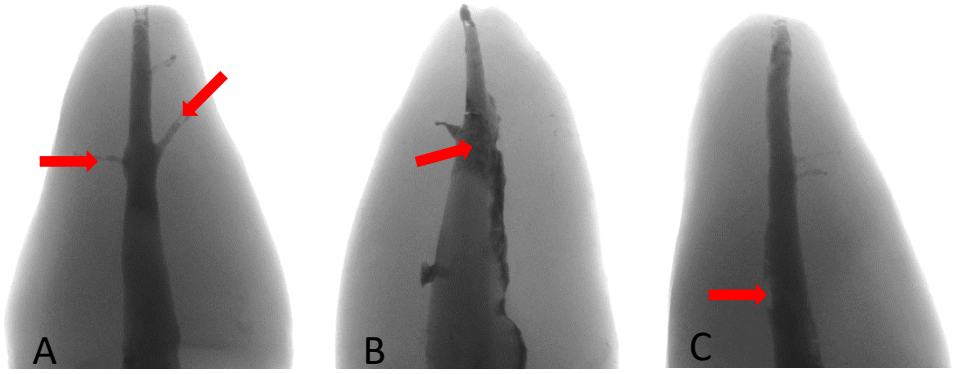

Figure 26: Inverted colour of the reconstructed images showing the typical gaps and voids areas found in obturated natural incisors (red arrows). *A: lateral canals, B: junction between the warm GP and the matched single-cone in WVC group and C: canal irregularity*

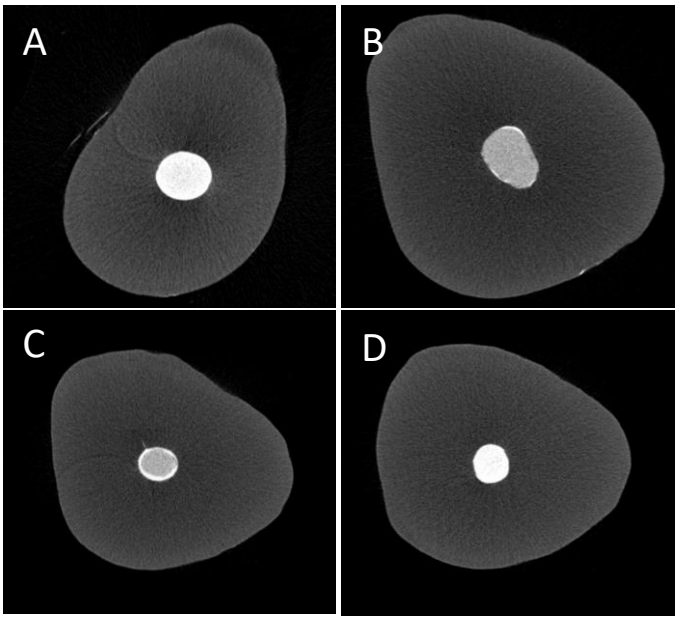

Figure 27: Cross-sectional images of obturated incisors *A: single-cone group, B: coronal part of WVC group, C: junction between the warm GP (grey) and matched single-cone (white) of WVC group and D: apical part of WVC group. Root canals were completely filled with filling materials. Note the difference in radiopacity between the matched GP cone (D) and warm GP (B) in WVC group*

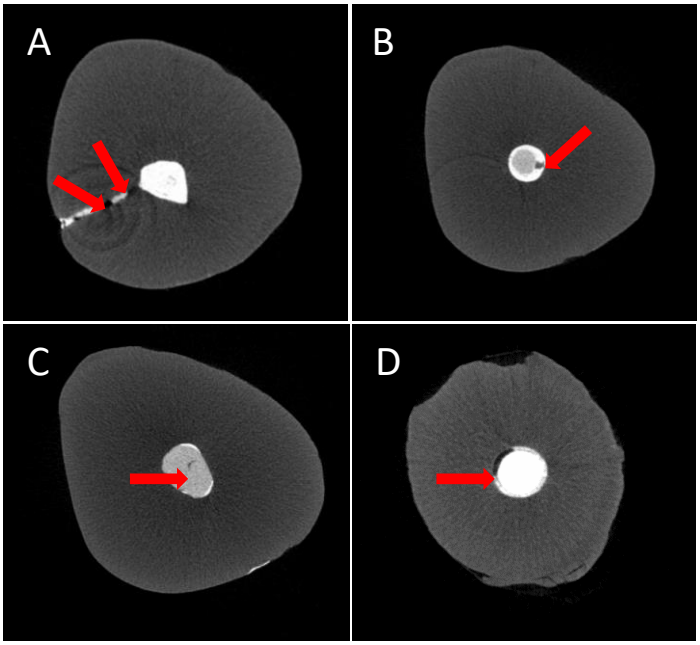

Figure 28: Cross-sectional images show the typical gaps and voids area found in natural incisors (red arrow). *A: gaps in a lateral canal, B: gaps at the junction between the warm GP and the matched single-cone, C: voids inside the warm GP and D: gaps at the canal irregularity*

3.5.2 Natural molar group

The mean empty root canal volume in the natural molar group was 9.21 ± 2.50 mm^3. There was no significant difference ($p > 0.05$) between each group for the same tooth type.

Typical obturated results are shown in Figure 29 and 31. The common gaps and voids areas were found at the isthmus (Figure 30A and 32A), the junction between warm GP and matched GP cones (Figure 30B and 32B), inside the root canal (Figure 30C and 32C) and within canal irregularities (Figure 30D and 32D). The mean gaps and voids volume percentage of each group was shown in Figure 34 and 36. The highest mean gaps and voids volume percentage was found in the BioRoot RCS single-cone group at all times. In contrast, the lowest mean gaps and voids volume percentage was found in the BioRoot RCS WVC group at all times.

There was no significant difference in the mean gap and void volume percentages ($p > 0.05$) when comparing between each sealer at the same time period. However, when comparing the same sealer at different times, there was a significant difference in the mean gap and void volume percentages immediately after obturation in comparison with 6 months after obturation of the AH Plus single-cone group ($p \leq 0.05$; Figure 33).

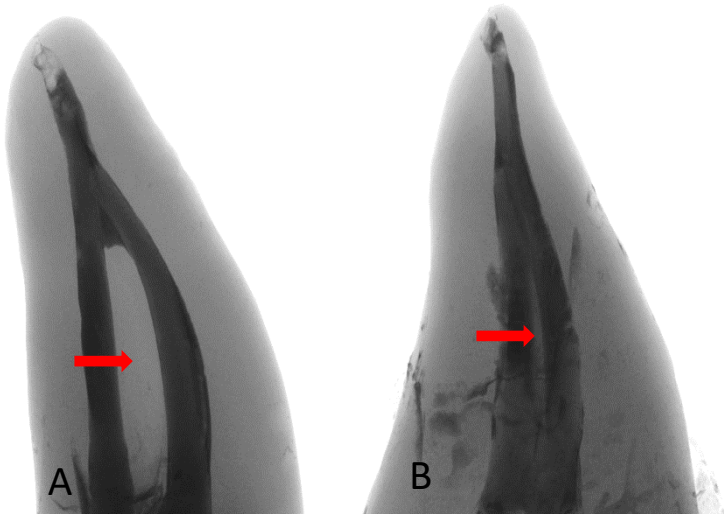

Figure 29: Inverted colour of the reconstructed images showing the typical µCT appearance of obturated molars *A: single-cone technique and B: WVC technique. Root canals are filled with root canal filling.*

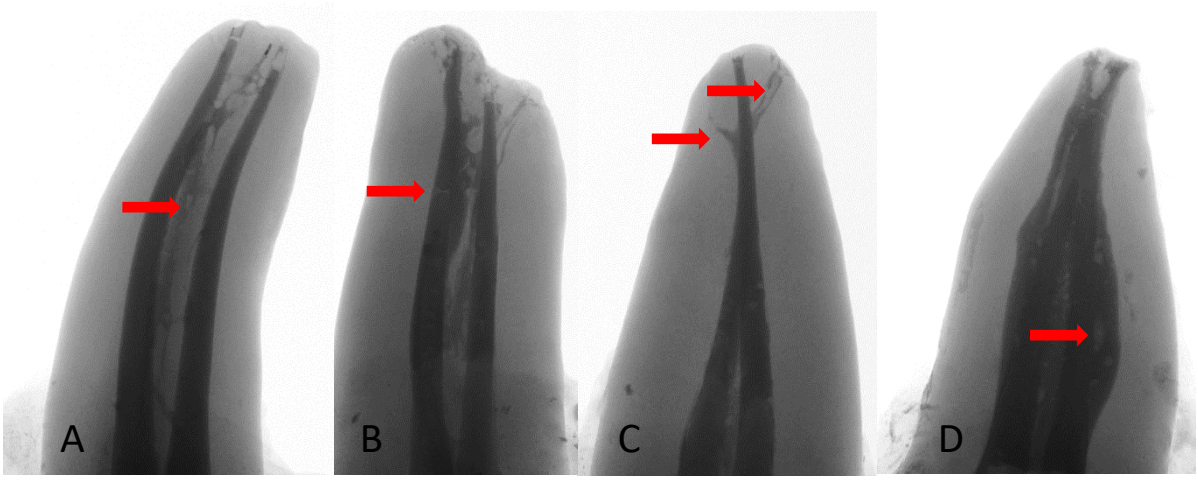

Figure 30: Inverted colour of the reconstructed images showing the gaps and voids areas found in obturated natural molars (red arrows). *A: isthmus area, B: junction between the warm GP and the matched single-cone in WVC group, C: lateral canal and D: canal irregularity*

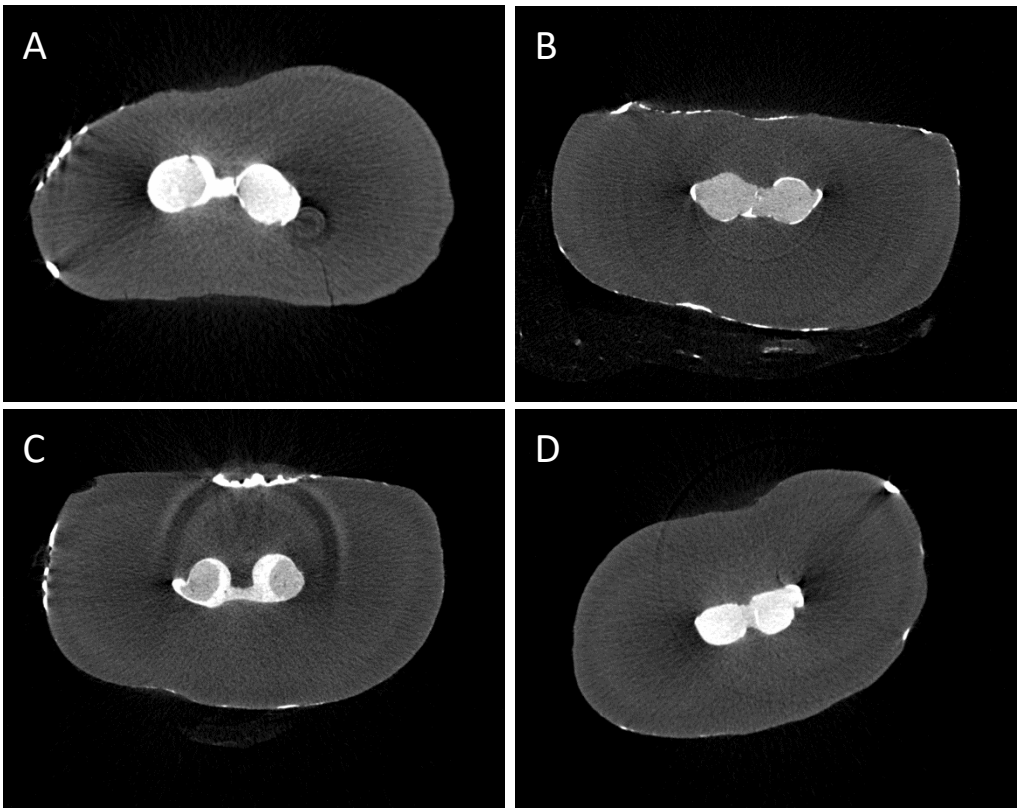

Figure 31: Cross-sectional µCT images of obturated natural molars *A: single-cone group, B: coronal part of WVC group, C: junction between the warm GP (grey) and matched single-cone (white) of WVC group and D: apical part of WVC group. Root canals were completely filled with filling materials. Note the difference in radiopacity between the matched GP cone (D) and warm GP (B) in WVC group*

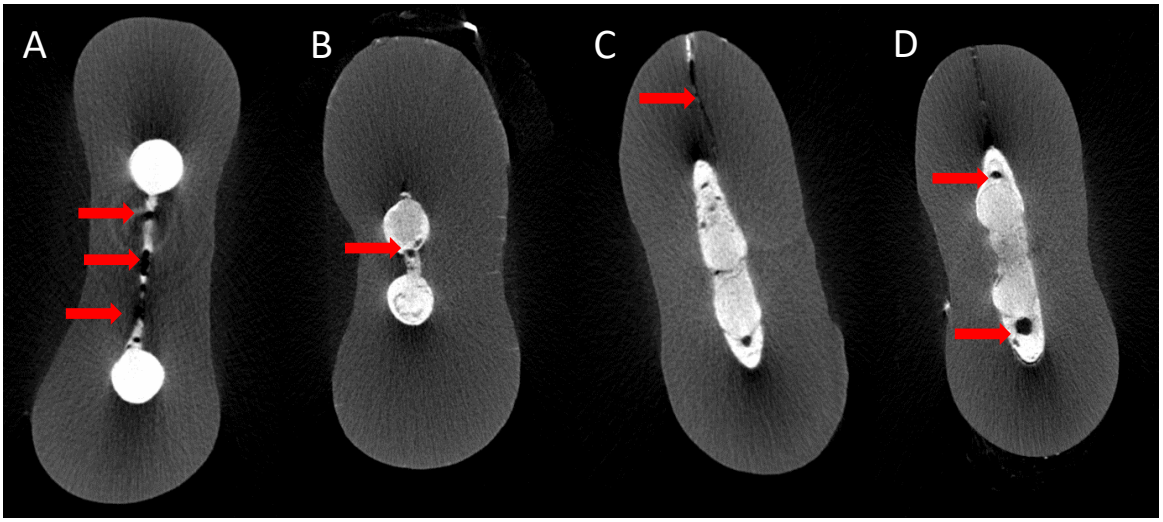

Figure 32: Cross-sectional µCT images show the gaps and voids areas found in obturated natural molars (red arrow). *A: gaps at the isthmus area, B: gaps at the junction between the warm GP and the matched single-cone, C: gaps at the lateral canal and D: gaps at the canal irregularity*

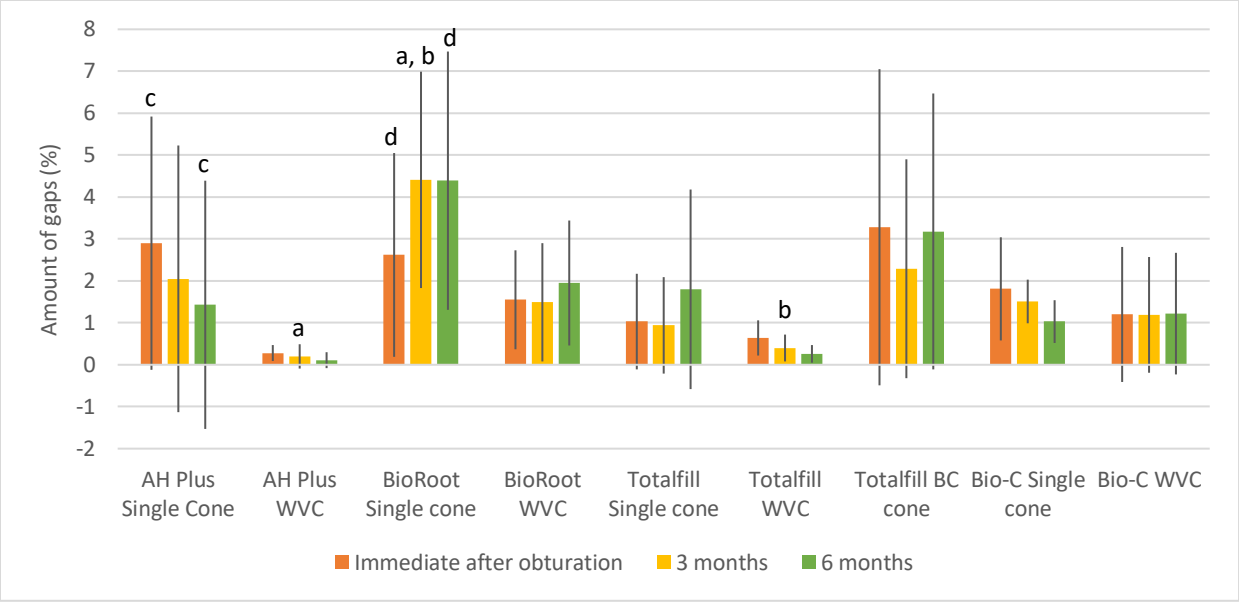

Figure 33: Mean percentage of gaps volume in natural incisors immediately after obturation, and also 3 months and 6 months later (n=5) (mean ± SD). *[a, b, c, d] The same letter indicates a significant difference (p < 0.05). When comparing the same sealer at different times, AH Plus and BioRoot RCS single-cones showed a significant difference immediately after obturation and 6 months later. When comparing different sealers all at 3 months, BioRoot RCS single-cones were significantly different from AH Plus WVC and Totalfill WVC groups*

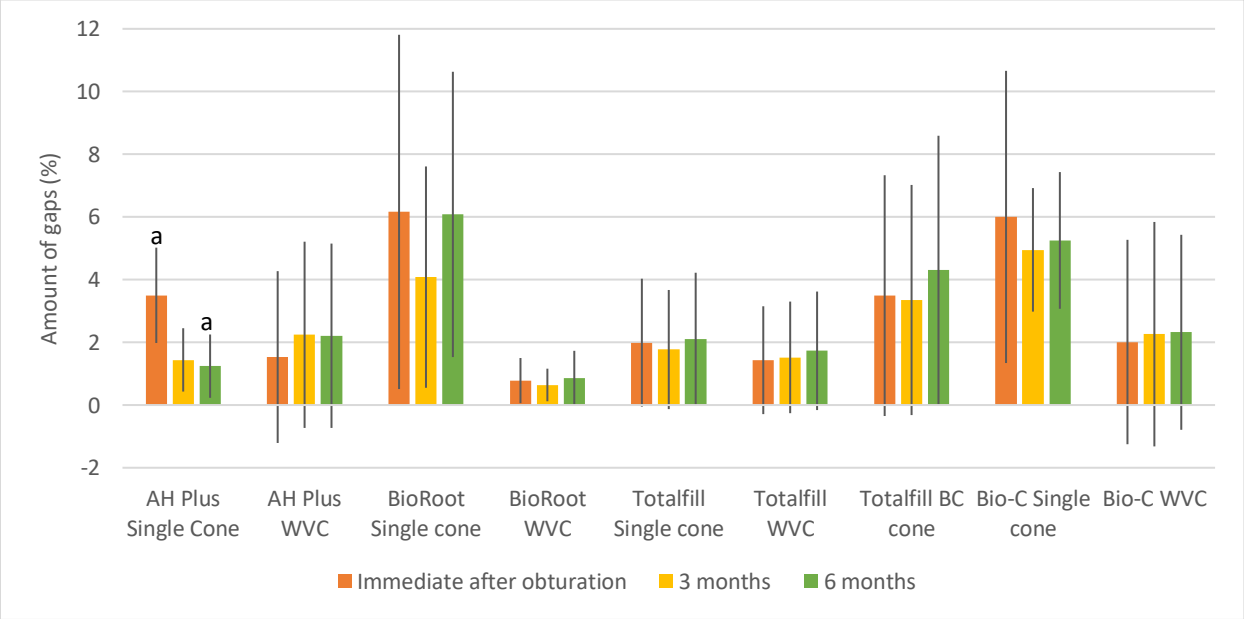

Figure 34: Mean percentage of gaps of natural molars from immediately after obturation, 3 months and 6 months (n=5) (mean ± SD). *[a] Same letter means a significant difference (p < 0.05). When compared the same sealer at different time, AH Plus has significant difference between at immediate after obturation and 6 months after obturation*

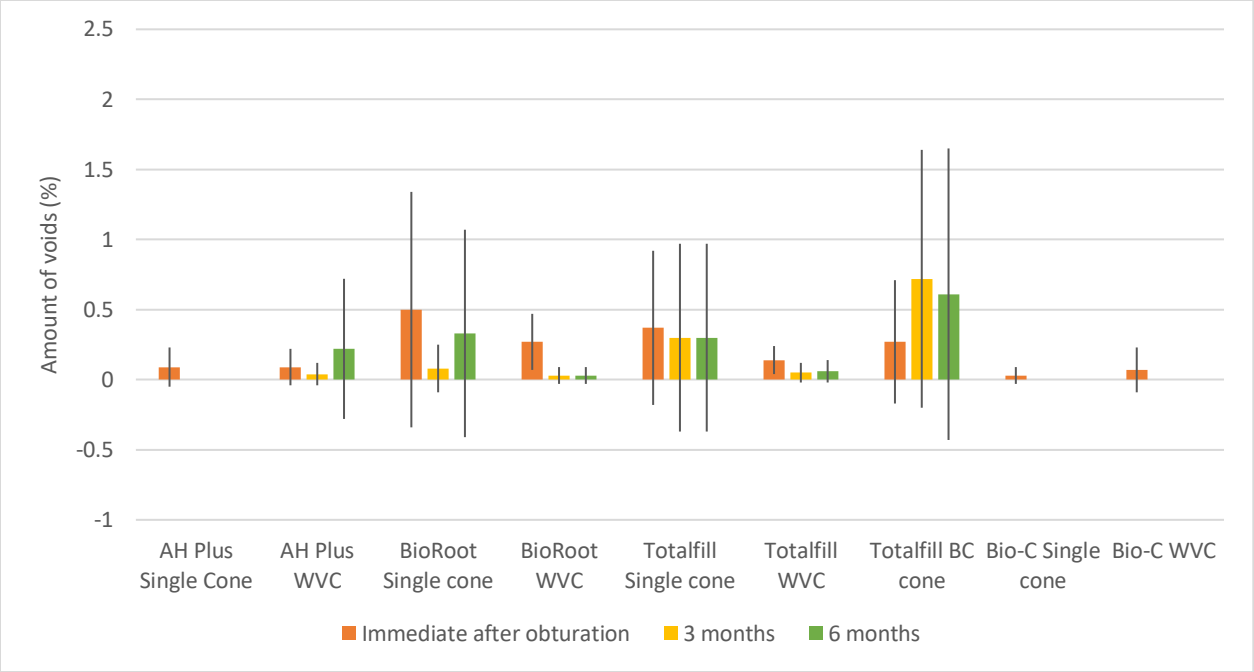

Figure 35: Mean percentage of voids volume in natural incisors immediately after obturation, and also 3 months and 6 months later (n=5) (mean ± SD). *No significant difference ($p > 0.05$) of the mean percentage of voids volume was found between each group*

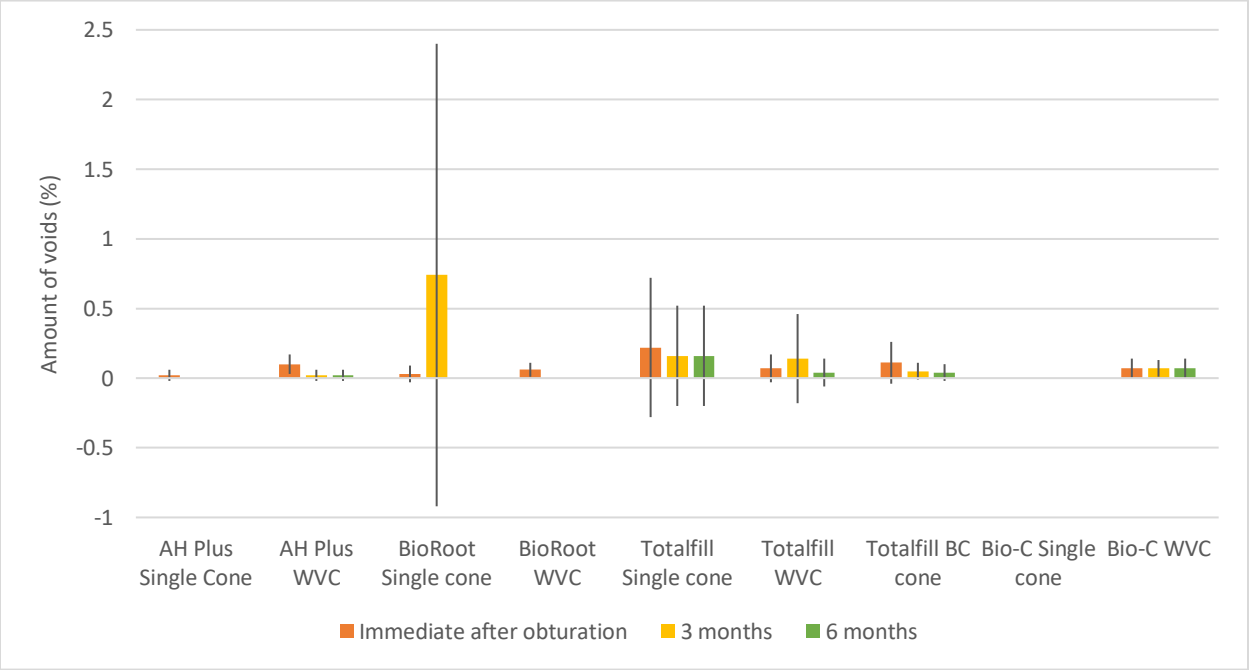

Figure 36: Mean percentage of voids volume in natural molars immediately after obturation, and also 3 months and 6 months later (n=5) (mean ± SD). *No significant difference ($p > 0.05$) of the mean percentage of voids volume was found between each group*

3.5.3 Polymer incisor group

The mean empty root canal volume in the natural molar group was 7.89 ± 0.38 mm^3. There was no significant difference ($p > 0.05$) between each group for the same tooth type.

Typical obturated results are shown in Figure 37A, 37B and 38. The common gaps and voids areas were found along the root length in the single-cone group and at the junction between warm GP and matched single-cones in the WVC group (Figure 37C, 37D and 39). The mean gaps and voids volume percentages of each group were shown in Figure 43 and 45. The highest mean gaps and voids volume percentage was found in Bio-C single-cone group at all times. In contrast, the lowest mean gaps and voids volume percentage was found in the Totalfill WVC group at all times.

There was no significant difference ($p > 0.05$) between each sealer at the same time period. However, when comparing the same sealer at different time periods, there was a significant difference between immediately after obturation and 6 months after obturation of the Bio-C single-cone group ($p \leq 0.05$) (Figure 43).

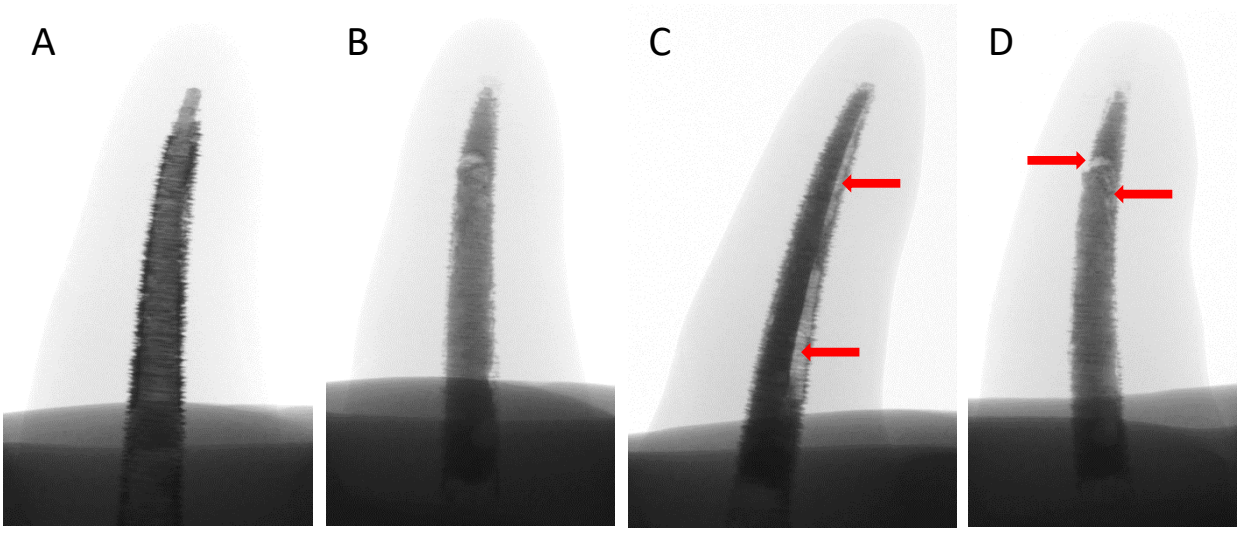

Figure 37: Inverted colour of uCT reconstructed images showing typical obturated polymer incisors and the gaps and voids areas (red arrows). *A: single-cone technique, B: WVC technique, C: gaps along the root length and D: gaps and voids at the junction between warm GP and matched single-cone in WVC technique*

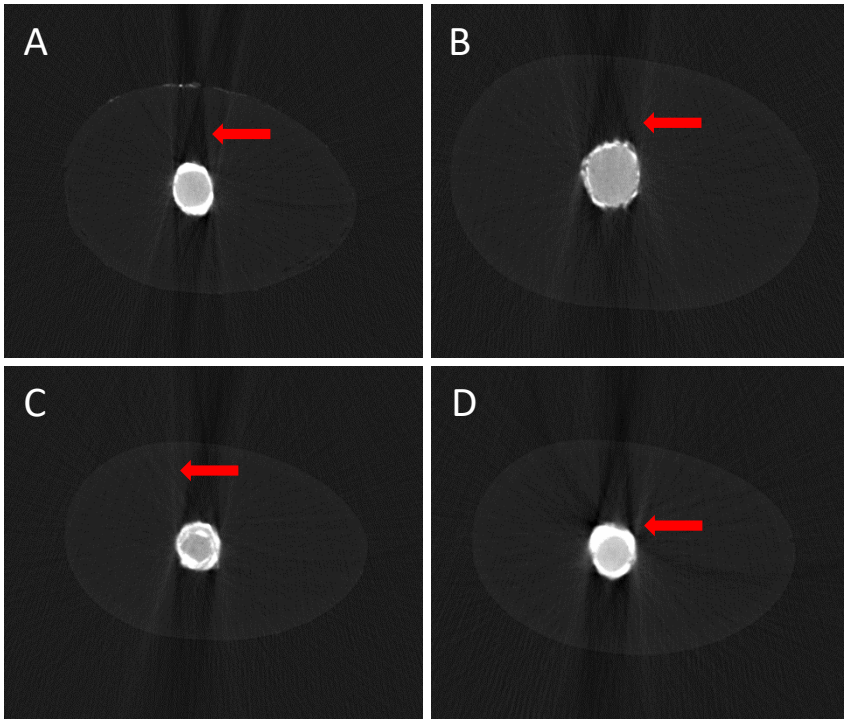

Figure 38: Cross-sectional µCT images of obturated polymer incisors *A: single-cone group, B: coronal part of WVC group, C: junction between the warm GP (grey) and matched single-cone (white) of WVC group and D: apical part of WVC group. Note the scattering defect (red colour) which has colour that resemble to the root filling material*

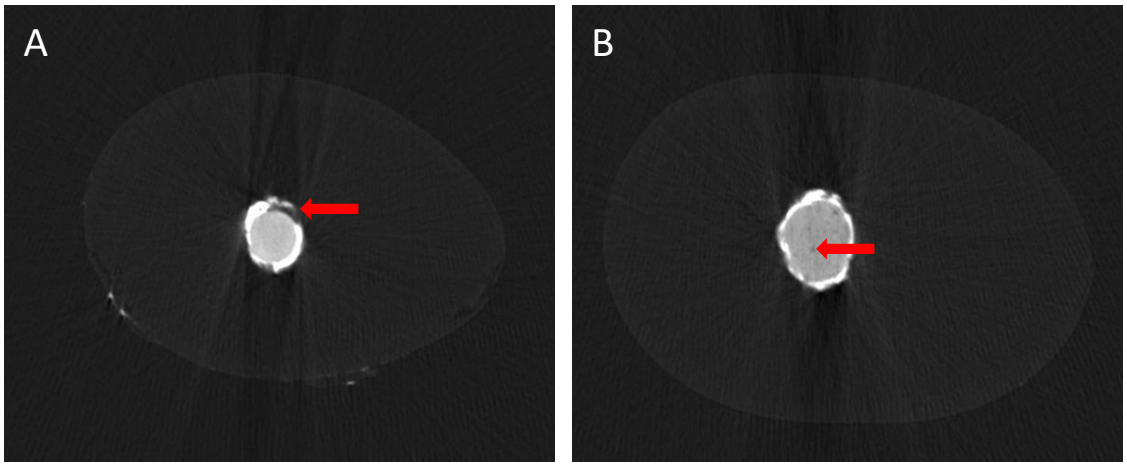

Figure 39: Cross-sectional µCT images show the gaps and voids area found in obturated polymer incisors (red arrow). *A: gaps and B: voids. Gaps were usually found in the single-cone group and the apical part of the WVC group. Voids were usually found in the coronal and middle part of the WVC group*

3.5.4 Polymer molar group

The mean empty root canal volume in the natural molar group was 9.04 ± 0.48 mm^3. There was no significant difference ($p > 0.05$) between each group for the same tooth type.

Typical obturated results are shown in Figure 40A, 40B and 41. The common gaps areas were found at the isthmus area (Figure 40C and 42A), at the junction between warm GP and matched single-cones in the WVC group (Figure 40D and 42B) and along the root length in the single-cone group (Figure 40C). The isthmus area of the WVC group was usually filled (Figure 41B-D), whereas the isthmus area of the single-cone group was usually empty (Figure 40C, 41A and 42A). In the latter group, the filling material was usually coated on the root canal wall only. The mean gaps and voids volume percentages of each group were shown in Figure 44. The highest mean gaps and voids volume percentage was found in the Totalfill BC cone group at all times. In contrast, the lowest mean gaps and voids volume percentage was found in the Bio-C WVC group immediately after obturation and in the Totalfill WVC group 3 months and 6 months after obturation. Voids was not found in the polymer molars.

When comparing between each sealer at the same time period, there were significant differences immediately after obturation between the Totalfill WVC and the Totalfill BC cone group and between the Totalfill WVC and the Bio-C single-cone group ($p \leq 0.05$). Other significant differences were found between the Bio-C WVC and the Totalfill BC cone group and between the Bio-C WVC and the Bio-C single-cone group ($p \leq 0.05$) (Figure 44).

At the 3-month period, there were significant differences between the Totalfill WVC and the Totalfill BC cone group and between the Totalfill WVC and the Bio-C single-cone group ($p \leq 0.05$) (Figure 44).

At the 6-month period, significant differences were found in the same groups as identified immediately after obturation, which were between the Totalfill WVC and the Totalfill BC cone group and between the Totalfill WVC and the Bio-C single-cone group ($p \leq 0.05$). Other significant differences were found between the Bio-C WVC and the Totalfill BC cone group and between the Bio-C WVC and the Bio-C single-cone group ($p \leq 0.05$) (Figure 40).

When comparing the same sealer at different time periods, there was a significant difference immediately after obturation compared with 3 months after obturation of the Totalfill WVC group ($p \leq 0.05$) (Figure 40).

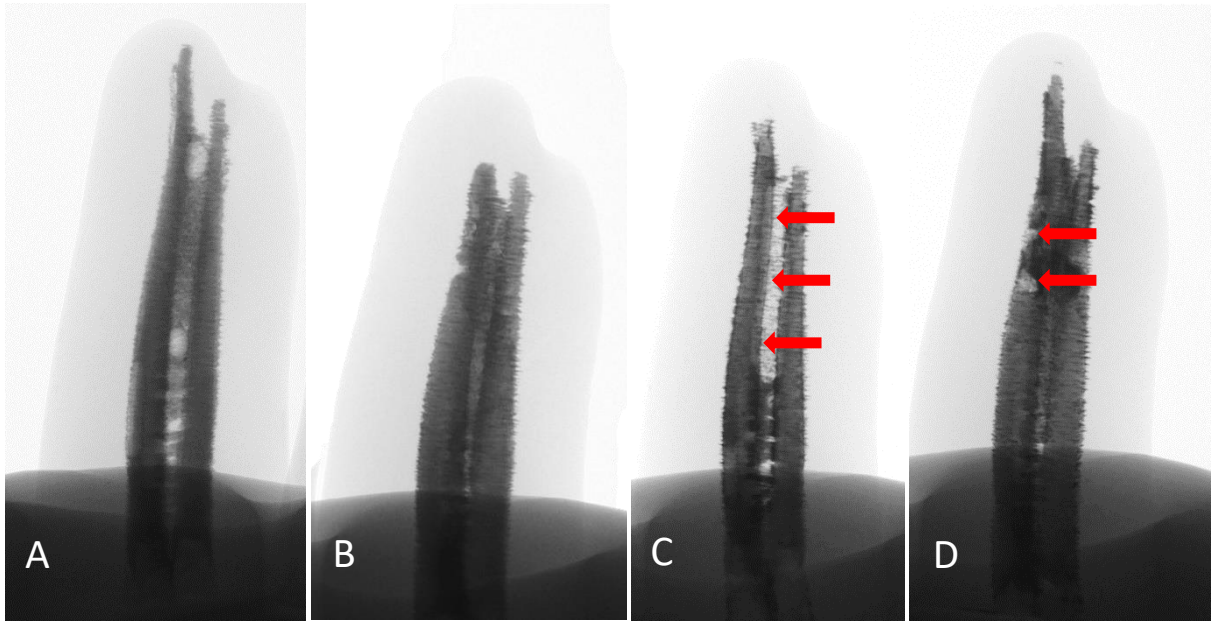

Figure 40: Inverted colour of the reconstructed images showing typical obturated polymer molars and the gaps and voids areas (red arrows). *A: single-cone technique, B: WVC technique, C: gaps along the root length and D: gaps and voids at the junction between warm GP and matched single-cone in the WVC technique. The itshmus area (red arrow) in the single-cone is usually empty (no filling material was showed radiographically), whereas in the WVC group, the itshmus area is usually filled with filling material*

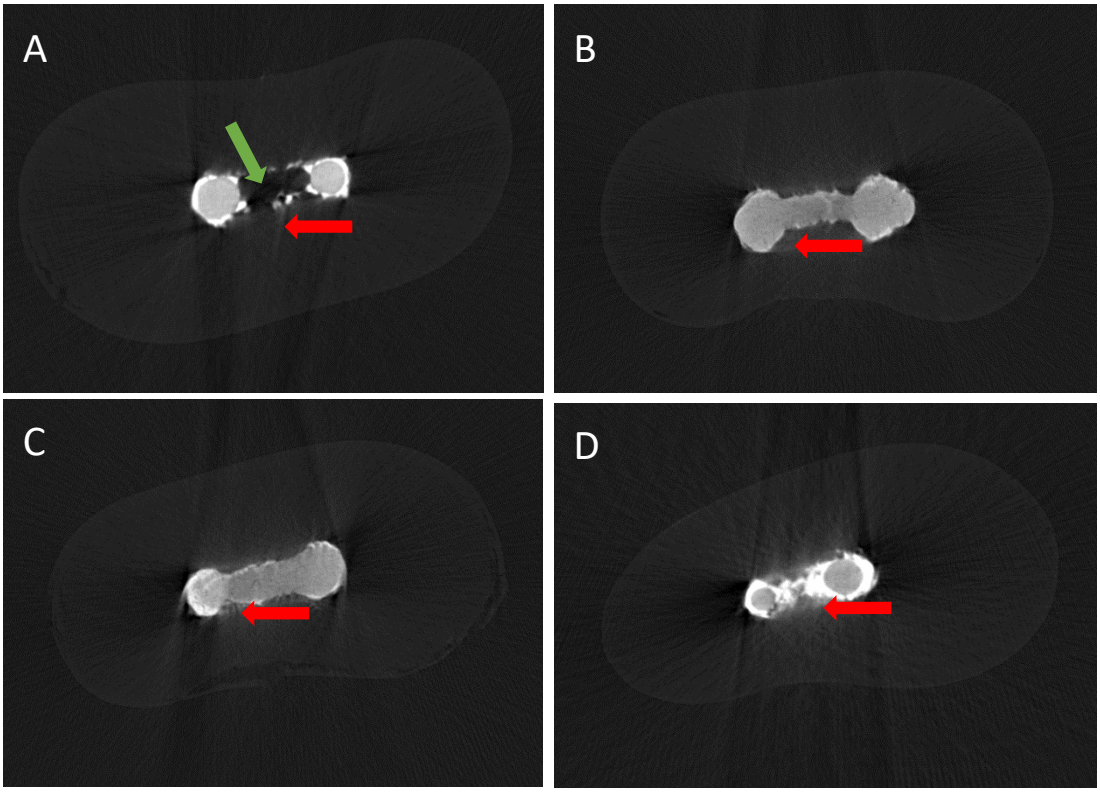

Figure 41: Cross-sectional µCT images show the typical obturated polymer molars *A: single-cone group, B: coronal part of WVC group, C: junction between the warm GP (grey) and matched single-cone (white) of WVC group and D: apical part of WVC group. The isthmus area (green arrow) in single-cone group usually has no root canal filling. Note the scattering defect (red colour) which has colour that resemble to the root filling material*

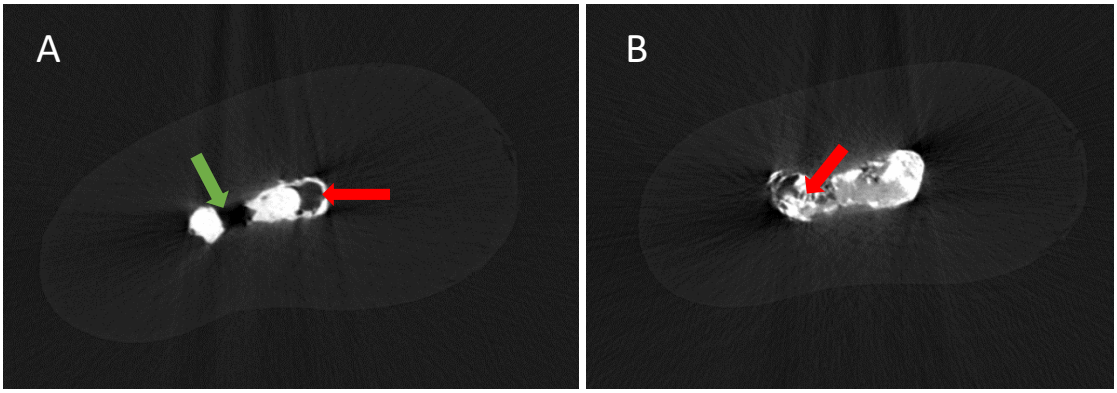

Figure 42: Cross-sectional µCT images of the gaps and voids areas found in obturated polymer molars. *A: gaps at the isthmus area (green arrow) and voids (red arrow) in single-cone group. Gaps and voids area in the single-cone group are usually large and found along the root length. B: gaps and voids in WVC group. Gaps and voids area in the WVC group are usually small, scatter and localised around the junction between the warm GP and matched single-cone of WVC group*

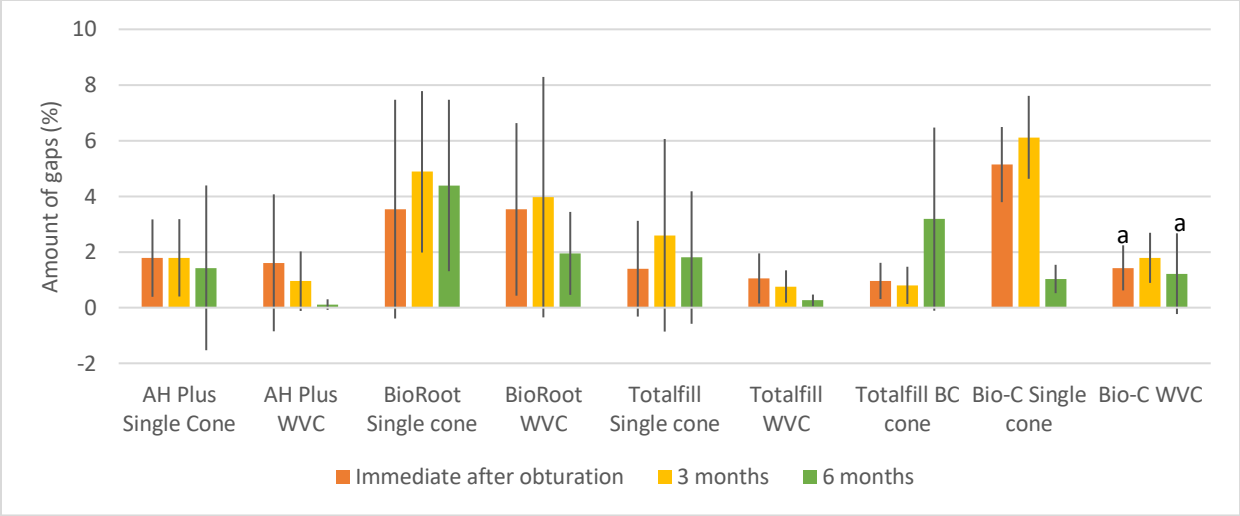

Figure 43: Mean percentage of gaps of polymer incisors from immediatly after obturation, 3 months and 6 months (n=5) (mean ± SD). *[a] Same letter means a significant difference (p < 0.05). When compared the same sealer at different time, Bio-C has significant difference between at immediate after obturation and 6 months after obturation*

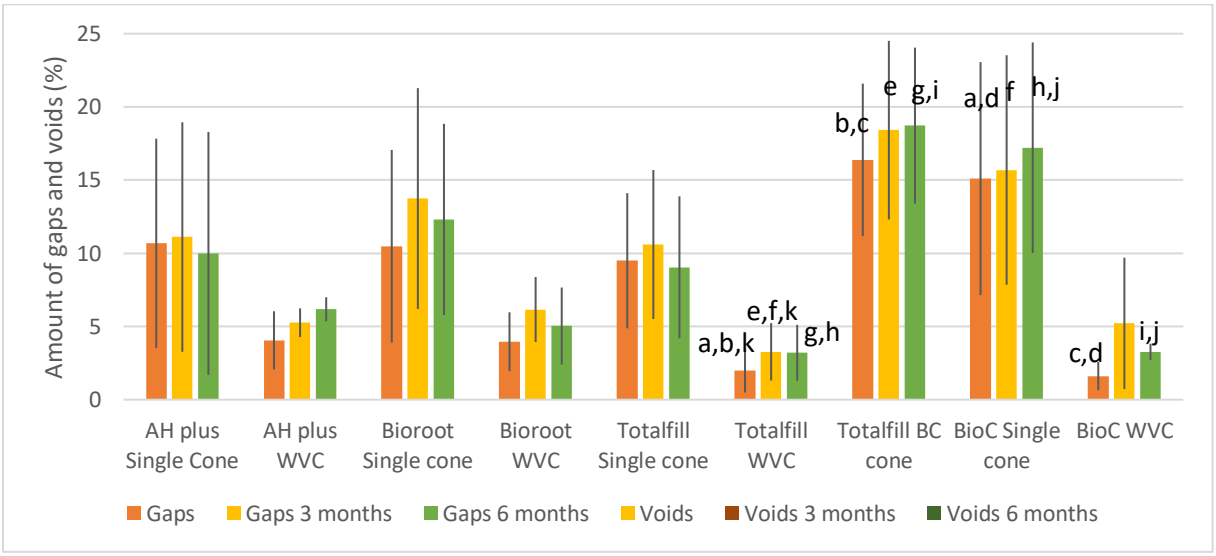

Figure 44: Mean percentage of gaps of polymer molars from immediately after obturation, 3 months and 6 months (n=5) (mean ± SD). *[a ,b, c, ,d, e, f, g, h, i, j, k] Same letter means a significant difference (p < 0.05). When compared between each sealer from the same period, there are significant difference at immediately after obturation and 6-month period between the Totalfill WVC and the Totalfill BC cone group and between the Totalfill WVC and the Bio-C single-cone group, between the Bio-C WVC and the Totalfill BC cone group and between the Bio-C WVC and the Bio-C single-cone group. At the 3-month period, there are significant differences between the Totalfill WVC and the Totalfill BC cone group and between the Totalfill WVC and the Bio-C single-cone group When comparing the same sealer at a different period, there is a significant difference between immediately after obturation and 3 months after obturation of the Totalfill WVC group*

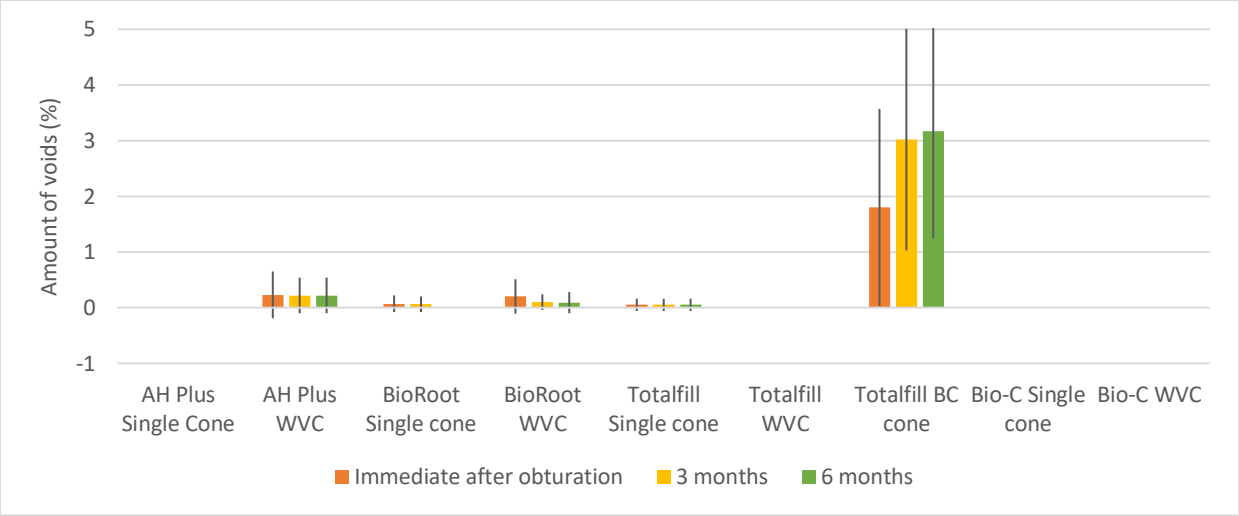

Figure 45: Mean percentage of voids volume in polymer incisors immediately after obturation, and also 3 months and 6 months later (n=5) (mean ± SD). *No significant difference ($p > 0.05$) of the mean percentage of voids volume was found between each group*

3.6 Calcium leachate analysis

The mean amount of calcium ions leaching from each sealer at 3 months is shown in Table 4. The highest amount of calcium ions released from incisor, molar, polymer incisor and polymer molar was found in the Totalfill BC cone, the Totalfill WVC, BioRoot RCS WVC and the BioRoot RCS single-cones, respectively. AH Plus released the least amount of calcium ions in every tooth type.

Table 4: The mean amount of calcium ions leaching from each sealer at 3 months (n=2; ppm).

Tooth type	AH Plus single-cone	AH Plus WVC	BioRoot RCS single-cone	BioRoot RCS WVC	Totalfill single-cone	Totalfill WVC	Totalfill BC cone	Bio-C single-cone	Bio-C WVC
Incisor	0	0	40.26	19.84	88.45	7.05	231.16	16.65	7.58
Molar	0.95	1.39	0.79	1.07	6.09	28.68	8.22	13.21	0.3
Polymer incisor	66.51	56.02	99.29	104.37	87.16	77.40	86.79	79.93	85.18
Polymer molar	62.49	67.41	250.83	225.62	138.77	94.49	113.80	78.85	75.08

The mean amount of calcium ions leaching and SD from each sealer at 6 months is shown in Table 5. The highest amount of calcium ions released from natural incisors and molars was found in the BioRoot RCS single-cone group. The highest amount of calcium ions released from polymer incisors was found in the Total fill BC cone group. In contrast, the highest amount of calcium ions released from polymer molars was found in the Bio-C WVC group.

Table 5: The mean and standard deviation of calcium ions leaching from each sealer at 6 months (n=3; ppm)

Tooth type	AH Plus single-cone	AH Plus WVC	BioRoot RCS single-cone	BioRoot RCS WVC	Totalfill single-cone	Totalfill WVC	Totalfill BC cone	Bio-C single-cone	Bio-C WVC
Incisor	8.34 ±3.65	12.19 ±9.23	98.96 ±8.14	46.73 ±26.50	33.15 ±5.82	9.01 ±11.52	12.79 ±13.84	5.61 ±4.12	2.77 ±2.64
Molar	11.39 ±1.32	14.89 ±5.37	158.97 ±52.58	99.87 ±26.15	82.79 ±27.77	24.40 ±39.95	44.68 ±4.87	15.88 ±15.29	7.86 ±4.84
Polymer incisor	7.47 ±0.23	17.00 ±8.70	5.83 ±2.09	21.20 ±10.84	38.36 ±22.13	30.11 ±12.24	14.46 ±3.65	22.88 ±12.27	13.05 ±6.25
Polymer molar	8.57 ±1.51	5.72 ±1.99	6.19 ±0.58	5.94 ±1.19	6.86 ±0.52	4.60 ±1.20	6.10 ±2.77	11.27 ±10.98	47.50 ±3.02

CHAPTER IV

DISCUSSION

In general, the objectives of root canal fillings are: to serve as a barrier to prevent leakage of oral fluids to the periodontium through the root canal system and entomb microorganisms remaining after the root canal disinfection process (117). Recently, several HCSC-based sealers have been developed. These sealers are claimed to slightly expand on setting (43, 44) which help promoting the sealing ability of the sealer. Moreover, they also have a bactericidal property (42) which promotes the goals of the root canal treatment. Nevertheless, some HCSC-based sealers' properties are altered by heat. Thus, this study aimed to compare the root canal filling quality of three HCSC-based sealers with AH Plus when obturating canals using the WVC and the single-cone techniques.

Currently, polymer printed teeth are frequently used as models for studying in endodontics because they are manufactured reproducibly eliminating variability from studies. Manufacturing 3D polymer models is not complicated as it does not require debinding and sintering required for 3D ceramic printing. Thus, the 3D polymer model is dimensionally stable as there is no thermal expansion or shrinkage during a sintering process. This study firstly hypothesized that as the 3D polymer teeth are impermeable; this would prevent environmental fluid from interacting with HCSC-based sealers. Previous study showed that moisture is essential to the setting reaction of the HCSC-based sealers (39-41); therefore, the impermeable polymer teeth may result in inaccurate setting time and the amount of calcium ion leaching. However, this hypothesis was rejected as the percentage of gaps and voids volumes following root canal obturation using different techniques as well as ions

leaching derived from polymer teeth and natural teeth were not significant difference. Using polymer teeth to test the root canal filling quality also minimize the critical effect from the variation of the natural root canal anatomy (92).

4.1 Material characterisation

Calcium ions play an essential role in tooth remineralisation and human dental pulp stem cell growth and differentiation (118), so it has been suggested materials that release calcium ions may promote healing. The EDX data showed that all calcium silicate-based sealers were composed primarily of calcium, silicon and oxygen which agrees with previous studies (119-121). The amount of calcium ions leached from the BioRoot RCS groups was the same as shown in previous studies (120, 121). In contrast calcium ions leached from the Totalfill BC and Bio-C groups were lower than previous studies (119, 121, 122).

One of the important features of a sealer is the ability to penetrate and fill the space in the irregularities of the root canal as well as dentinal tubules (sealer penetration and flowability). A previous study showed that smaller particle size promoted dentinal tubule penetration (123). SEM analysis in the present study showed that Bio-C had the smallest particle size of all the sealers; therefore, it would have been expected to penetrate into the dentinal tubule better than the other sealants. Another publication found Bio-C had the highest flowability compared with Totalfill BC and AH Plus (59). However, particle size is not the only factor that affects sealer penetration which is also influenced by shear rate, temperature and time from mixing (124). A previous study showed that adding a water-soluble polymer can improve the flow rate of the BioRoot RCS (125). Thus, the particle size does not necessarily directly correlate with the flowability and sealer penetration.

The EDS analysis of every GP type showed a definite peak of zinc, which is the main component of GP. In addition to zinc, the BC cone showed a small presence of calcium. The SEM analysis of the BC cone also confirmed the calcium coating on the GP surface. The calcium-coated surface of the GP was aimed to generate the interaction between the GP and the sealer (Monoblock concept). However, the high amount of voids volume percentage found in the BC cone group meant there were spaces preventing the contact between the GP and the sealer. Thus, the interaction between these filling materials may be compromised.

4.2 The potential of HA-3DPT for replacing human teeth for in-vitro endodontic research

The Admatec printer is a new ceramic printing machine that can automatically collect and reuse ceramic slurries resulting in a reduction of the printing cost. In order make a compatible slurry suspension, the suspension needs to have specific characteristics. In particular, according to the Admatec study (114), the suspension should present a shear thinning behaviour and have a dynamic viscosity that is below 600 Pa·s for a shear rate of 0.1 s^{-1} and below 10 Pa·s for shear rates between 10 and 300 s^{-1}.

The major problem encountered in this study attempting to print 3D HA teeth was the unstable ceramic suspension as the HA slurry kept thickening over time. Based on a preliminary test, it took around 4 hours to create a tooth model which was 16 mm in length. Therefore, in this case, the slurry needed to be stable for at least 4 hours after mixing.

The initial target for HA solid loading to reproduce a realistic tooth model was set to 60% to replicate the approximate percentage of HA

found in human dentine (126). The mechanical mixer could homogeneously mix the HA slurry up to 60%. However, despite altering the resin and dispersant ratio, it was only possible to achieve 45% or less solid loading in order for it to be stable enough for the complete duration of the printing. One possible explanation for the instability of the 50% HA loaded slurry could possibly be due to the use of a strong vibrator to mix the slurry, which generated heat that promoted the mixing and flowability. When it cooled down, the slurry agglomerated and thickened.

This study showed that both 40% and 45% HA slurries had the potential to be printed by the Admatec printer to produce a simple single root replica as their viscosity corresponded with the criteria described above. There was a further problem with these slurries as they flooded out of the collector unit (Figure 46) because the dynamic viscosity of the slurry was too low, however, both slurries' viscosities were higher than the Admatec alumina slurry that proved to be printable (114). This could mean that the optimal range of the viscosity may differ between different materials.

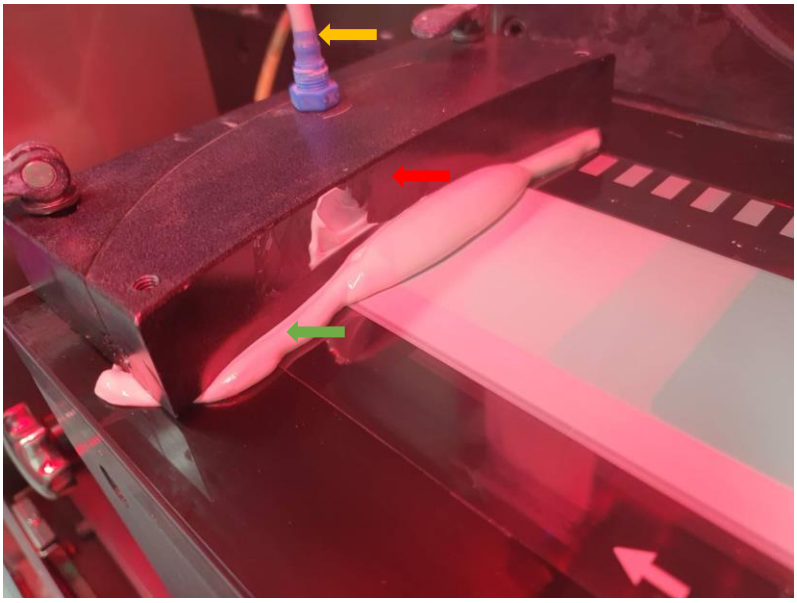

Figure 46: Slurry flooded out of the collector unit (red arrow). *The slurry flooded out (green arrow) of the collector unit which should not be found in the general printing process. In general, all slurry should be collected by the collector unit and circulate back to the slurry pool by the plastic tube (yellow arrow)*

This study tested the viscosity of both slurries an hour after mixing because this was the time taken before starting printing. It would have been better to test the viscosity at a different time points because of the instability of the slurry to make sure that the Admatec's criteria (114) were achievable.

Another problem encountered during model development was that the printer could not create the root canal. According to the manufacturer, the machine had an X-Y resolution of 50 µm with a Z resolution of 10 µm. The minimum feature size that could be printed from the machine was 0.3 to 0.4 mm. In general, the root canal was enlarged to file size 25 or 30 which had a tip size diameter equal to 0.25 and 0.30 mm, respectively. This meant the root canal diameter at the LT level was at least equivalence to 0.25 mm. The taper of the rotary file used nowadays was range from 4% to 9%, which meant the root canal diameter was approximately 0.04 to 0.09 mm larger for each mm upward

coronally. Hence, the printer's resolution less than 0.25 mm was required to print the entire instrumented root canal. The Admatec printer's resolutions are sufficiently high enough to be able to print most of the instrumented root canal part except the root canal at the LT level, so the problem may be the material characteristics or the machine settings Which requires further investigation to resolve this issue.

The radiopacity of the HA printed root was investigated because poor radiopacity is a problem associated with the polymer printed root discussed. The HA printed root's radiopacity was equivalent to human dentine which means that the HA printed root may be more suitable for gaps and voids volume percentage calculation than the polymer tooth. Nonetheless, when the printed root was debound and sintered, the radiopacity may have increased as the structure was compressed together. The general shrinkage rate of the model printed from the Admaflex machine is 20% (114).

Further research after identification of a suitable concentration of HA slurry and parameters for 3DP remains to identify an appropriate time and temperature used for debinding and sintering. To date, there is no study regarding a suitable time and temperature to be used for debinding and sintering HA printed root with Admaflex's technique. Future research should characterise the HA printed root after debinding and sintering and identify shrinkage, hardness, microscopic structure and radiopacity to enable adjustment to mimic the properties of natural dentine.

4.3 Discussion on µCT measurement

Previous studies used various methods such as dye leakage and bacterial infiltration to evaluate root canal filling quality (127, 128). However, the dye leakage data was either linear or volumetric, where the dye penetrated around voids or within the root fillings (129) and the bacterial infiltration technique could reveal the gaps that extend along the full length of the root canal only (130). The present study used µCT to measure the gaps and voids volume percentage volume because it allowed 3D investigation of internal structures at the micron scale in a nondestructive way.

µCT has been used in several endodontic studies for a quantitative assessment of parameters which include: material removal in the retreatment (131), amount of debris remaining following root canal preparation (132) and the quality of root canal filling (133) because of its high resolution and sensitivity. On the other hand, the sensitivity of µCT may be too high for measuring the gaps and voids percentage; even a small change in temperature, position or moisture status of the tooth can significantly affect the measurement. To the best of the authors' knowledge, no study has previously reported the effect of temperature, sample position, or moisture on the quantitative measurement of µCT in model set-ups used in endodontic research. This study hypothesized that these parameters would affect the quantitative measurement as the reconstruction process of the µCT is based on 2D projected images. If the tooth position or angle is changed, the 2D projected images will be affected and generate different reconstructed images. Tooth moisture and temperature can also affect the measurement as they may affect the HCSC-based sealer. As HCSC-based sealer needs moisture to undergo a hydration reaction (134), this sealer will dry out and shrink when placed in dry environment (135). Nevertheless, this hypothesis was rejected as

there was no significant difference between the gaps and voids percentage among the parameters.

ImageJ was used to measure the effect of each parameter rather than the CTAn software because CTAn cannot flawlessly detect the difference between the empty canal and the polymer as the radiodensity of both areas are almost similar. In order to detect the outline of the root canal, the threshold value was adjusted which resulted in a lot of signal noise (Figure 47). This problem was not apparent in the gaps and voids measurements as most of the root canal was filled with the radiopaque filling materials and CTAn could easily detect the difference between the filling materials and the empty space (gaps and voids).

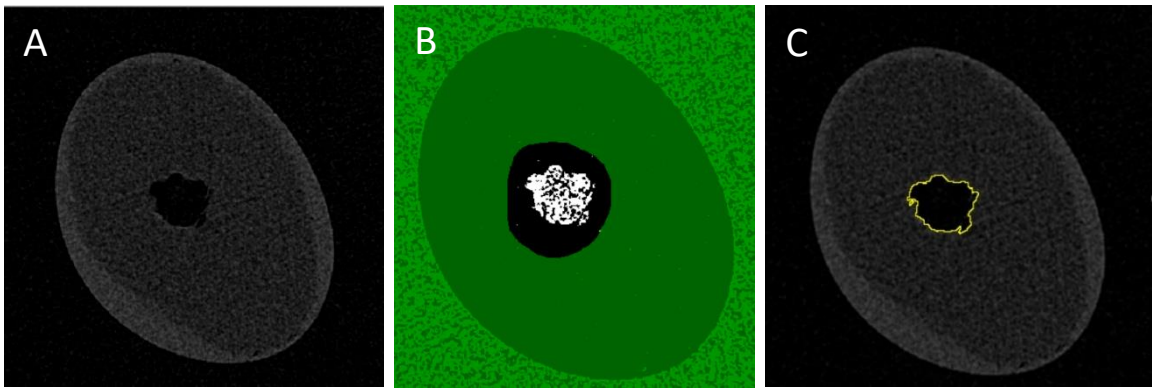

Figure 47: a µCT image of a polymer tooth viewed using different software*; A: an original image, B: the CTAn image. Note the black spot (noise) within the root canal (white area). The software calculated the white area as a root canal volume; therefore, the root canal volume measured by CTAn was lower than the actual volume and C: the ImageJ image. Note the yellow outline of the root canal. The software calculated the area that was encircled within the yellow outline; therefore, the root canal volume measured by imageJ was equal to the actual root canal volume*

Although this study showed that the temperature, sample position and moisture had no significant impact on the quantitative measurement using µCT, these factors still affected the measurement. The impact of these factors was at one to two decimal places (0.x-0.0x mm^3). The impact also increased with the length of the tested sample. As a consequence, these factors should be controlled and the

quantitative data from µCT should be reported as a proportion rather than an exact value. A larger sample size is needed to confirm the impact of these factors.

4.4 Quality of root canal obturation with different sealers and techniques

A factor that influences root canal filling quality is the amount of filling material used; therefore, the amount of material introduced into the canal during obturation needs to be controlled to prevent bias. Teeth used in this study demonstrated no significant difference in the root canal volume between each tooth; therefore, there should not be any difference in the volume of sealer used in each tooth. This study used standardized matched GP cones and the canal volume to manipulate the amount of sealer used in each root filled specimen.

The threshold used in this study varied between the single-cone part (150−255) and the WVC part (130−255) because the thermoplasticised GP had a lower radiopacity than the GP cone (Figure 48). The main difficulty with setting the threshold and measuring was at the junction between the thermoplasticised GP and the GP cone in the WVC group as it contained a mixture of both GPs. The present study used the root portion as the reference point. If the GP was in the middle portion, the threshold range from 130−255 was used; otherwise, the threshold range from 150−255 was used for the areas where the GP cone was present.

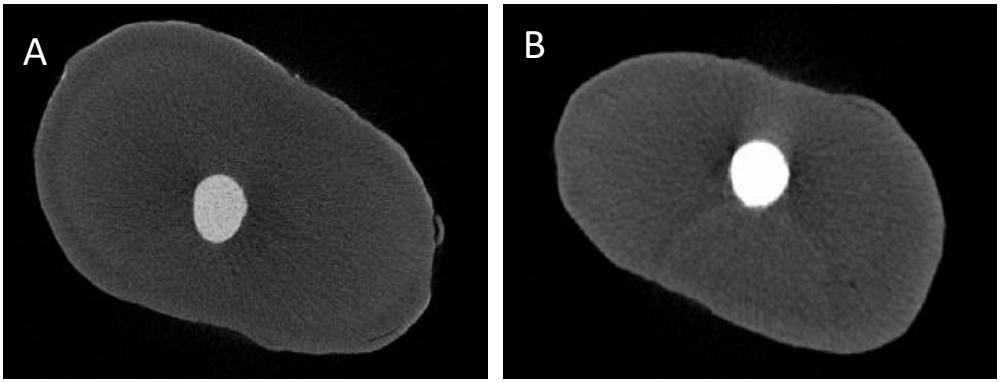

Figure 48: µCT images of the filled root canal; *A: with WVC and B: with single-cone technique. Note the brighter colour of the GP in the single-cone group compared with the warm GP in the WVC group (higher radiopacity)*

BioRoot RCS demonstrated the highest gaps and voids volume percentage in almost every tooth type and different time periods, which may be related to two reasons. BioRoot RCS has a high viscosity, which means it is difficult to manipulate the sealer and allow it to flow into the irregularities of the root canal system. This material is also hand-mixed, which could lead to entrapment of air within the material during mixing (136) and therefore, the material could contain voids even prior to its application into the root canals system.

Another group that had a high percentage of gaps and voids volume percentage was the Totalfill BC filled with BC cones group, which may be related to the size of GP cone used. BC cones have a taper of 0.04% which is smaller than the taper size of both the ProTaper Gold F2 (taper of 0.08% which varies along the length) and the F3 (taper of 0.09% and varies along the length). Consequently, there was not enough GP to force the sealer into any spaces. According to Pascal's law: the pressure in an enclosed fluid is uniform in all directions (137), so as large volume of GP as possible is needed to entirely fill a root canal space and generate force to push the sealer into the root canal irregularities and dentinal tubule.

The present study found that gaps and voids volume percentage of AH Plus in both natural tooth groups after 6-months was significantly lower than immediately after obturation. This finding was in agreement with previous studies which identified that AH Plus slightly expands on setting (138-140). These studies claimed that the expansion of the AH Plus was likely due to water absorption (138-140).

When considering the obturation technique, there remains controversy with respect to the quality of the root canal filling between the single-cone and the WVC. This study found no significant difference in terms of the gaps and voids volume percentage between both techniques. Nevertheless, the gaps and voids volume percentage found in the WVC group was usually located at the junction between thermoplasticised GP and the matched GP cone and the apical-third area (single-cone part). In the single-cone group, gaps and voids were found along the whole root length. Moreover, the obturation materials in the single-cone group usually coated only the wall surface but did not fill the space of the isthmus (Figure 31B).

Despite the concern that heat may change the viscosity and potential flow of HCSC-based sealers (141) which could affect the filling quality when using HCSC-based sealers with WVC, the present study found that most of the irregularities (isthmus and lateral canals) in the WVC group were almost completely filled with GP instead (Figure 40B-D). However, the area that could have been affected by the heat was at the junction between the single-cone part and the WVC part because the GP cone could prevent substitution of heated affected-sealer with warm GP.

Data derived from polymer teeth was similar to the results obtained from natural teeth. However, there were some limitations to the polymer teeth. Firstly, the polymer tooth had low radiopacity which made it difficult to be detected by the X-ray. Hence, a higher amount of X-ray was needed to detect the polymer tooth. Neverteless, root canal filling materials were also received a higher amount of X-ray, resulted in X-ray beam scattering defect (Figure 38 and 41). Secondly, the root canal wall of the polymer tooth was rough (Figure 49). This study used 11 µm intervals, which meant that the µCT combined the data in-between to form one image (Figure 50). Uneven root canal walls made the outline of the root canal blur (Figure 50C and 50D). These factors were not found in natural tooth as the dentine had more radiopacity than the polymer and the prepared-natural root canal was smooth continuous tapering (Figure 50A and 50B).

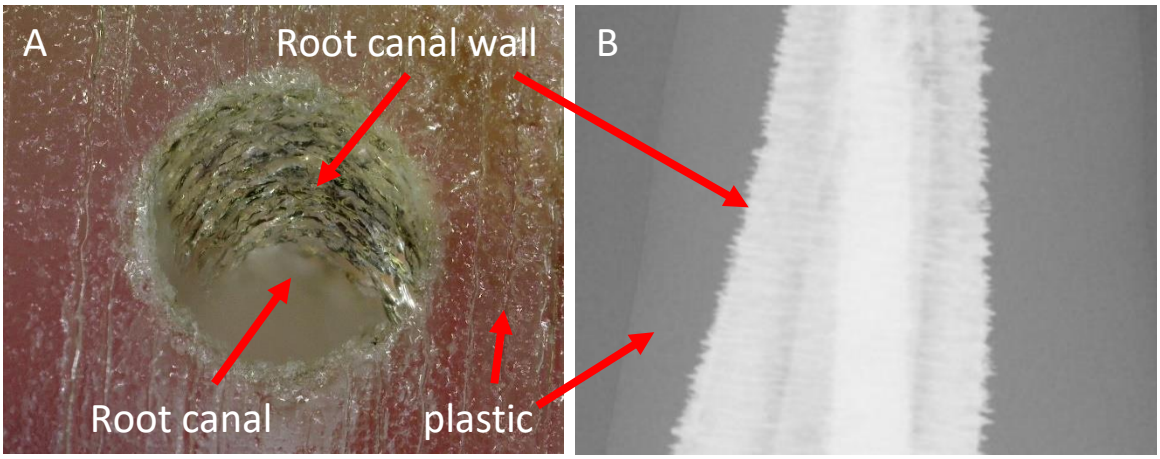

Figure 49: Polymer root canal wall images; *A: 200x of polymer root canal wall (focus stacking) from the microscope and B: the X-ray image of the filled polymer root canal. Note the roughness of the root canal wall*

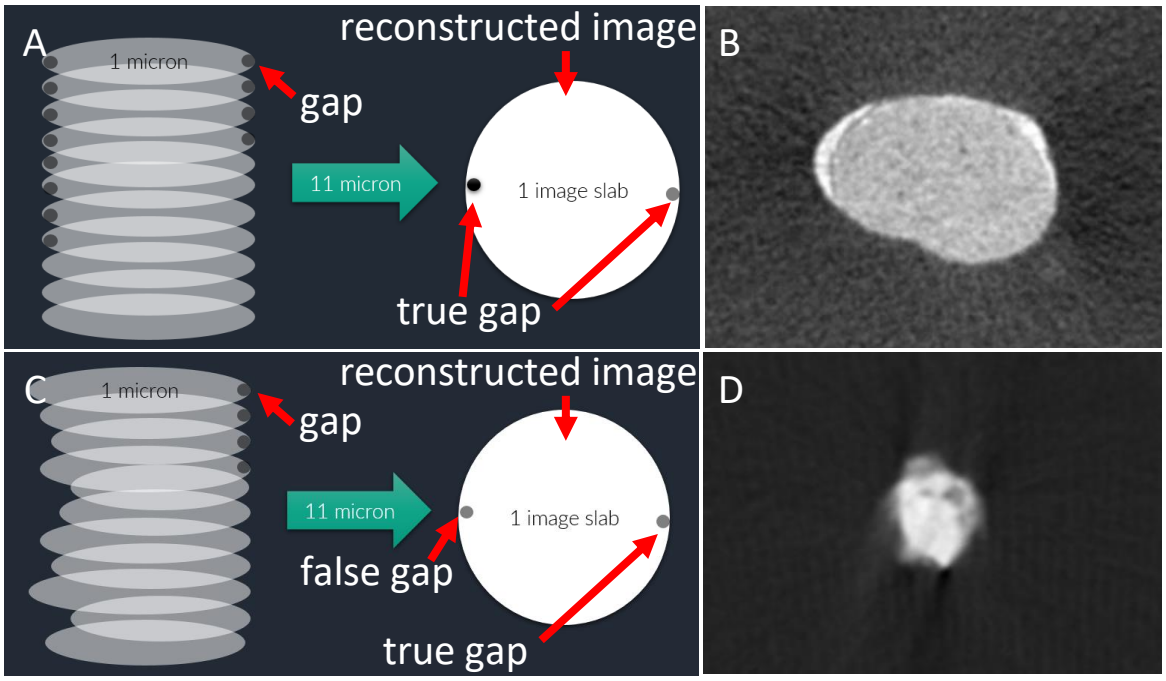

***Figure 50: µCT reconstruction process**; A: schematic reconstructed process of a natural tooth. The software merges 11 of 1 µm images into one image slab. More gaps (grey circle) result in a darker area (black circle), B: a µCT image of a natural tooth. Notice a clear root canal outline, C: schematic reconstructed process of a polymer tooth. An uneven wall result in an identical grey area (false gaps) and D: a µCT image of a polymer tooth. Notice a blur root canal outline*

The high standard deviation of the gaps and voids volume percentage data was considered normal in the gaps and voids study because of the variation in tooth morphology. The round continuously tapered canal was filled almost entirely (Figure 51A) resulting in a low percentage of gaps and voids. In contrast, some incisors in this study had lateral canals and the size and level of the isthmus in molars were different. The polymer molars also had an isthmus in every tooth. The amount of obturation materials distributed into these morphologies, especially in the single-cone group, varied (Figure 5B) which resulted in a wide range of data.

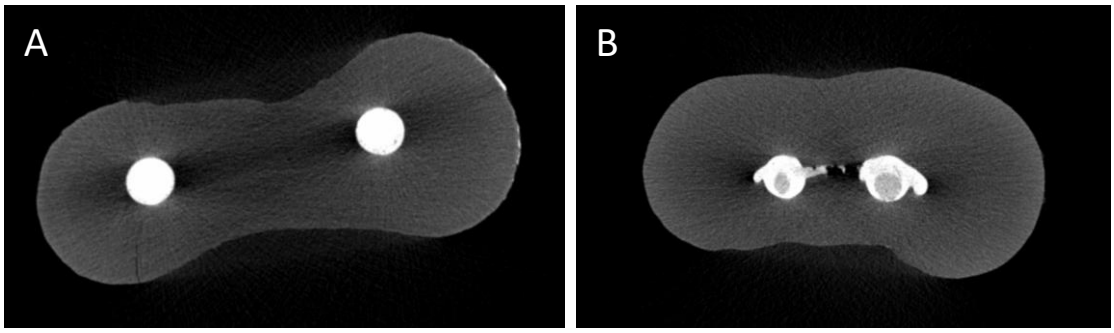

Figure 51: The µCT images of filled natural molar; *A: gap-free in round canals and B: gaps in an oval canal. The amount of filling materials inside the isthmus area were varies among the samples which result in high standard variation of the data*

The range of the gaps and voids percentage volumes found in this study was less than 5% in the natural teeth and polymer incisors. This amount of gaps and voids volume may not be clinically significant, which mean all sealers used in this study are able to be used clinically. This corresponded with previous studies (142-144). Moreover, the gaps and voids volume percentages alone could not represent the potential clinical outcome which depends on many factors, including disinfection.

4.5 Leachate analysis

In this study the root surface was coated with collagen to imitate the PDL, which may have slowed the leaching rate. However, there is no previous study on how the PDL effects the rate of leaching. The problems with using the collagen gel alone were that it had a long setting time and it detached from the root surface when the root was immersed in HBSS.

To overcome these problems, agarose was used as a matrix for collagen. Agarose does not affect the collagen's structural or formation topology and vice versa (145). Moreover, the collagen-agarose co-gels were found to improve the mechanical and structural properties (146). The present study used 1% collagen-agarose co-gels as previously

described (146). However, the leachate rate of ions at different gel concentrations must be measured and compared with the leachate rate of the natural PDL in the future to reproduce the *in vivo* environment.

Calcium ion leaching is considered as a biological property of the sealer, as it stimulates bone regeneration (147). A previous study raised the point that a prolonged ion release may compromise the sealing ability of the hydraulic cement (148). Nevertheless, the present study showed that ion leaching was not related to the solubility and sealer wash out, as the gaps and voids percentage volumes were not significantly different between each time period.

This study found that the amount of calcium ion leachate from the natural molars was lower than the natural incisors at 3-months. Conversely, the calcium ion leachate at 6-months from molars was higher than from the incisors. This indicated that calcium ion took longer to elute from the molars than the incisors which could be explained by the apical foramen diameter and the amount of the dentinal tubules. The apical foramina of the incisors in the present study was enlarged to size 30 (0.3 mm) which was larger than the molars (size 25; 0.25 mm). The amount of dentinal tubules in the molars is lower than the incisors (149); therefore, the leaching rate was slower in molars than incisors.

The high release of calcium ion from BioRoot RCS and Totalfill BC were also found from polymer teeth. However, when compared with natural teeth, all polymer groups released more calcium ions in 3-months than after 6 months which have arisen from calcium ions reacting with the dentine in natural teeth

CHAPTER V

CONCLUSION

All HCSC-based sealers were composed of calcium, silicon and zirconium. The highest amount of calcium was found in BioRoot RCS, followed by Totalfill BC and Bio-C, respectively. Bio-C had the smallest particle size. All GP contains zinc as the main constituent, whereas calcium was found in GP pellet and BC cone.

This study showed the potential to develop 3DPT with HA. 40% and 45% solid loading of HA slurry showed the potential to be printed by Admaflex 130. The viscosity and stability of the slurry needed to be tested and adjusted further to enable more predictable printing. The tooth's dimension before debinding and sintering was the same as in the digital model. Further investigation on the radiopacity, debinding and sintering parameters and the tooth's dimension after debinding and sintering were required.

Polymer teeth could be used in endodontic research about the root canal filling quality and amount of calcium ion leaching where the natural teeth are inaccessible. Increasing the radiopacity of the polymer teeth could improve the reliability of the result. Tooth's position, temperature and moisture condition had no significant effect on the quantitative measurement of µCT. All HCSC-based sealers could be used to obturate the root canal by the WVC or the single cone technique. Gutta-percha mass was still needed to adapt the sealers into the root canal wall and irregularity. At the 3-month period, the differences were found between the Totalfill WVC and the Totalfill BC cone group and between the Totalfill WVC and the Bio-C single-cone group.

The Totalfill BC and the BioRoot RCS obturated with single cone technique should be used whenever the clinician needs the effects of calcium ion released from the sealer.

REFERENCES

1. Kakehashi S, Stanley HR, Fitzgerald RJ. The Effects of Surgical Exposures of Dental Pulps in Germ-Free and Conventional Laboratory Rats. Oral Surg Oral Med Oral Pathol. 1965;20:340-9.
2. Paque F, Peters OA. Micro-computed tomography evaluation of the preparation of long oval root canals in mandibular molars with the self-adjusting file. J Endod. 2011;37(4):517-21.
3. Ercan E, Ozekinci T, Atakul F, Gul K. Antibacterial activity of 2% chlorhexidine gluconate and 5.25% sodium hypochlorite in infected root canal: in vivo study. J Endod. 2004;30(2):84-7.
4. Peters OA. Current challenges and concepts in the preparation of root canal systems: a review. J Endod. 2004;30(8):559-67.
5. Torabinejad M, Walton R.E. Principles and practice of endodontics. Philadelphia: Saunders; 2002.
6. Endodontology ESo. Quality guidelines for endodontic treatment: consensus report of the European Society of Endodontology. International Endodontic Journal. 2006;39(12):921-30.
7. Grossman LI. Endodontic Practice: Lea & Febiger; 1978.
8. Gutmann J. History of endodontics. Ingle's Endodontics. 2008.
9. Friedman CM, Sandrik JL, Heuer MA, Rapp GW. Composition and mechanical properties of gutta-percha endodontic points. Journal of dental research. 1975;54(5):921-5.
10. Combe EC, Cohen BD, Cummings K. Alpha- and beta-forms of gutta-percha in products for root canal filling. Int Endod J. 2001;34(6):447-51.
11. Lottanti S, Tauböck TT, Zehnder M. Shrinkage of backfill gutta-percha upon cooling. J Endod. 2014;40(5):721-4.
12. Meyer K, Kollmar F, Schirrmeister J, Schneider F, Hellwig E. Analysis of shrinkage of different gutta-percha types using optical measurement methods. Schweizer Monatsschrift für Zahnmedizin = Revue mensuelle suisse d'odonto-stomatologie = Rivista mensile svizzera di odontologia e stomatologia / SSO. 2006;116:356-61.
13. Orstavik D. Antibacterial properties of root canal sealers, cements and pastes. Int Endod J. 1981;14(2):125-33.
14. Orstavik D. Antibacterial properties of endodontic materials. Int Endod J. 1988;21(2):161-9.
15. Gorduysus M, Avcu N. Evaluation of the radiopacity of different root canal sealers. Oral Surg Oral Med Oral Pathol Oral Radiol Endod. 2009;108(3):e135-40.
16. Borges AH, Pedro FL, Semanoff-Segundo A, Miranda CE, Pecora JD, Cruz Filho AM. Radiopacity evaluation of Portland and MTA-based cements by digital radiographic system. J Appl Oral Sci. 2011;19(3):228-32.
17. Michaud RA, Burgess J, Barfield RD, Cakir D, McNeal SF, Eleazer PD. Volumetric expansion of gutta-percha in contact with eugenol. J Endod. 2008;34(12):1528-32.
18. Tilakchand M, Jain A, Naik B. Expansion of Gutta-percha in contact with various concentrations of zinc oxide-eugenol sealer: A three-dimensional volumetric study using spiral computed tomography. J Conserv Dent. 2016;19(4):317-22.
19. Upadhyay V, Upadhyay M, Panday RK, Chturvedi TP, Bajpai U. A SEM evaluation of dentinal adaptation of root canal obturation with GuttaFlow and conventional obturating material. Indian J Dent Res. 2011;22(6):881.
20. Barnett F, Trope M, Rooney J, Tronstad L. In vivo sealing ability of calcium hydroxide-containing root canal sealers. Endod Dent Traumatol. 1989;5(1):23-6.
21. Manhart MJ. The calcium hydroxide method of endodontic sealing. Oral Surg Oral Med Oral Pathol. 1982;54(2):219-24.

22. Nerwich A, Figdor D, Messer HH. pH changes in root dentin over a 4-week period following root canal dressing with calcium hydroxide. J Endod. 1993;19(6):302-6.
23. Estrela C, Sydney GB, Bammann LL, Felippe Junior O. Mechanism of action of calcium and hydroxyl ions of calcium hydroxide on tissue and bacteria. Braz Dent J. 1995;6(2):85-90.
24. Heithersay GS. Calcium hydroxide in the treatment of pulpless teeth with associated pathology. J Br Endod Soc. 1975;8(2):74-93.
25. Tagger M, Tagger E, Kfir A. Release of calcium and hydroxyl ions from set endodontic sealers containing calcium hydroxide. J Endod. 1988;14(12):588-91.
26. Gordon TM, Alexander JB. Influence on pH level of two calcium hydroxide root canal sealers in vitro. Oral Surg Oral Med Oral Pathol. 1986;61(6):624-8.
27. Kaplan AE, Picca M, Gonzalez MI, Macchi RL, Molgatini SL. Antimicrobial effect of six endodontic sealers: an in vitro evaluation. Endod Dent Traumatol. 1999;15(1):42-5.
28. Waltimo TM, Boiesen J, Eriksen HM, Orstavik D. Clinical performance of 3 endodontic sealers. Oral Surg Oral Med Oral Pathol Oral Radiol Endod. 2001;92(1):89-92.
29. Beltes P, Koulaouzidou E, Kotoula V, Kortsaris AH. In vitro evaluation of the cytotoxicity of calcium hydroxide-based root canal sealers. Endod Dent Traumatol. 1995;11(5):245-9.
30. Huang FM, Tai KW, Chou MY, Chang YC. Cytotoxicity of resin-, zinc oxide-eugenol-, and calcium hydroxide-based root canal sealers on human periodontal ligament cells and permanent V79 cells. Int Endod J. 2002;35(2):153-8.
31. Tyagi S, Mishra P, Tyagi P. Evolution of root canal sealers: An insight story. European Journal of General Dentistry. 2013;2(3):199-218.
32. Hammad M, Qualtrough A, Silikas N. Extended setting shrinkage behavior of endodontic sealers. J Endod. 2008;34(1):90-3.
33. McMichen FR, Pearson G, Rahbaran S, Gulabivala K. A comparative study of selected physical properties of five root-canal sealers. Int Endod J. 2003;36(9):629-35.
34. Nunes VH, Silva RG, Alfredo E, Sousa-Neto MD, Silva-Sousa YT. Adhesion of Epiphany and AH Plus sealers to human root dentin treated with different solutions. Braz Dent J. 2008;19(1):46-50.
35. Cohen BI, Pagnillo MK, Musikant BL, Deutsch AS. Formaldehyde evaluation from endodontic materials. Oral Health. 1998;88(12):37-9.
36. Shenoi PR, Badole GP, Khode RT. Evaluation of softening ability of Xylene & Endosolv-R on three different epoxy resin based sealers within 1 to 2 minutes - an in vitro study. Restor Dent Endod. 2014;39(1):17-23.
37. Garrido AD, Lia RC, Franca SC, da Silva JF, Astolfi-Filho S, Sousa-Neto MD. Laboratory evaluation of the physicochemical properties of a new root canal sealer based on Copaifera multijuga oil-resin. Int Endod J. 2010;43(4):283-91.
38. Koch KA, Brave D. EndoSequence: melding endodontics with restorative dentistry, part 3. Dent Today. 2009;28(3):88, 90, 2 passim.
39. Fridland M, Rosado R. Mineral trioxide aggregate (MTA) solubility and porosity with different water-to-powder ratios. J Endod. 2003;29(12):814-7.
40. Sarkar NK, Caicedo R, Ritwik P, Moiseyeva R, Kawashima I. Physicochemical basis of the biologic properties of mineral trioxide aggregate. J Endod. 2005;31(2):97-100.
41. Camilleri J. Characterization of hydration products of mineral trioxide aggregate. Int Endod J. 2008;41(5):408-17.
42. Islam I, Chng HK, Yap AU. Comparison of the physical and mechanical properties of MTA and portland cement. J Endod. 2006;32(3):193-7.
43. Trope M, Bunes A, Debelian G. Root filling materials and techniques: bioceramics a new hope? Endodontic Topics. 2015;32(1):86-96.

44. Debelian G, Trope M. The use of premixed bioceramic materials in endodontics. Giornale Italiano di Endodonzia. 2016;30(2):70-80.
45. Viapiana R, Guerreiro-Tanomaru JM, Hungaro-Duarte MA, Tanomaru-Filho M, Camilleri J. Chemical characterization and bioactivity of epoxy resin and Portland cement-based sealers with niobium and zirconium oxide radiopacifiers. Dent Mater. 2014;30(9):1005-20.
46. Valles M, Mercade M, Duran-Sindreu F, Bourdelande JL, Roig M. Influence of light and oxygen on the color stability of five calcium silicate-based materials. J Endod. 2013;39(4):525-8.
47. Camps J, Jeanneau C, El Ayachi I, Laurent P, About I. Bioactivity of a Calcium Silicate-based Endodontic Cement (BioRoot RCS): Interactions with Human Periodontal Ligament Cells In Vitro. J Endod. 2015;41(9):1469-73.
48. Arias-Moliz MT, Camilleri J. The effect of the final irrigant on the antimicrobial activity of root canal sealers. Journal of dentistry. 2016;52:30-6.
49. Camilleri J. Sealers and warm gutta-percha obturation techniques. J Endod. 2015;41(1):72-8.
50. Viapiana R, Moinzadeh AT, Camilleri L, Wesselink PR, Tanomaru Filho M, Camilleri J. Porosity and sealing ability of root fillings with gutta-percha and BioRoot RCS or AH Plus sealers. Evaluation by three ex vivo methods. Int Endod J. 2016;49(8):774-82.
51. Loushine BA, Bryan TE, Looney SW, Gillen BM, Loushine RJ, Weller RN, et al. Setting properties and cytotoxicity evaluation of a premixed bioceramic root canal sealer. J Endod. 2011;37(5):673-7.
52. Candeiro GT, Correia FC, Duarte MA, Ribeiro-Siqueira DC, Gavini G. Evaluation of radiopacity, pH, release of calcium ions, and flow of a bioceramic root canal sealer. J Endod. 2012;38(6):842-5.
53. Scarparo RK, Haddad D, Acasigua GA, Fossati AC, Fachin EV, Grecca FS. Mineral trioxide aggregate-based sealer: analysis of tissue reactions to a new endodontic material. J Endod. 2010;36(7):1174-8.
54. Nagas E, Uyanik MO, Eymirli A, Cehreli ZC, Vallittu PK, Lassila LV, et al. Dentin moisture conditions affect the adhesion of root canal sealers. J Endod. 2012;38(2):240-4.
55. Gomes-Filho JE, Watanabe S, Bernabe PF, de Moraes Costa MT. A mineral trioxide aggregate sealer stimulated mineralization. J Endod. 2009;35(2):256-60.
56. Huffman BP, Mai S, Pinna L, Weller RN, Primus CM, Gutmann JL, et al. Dislocation resistance of ProRoot Endo Sealer, a calcium silicate-based root canal sealer, from radicular dentine. Int Endod J. 2009;42(1):34-46.
57. Sagsen B, Ustun Y, Demirbuga S, Pala K. Push-out bond strength of two new calcium silicate-based endodontic sealers to root canal dentine. Int Endod J. 2011;44(12):1088-91.
58. Hatibovic-Kofman S, Raimundo L, Zheng L, Chong L, Friedman M, Andreasen JO. Fracture resistance and histological findings of immature teeth treated with mineral trioxide aggregate. Dent Traumatol. 2008;24(3):272-6.
59. Zordan-Bronzel CL, Esteves Torres FF, Tanomaru-Filho M, Chavez-Andrade GM, Bosso-Martelo R, Guerreiro-Tanomaru JM. Evaluation of Physicochemical Properties of a New Calcium Silicate-based Sealer, Bio-C Sealer. J Endod. 2019;45(10):1248-52.
60. Asgary S, Shahabi S, Jafarzadeh T, Amini S, Kheirieh S. The properties of a new endodontic material. J Endod. 2008;34(8):990-3.
61. Callahan R. Rosin solution for the sealing of the dentinal tubuli and as an adjuvant in the filling of root-canals. J Allied Dent Soci. 1914;39:53-63.
62. Peng L, Ye L, Tan H, Zhou X. Outcome of root canal obturation by warm gutta-percha versus cold lateral condensation: a meta-analysis. J Endod. 2007;33(2):106-9.
63. Schilder H. Filling root canals in three dimensions. Dent Clin North Am. 1967:723-44.
64. Peters DD. Two-year in vitro solubility evaluation of four Gutta-percha sealer obturation techniques. J Endod. 1986;12(4):139-45.
65. Holcomb JQ, Pitts DL, Nicholls JI. Further investigation of spreader loads required to cause vertical root fracture during lateral condensation. J Endod. 1987;13(6):277-84.

66. Lertchirakarn V, Palamara JE, Messer HH. Load and strain during lateral condensation and vertical root fracture. J Endod. 1999;25(2):99-104.
67. Ho ES, Chang JW, Cheung GS. Quality of root canal fillings using three gutta-percha obturation techniques. Restor Dent Endod. 2016;41(1):22-8.
68. Brothman P. A comparative study of the vertical and the lateral condensation of gutta-percha. J Endod. 1981;7(1):27-30.
69. Goldberg F, Artaza LP, De Silvio A. Effectiveness of different obturation techniques in the filling of simulated lateral canals. J Endod. 2001;27(5):362-4.
70. Buchanan LS. The continuous wave of condensation technique: a convergence of conceptual and procedural advances in obturation. Dent Today. 1994;13(10):80, 2, 4-5.
71. Lea CS, Apicella MJ, Mines P, Yancich PP, Parker MH. Comparison of the obturation density of cold lateral compaction versus warm vertical compaction using the continuous wave of condensation technique. J Endod. 2005;31(1):37-9.
72. Buchanan LS. The predefined endodontic preparation: instrument and technique updates for the greater taper system. Dent Today. 2001;20(1):56-60, 2-5.
73. Gordon MP, Love RM, Chandler NP. An evaluation of .06 tapered gutta-percha cones for filling of .06 taper prepared curved root canals. Int Endod J. 2005;38(2):87-96.
74. Ozawa T, Taha N, Messer HH. A comparison of techniques for obturating oval-shaped root canals. Dent Mater J. 2009;28(3):290-4.
75. Horsted-Bindslev P, Andersen MA, Jensen MF, Nilsson JH, Wenzel A. Quality of molar root canal fillings performed with the lateral compaction and the single-cone technique. J Endod. 2007;33(4):468-71.
76. Tasdemir T, Er K, Yildirim T, Buruk K, Celik D, Cora S, et al. Comparison of the sealing ability of three filling techniques in canals shaped with two different rotary systems: a bacterial leakage study. Oral Surg Oral Med Oral Pathol Oral Radiol Endod. 2009;108(3):e129-34.
77. Pommel L, Camps J. In vitro apical leakage of system B compared with other filling techniques. J Endod. 2001;27(7):449-51.
78. Yucel AC, Ciftci A. Effects of different root canal obturation techniques on bacterial penetration. Oral Surg Oral Med Oral Pathol Oral Radiol Endod. 2006;102(4):e88-92.
79. Clark-Holke D, Drake D, Walton R, Rivera E, Guthmiller JM. Bacterial penetration through canals of endodontically treated teeth in the presence or absence of the smear layer. J Dent. 2003;31(4):275-81.
80. Monticelli F, Sadek FT, Schuster GS, Volkmann KR, Looney SW, Ferrari M, et al. Efficacy of two contemporary single-cone filling techniques in preventing bacterial leakage. J Endod. 2007;33(3):310-3.
81. Jafari F, Jafari S. Importance and methodologies of endodontic microleakage studies: A systematic review. J Clin Exp Dent. 2017;9(6):e812-e9.
82. Schafer E, Olthoff G. Effect of three different sealers on the sealing ability of both thermafil obturators and cold laterally compacted Gutta-Percha. J Endod. 2002;28(9):638-42.
83. Wu MK, Wesselink PR. Endodontic leakage studies reconsidered. Part I. Methodology, application and relevance. Int Endod J. 1993;26(1):37-43.
84. Souza EM, Pappen FG, Shemesh H, Bonanato-Estrela C, Bonetti-Filho I. Reliability of assessing dye penetration along root canal fillings using methylene blue. Aust Endod J. 2009;35(3):158-63.
85. Mente J, Ferk S, Dreyhaupt J, Deckert A, Legner M, Staehle HJ. Assessment of different dyes used in leakage studies. Clin Oral Investig. 2010;14(3):331-8.
86. Wanted: a base of evidence. J Endod. 2007;33(12):1401-2.
87. Wu MK, Wesselink PR, Boersma J. A 1-year follow-up study on leakage of four root canal sealers at different thicknesses. Int Endod J. 1995;28(4):185-9.
88. Belli S, Zhang Y, Pereira PN, Pashley DH. Adhesive sealing of the pulp chamber. J Endod. 2001;27(8):521-6.

89. Fogel HM. Microleakage of posts used to restore endodontically treated teeth. J Endod. 1995;21(7):376-9.
90. Hammad M, Qualtrough A, Silikas N. Evaluation of root canal obturation: a three-dimensional in vitro study. J Endod. 2009;35(4):541-4.
91. Ricucci D, Grondahl K, Bergenholtz G. Periapical status of root-filled teeth exposed to the oral environment by loss of restoration or caries. Oral Surg Oral Med Oral Pathol Oral Radiol Endod. 2000;90(3):354-9.
92. De-Deus G. Research that matters – root canal filling and leakage studies. International Endodontic Journal. 2012;45(12):1063-4.
93. Verissimo DM, do Vale MS. Methodologies for assessment of apical and coronal leakage of endodontic filling materials: a critical review. J Oral Sci. 2006;48(3):93-8.
94. Arai Y, Tammisalo E, Iwai K, Hashimoto K, Shinoda K. Development of a compact computed tomographic apparatus for dental use. Dentomaxillofac Radiol. 1999;28(4):245-8.
95. Huang YD, Wu J, Sheu RJ, Chen MH, Chien DL, Huang YT, et al. Evaluation of the root and root canal systems of mandibular first premolars in northern Taiwanese patients using cone-beam computed tomography. J Formos Med Assoc. 2015;114(11):1129-34.
96. Weber MT, Stratz N, Fleiner J, Schulze D, Hannig C. Possibilities and limits of imaging endodontic structures with CBCT. Swiss Dent J. 2015;125(3):293-311.
97. Ozcan G, Sekerci AE, Cantekin K, Aydinbelge M, Dogan S. Evaluation of root canal morphology of human primary molars by using CBCT and comprehensive review of the literature. Acta Odontol Scand. 2016;74(4):250-8.
98. Scarfe WC, Farman AG, Sukovic P. Clinical applications of cone-beam computed tomography in dental practice. J Can Dent Assoc. 2006;72(1):75-80.
99. Swain MV, Xue J. State of the art of Micro-CT applications in dental research. Int J Oral Sci. 2009;1(4):177-88.
100. du Plessis A, Broeckhoven C. Looking deep into nature: A review of micro-computed tomography in biomimicry. Acta Biomaterialia. 2019;85:27-40.
101. Briseno-Marroquin B, Paque F, Maier K, Willershausen B, Wolf TG. Root Canal Morphology and Configuration of 179 Maxillary First Molars by Means of Micro-computed Tomography: An Ex Vivo Study. J Endod. 2015;41(12):2008-13.
102. Grande NM, Plotino G, Gambarini G, Testarelli L, D'Ambrosio F, Pecci R, et al. Present and future in the use of micro-CT scanner 3D analysis for the study of dental and root canal morphology. Ann Ist Super Sanita. 2012;48(1):26-34.
103. Peters OA, Paque F. Root canal preparation of maxillary molars with the self-adjusting file: a micro-computed tomography study. J Endod. 2011;37(1):53-7.
104. Gross BC, Erkal JL, Lockwood SY, Chen C, Spence DM. Evaluation of 3D printing and its potential impact on biotechnology and the chemical sciences. Anal Chem. 2014;86(7):3240-53.
105. Cohen A, Laviv A, Berman P, Nashef R, Abu-Tair J. Mandibular reconstruction using stereolithographic 3-dimensional printing modeling technology. Oral Surg Oral Med Oral Pathol Oral Radiol Endod. 2009;108(5):661-6.
106. Ikuta K, Yamada A, Niikura F. Real three-dimensional microfabrication for biodegradable polymers: demonstration of high-resolution and biocompatibility for implantable microdevices. Conf Proc IEEE Eng Med Biol Soc. 2004;4:2679-82.
107. Chia HN, Wu BM. Recent advances in 3D printing of biomaterials. J Biol Eng. 2015;9:4.
108. Doraiswamy A, Dunaway TM, Wilker JJ, Narayan RJ. Inkjet printing of bioadhesives. J Biomed Mater Res B Appl Biomater. 2009;89(1):28-35.
109. Venturi M, Pasquantonio G, Falconi M, Breschi L. Temperature change within gutta-percha induced by the System-B Heat Source. Int Endod J. 2002;35(9):740-6.

110. Permar D, Melfi RC. Permar's oral embryology and microscopic anatomy a textbook for students in dental hygiene. Philadelphia: Lea & Febiger; 1994.
111. Xia Y, Zhou P, Cheng X, Xie Y, Liang C, Li C, et al. Selective laser sintering fabrication of nano-hydroxyapatite/poly-epsilon-caprolactone scaffolds for bone tissue engineering applications. Int J Nanomedicine. 2013;8:4197-213.
112. Heo SJ, Kim SE, Wei J, Hyun YT, Yun HS, Kim DH, et al. Fabrication and characterization of novel nano- and micro-HA/PCL composite scaffolds using a modified rapid prototyping process. J Biomed Mater Res A. 2009;89(1):108-16.
113. Shao H, He J, Lin T, Zhang Z, Zhang Y, Liu S. 3D gel-printing of hydroxyapatite scaffold for bone tissue engineering. Ceramics International. 2019;45(1):1163-70.
114. Au - Gonzalez P, Au - Schwarzer E, Au - Scheithauer U, Au - Kooijmans N, Au - Moritz T. Additive Manufacturing of Functionally Graded Ceramic Materials by Stereolithography. JoVE. 2019(143):e57943.
115. ØRSTAVIK D. Materials used for root canal obturation: technical, biological and clinical testing. Endodontic Topics. 2005;12(1):25-38.
116. Formosa LM, Mallia B, Camilleri J. The effect of curing conditions on the physical properties of tricalcium silicate cement for use as a dental biomaterial. Int Endod J. 2012;45(4):326-36.
117. Saunders WP, Saunders EM. Coronal leakage as a cause of failure in root-canal therapy: a review. Endodontics & dental traumatology. 1994;10(3):105-8.
118. An S, Gao Y, Ling J, Wei X, Xiao Y. Calcium ions promote osteogenic differentiation and mineralization of human dental pulp cells: implications for pulp capping materials. J Mater Sci Mater Med. 2012;23(3):789-95.
119. Reszka P, Nowicka A, Dura W, Marek E, Lipski M. SEM and EDS study of TotalFill BC Sealer and GuttaFlow Bioseal root canal sealers. Dent Med Probl. 2019;56(2):167-72.
120. Siboni F, Taddei P, Zamparini F, Prati C, Gandolfi MG. Properties of BioRoot RCS, a tricalcium silicate endodontic sealer modified with povidone and polycarboxylate. Int Endod J. 2017;50 Suppl 2:e120-e36.
121. Reszka P, Nowicka A, Lipski M, Dura W, Drozdzik A, Wozniak K. A Comparative Chemical Study of Calcium Silicate-Containing and Epoxy Resin-Based Root Canal Sealers. Biomed Res Int. 2016;2016:9808432.
122. Lopez-Garcia S, Lozano A, Garcia-Bernal D, Forner L, Llena C, Guerrero-Girones J, et al. Biological Effects of New Hydraulic Materials on Human Periodontal Ligament Stem Cells. J Clin Med. 2019;8(8).
123. Akcay M, Arslan H, Durmus N, Mese M, Capar ID. Dentinal tubule penetration of AH Plus, iRoot SP, MTA fillapex, and guttaflow bioseal root canal sealers after different final irrigation procedures: A confocal microscopic study. Lasers Surg Med. 2016;48(1):70-6.
124. Desai S, Chandler N. Calcium hydroxide-based root canal sealers: a review. J Endod. 2009;35(4):475-80.
125. Camilleri J. Evaluation of selected properties of mineral trioxide aggregate sealer cement. J Endod. 2009;35(10):1412-7.
126. Nanci A. Ten Cate's Oral Histology-E-Book: Development, Structure, and Function: Elsevier Health Sciences; 2017.
127. Xu Q, Fan MW, Fan B, Cheung GS, Hu HL. A new quantitative method using glucose for analysis of endodontic leakage. Oral Surg Oral Med Oral Pathol Oral Radiol Endod. 2005;99(1):107-11.
128. Shemesh H, Wu MK, Wesselink PR. Leakage along apical root fillings with and without smear layer using two different leakage models: a two-month longitudinal ex vivo study. Int Endod J. 2006;39(12):968-76.
129. Huang Y, Celikten B, de Faria Vasconcelos K, Ferreira Pinheiro Nicolielo L, Lippiatt N, Buyuksungur A, et al. Micro-CT and nano-CT analysis of filling quality of three different endodontic sealers. Dentomaxillofac Radiol. 2017;46(8):20170223.

130. Wu MK, Bud MG, Wesselink PR. The quality of single cone and laterally compacted gutta-percha fillings in small and curved root canals as evidenced by bidirectional radiographs and fluid transport measurements. Oral Surg Oral Med Oral Pathol Oral Radiol Endod. 2009;108(6):946-51.
131. Da Rosa RA, Santini MF, Cavenago BC, Pereira JR, Duarte MA, So MV. Micro-CT Evaluation of Root Filling Removal after Three Stages of Retreatment Procedure. Braz Dent J. 2015;26(6):612-8.
132. Robinson JP, Lumley PJ, Claridge E, Cooper PR, Grover LM, Williams RL, et al. An analytical Micro CT methodology for quantifying inorganic dentine debris following internal tooth preparation. Journal of dentistry. 2012;40(11):999-1005.
133. Keles A, Alcin H, Kamalak A, Versiani MA. Micro-CT evaluation of root filling quality in oval-shaped canals. Int Endod J. 2014;47(12):1177-84.
134. Camilleri J. Mineral trioxide aggregate: present and future developments. Endodontic Topics. 2015;32(1):31-46.
135. Almudaiheem JA. Prediction of Drying Shrinkage of Portland Cement Paste: Influence of Shrinkage Mechanisms. Journal of King Saud University - Engineering Sciences. 1991;3(1):69-86.
136. Mutal L, Gani O. Presence of pores and vacuoles in set endodontic sealers. Int Endod J. 2005;38(10):690-6.
137. Parr A. Chapter | one - Fundamental Principles. In: Parr A, editor. Hydraulics and Pneumatics (Third Edition). Oxford: Butterworth-Heinemann; 2011. p. 1-29.
138. Flores DS, Rached FJ, Jr., Versiani MA, Guedes DF, Sousa-Neto MD, Pecora JD. Evaluation of physicochemical properties of four root canal sealers. Int Endod J. 2011;44(2):126-35.
139. Marin-Bauza GA, Silva-Sousa YT, da Cunha SA, Rached-Junior FJ, Bonetti-Filho I, Sousa-Neto MD, et al. Physicochemical properties of endodontic sealers of different bases. J Appl Oral Sci. 2012;20(4):455-61.
140. Versiani MA, Carvalho-Junior JR, Padilha MI, Lacey S, Pascon EA, Sousa-Neto MD. A comparative study of physicochemical properties of AH Plus and Epiphany root canal sealants. Int Endod J. 2006;39(6):464-71.
141. Qu W, Bai W, Liang YH, Gao XJ. Influence of Warm Vertical Compaction Technique on Physical Properties of Root Canal Sealers. J Endod. 2016;42(12):1829-33.
142. Selem LC, Li GH, Niu LN, Bergeron BE, Bortoluzzi EA, Chen JH, et al. Quality of obturation achieved by a non-gutta-percha-based root filling system in single-rooted canals. J Endod. 2014;40(12):2003-8.
143. Celikten B, C FU, A IO, Tufenkci P, Misirli M, K OD, et al. Micro-CT assessment of the sealing ability of three root canal filling techniques. J Oral Sci. 2015;57(4):361-6.
144. Naseri M, Kangarlou A, Khavid A, Goodini M. Evaluation of the quality of four root canal obturation techniques using micro-computed tomography. Iran Endod J. 2013;8(3):89-93.
145. Lake SP, Barocas VH. Mechanical and structural contribution of non-fibrillar matrix in uniaxial tension: a collagen-agarose co-gel model. Ann Biomed Eng. 2011;39(7):1891-903.
146. Lake SP, Hald ES, Barocas VH. Collagen-agarose co-gels as a model for collagen-matrix interaction in soft tissues subjected to indentation. J Biomed Mater Res A. 2011;99(4):507-15.
147. Lee MN, Hwang HS, Oh SH, Roshanzadeh A, Kim JW, Song JH, et al. Elevated extracellular calcium ions promote proliferation and migration of mesenchymal stem cells via increasing osteopontin expression. Exp Mol Med. 2018;50(11):1-16.
148. Koutroulis A, Kuehne SA, Cooper PR, Camilleri J. The role of calcium ion release on biocompatibility and antimicrobial properties of hydraulic cements. Sci Rep. 2019;9(1):19019.
149. Jittikarn S, Sitthichai W, Varisara S. Diameter and Density of Dentinal Tubule in Human Primary Teeth. Journal of the Dental Association of Thailand. 2017;67.